

10-8-2018

# Active Fault-Tolerant Control Design for Nonlinear Systems

Ali Reza Abbaspour

*Florida International University, aabba014@fiu.edu*

Follow this and additional works at: <https://digitalcommons.fiu.edu/etd>

 Part of the [Controls and Control Theory Commons](#), and the [Navigation, Guidance, Control and Dynamics Commons](#)

---

## Recommended Citation

Abbaspour, Ali Reza, "Active Fault-Tolerant Control Design for Nonlinear Systems" (2018). *FIU Electronic Theses and Dissertations*. 3917.

<https://digitalcommons.fiu.edu/etd/3917>

This work is brought to you for free and open access by the University Graduate School at FIU Digital Commons. It has been accepted for inclusion in FIU Electronic Theses and Dissertations by an authorized administrator of FIU Digital Commons. For more information, please contact [dcc@fiu.edu](mailto:dcc@fiu.edu).

FLORIDA INTERNATIONAL UNIVERSITY  
Miami, Florida

ACTIVE FAULT-TOLERANT CONTROL DESIGN FOR NONLINEAR  
SYSTEMS

A dissertation submitted in partial fulfillment of the  
requirements for the degree of  
DOCTOR OF PHILOSOPHY  
in  
ELECTRICAL AND COMPUTER ENGINEERING  
by  
Ali Reza Abbaspour

2018

To: Dean John L. Volakis  
College of Engineering and Computing

This dissertation, written by Ali Reza Abbaspour, and entitled Active Fault-Tolerant Control Design for Nonlinear Systems, having been approved in respect to style and intellectual content, is referred to you for judgment.

We have read this dissertation and recommend that it be approved.

---

Jean Andrian

---

Arif I. Sarwat

---

Arman Sargolzaei

---

Alexander Perez-Pons

---

Deng Pan

---

Kang K. Yen, Major Professor

Date of Defense: October 8, 2018

The dissertation of Ali Reza Abbaspour is approved.

---

Dean John L. Volakis  
College of Engineering and Computing

---

Andrés G. Gil  
Vice President for Research and Economic Development  
and Dean of the University Graduate School

Florida International University, 2018

© Copyright 2018 by Ali Reza Abbaspour

All rights reserved.

## DEDICATION

To my parents and my beloved wife.

## ACKNOWLEDGMENTS

I would like to express my sincere gratitude to my major professor, Dr. Kang K. Yen, for his continual support, patience, immense knowledge, and expertise. As my teacher and mentor, he has taught me more than I could ever thank him enough.

I would also like to thank my committee members, Dr. Arman Sargolzaei, Dr. Arif I. Sarwat, Dr. Alexander Perez-Pons, Dr. Jean Andrian, and Dr. Deng Pan. Their extensive scientific guidance helped me to significantly improve this dissertation.

I would like to acknowledge the Department of Electrical and Computer Engineering for providing me with a graduate assistantship, University Graduate School (UGS) for the Dissertation Year Fellowship (DYF) award, and SGA Graduate Scholarships, all of which facilitated the research of this dissertation. This work would not have been possible without their financial support.

My family was the most important reason to me in the pursuit of my studies to this level. I would like to thank my parents, whose love and guidance are with me from thousands of miles away in my home country (Iran). Most importantly, I wish to thank my loving and supportive wife, Parisa, whose companionship eased the difficulties during my studies.

ABSTRACT OF THE DISSERTATION  
ACTIVE FAULT-TOLERANT CONTROL DESIGN FOR NONLINEAR  
SYSTEMS

by

Ali Reza Abbaspour

Florida International University, 2018

Miami, Florida

Professor Kang K. Yen, Major Professor

Faults and failures in system components are the two main reasons for the instability and the degradation in control performance. In recent decades, fault-tolerant control (FTC) approaches were introduced to improve the resiliency of the control system against faults and failures. In general, FTC techniques are classified into two major groups: passive and active. Passive FTC systems do not rely on the fault information to control the system and are closely related to the robust control techniques while an active FTC system performs based on the information received from the fault detection and isolation (FDI) system, and the fault problem will be tackled more intelligently without affecting other parts of the system.

This dissertation technically reviews fault and failure causes in control systems and finds solutions to compensate for their effects. Recent achievements in FDI approaches, and active and passive FTC designs are investigated. Thorough comparisons of several different aspects are conducted to understand the advantages and disadvantages of different FTC techniques to motivate researchers to further developing FTC, and FDI approaches.

Then, a novel active FTC system framework based on online FDI is presented which has significant advantages in comparison with other state of the art FTC strategies. To design the proposed active FTC, a new FDI approach is introduced which uses

the artificial neural network (ANN) and a model based observer to detect and isolate faults and failures in sensors and actuators. In addition, the extended Kalman filter (EKF) is introduced to tune ANN weights and improve the ANN performance. Then, the FDI signal combined with a nonlinear dynamic inversion (NDI) technique is used to compensate for the faults in the actuators and sensors of a nonlinear system. The proposed scheme detects and accommodates faults in the actuators and sensors of the system in real-time without the need of controller reconfiguration. The proposed active FTC approach is used to design a control system for three different applications: Unmanned aerial vehicle (UAV), load frequency control system, and proton exchange membrane fuel cell (PEMFC) system. The performance of the designed controllers are investigated through numerical simulations by comparison with conventional control approaches, and their advantages are demonstrated.

## TABLE OF CONTENTS

CHAPTER	PAGE
1. INTRODUCTION . . . . .	1
1.1 Introduction . . . . .	1
1.2 Problem Statement . . . . .	1
1.3 Definition of Fault-Tolerant Controller . . . . .	5
1.3.1 Passive FTC . . . . .	6
1.3.2 Active FTC . . . . .	8
1.4 Motivations, and Summary of Contributions . . . . .	9
1.5 Dissertation Road-map . . . . .	11
2. LITERATURE REVIEW AND DESIGN FUNDAMENTALS . . . . .	13
2.1 Introduction . . . . .	13
2.2 Fault Detection and Isolation . . . . .	13
2.2.1 Model based FDI . . . . .	15
2.2.2 Knowledge-based Approaches . . . . .	21
2.2.3 Combined Model-Knowledge based Approach . . . . .	26
2.3 Active Fault Tolerant Control . . . . .	29
2.3.1 Switching-Based Active FTC . . . . .	30
2.3.2 Hierarchical Structure Active FTC . . . . .	31
2.3.3 Safe Parking Active FTC . . . . .	31
2.3.4 Analytical Feedback Compensation Active FTC . . . . .	32
2.3.5 Hybrid FTC . . . . .	33
3. ACTIVE FAULT TOLERANT CONTROL DESIGN . . . . .	34
3.1 Introduction . . . . .	34
3.2 Proposed FDI Method . . . . .	35
3.2.1 NNAS . . . . .	37
3.2.2 Neural network weight update law . . . . .	39
3.2.3 Stability Analysis of ANN Updating Based on EKF . . . . .	40
3.2.4 The Overall Stability of The NNAS . . . . .	42
3.3 Actuator FDI Design . . . . .	45
3.4 Sensor FDI Design . . . . .	45
3.5 Proposed Active FTC Design Resilient . . . . .	47
3.5.1 Nonlinear Feedback Linearization Controller . . . . .	48
3.5.2 Adaptive fault compensation feedback controller . . . . .	49
3.5.3 Active FTC Stability Analysis . . . . .	50
4. A NEURAL ADAPTIVE ACTIVE FTC DESIGN FOR UAV . . . . .	55
4.1 Introduction . . . . .	55
4.2 UAV Nonlinear Dynamic . . . . .	58
4.3 FDI Design . . . . .	60

4.3.1	NNAS . . . . .	61
4.3.2	Neural network weight update law . . . . .	62
4.3.3	Actuator FDI design . . . . .	63
4.4	Active FTC design . . . . .	65
4.4.1	Nonlinear Dynamic Inversion Controller . . . . .	65
4.4.2	Adaptive Fault Compensation Feedback Controller . . . . .	67
4.5	Numerical Simulations . . . . .	68
4.5.1	Fault in the Aileron . . . . .	70
4.5.2	Fault in the Elevator . . . . .	72
4.5.3	Fault in the Rudder . . . . .	75
4.6	Conclusion . . . . .	76
5	A NEURAL NETWORK-BASED ACTIVE FAULT-TOLERANT DESIGN FOR PRESSURE CONTROL IN PROTON EXCHANGE MEMBRANE FUEL CELLS . . . . .	79
5.1	Introduction . . . . .	79
5.2	PEMFC MODEL . . . . .	84
5.3	FD Design . . . . .	87
5.3.1	ANN Weight Update Law . . . . .	88
5.3.2	Actuator FD design for PEMFC . . . . .	90
5.4	Active FTC Design . . . . .	91
5.4.1	FBL Controller . . . . .	92
5.4.2	FTC Design . . . . .	92
5.4.3	Fault Analyzer . . . . .	93
5.5	Numerical Simulation . . . . .	93
5.5.1	Fault in the actuator . . . . .	95
5.5.2	Simultaneous Actuator Faults and Failure . . . . .	96
5.6	Conclusion . . . . .	98
6	RESILIENT CONTROL DESIGN FOR LOAD FREQUENCY CONTROL OF POWER GRID SYSTEM UNDER FALSE DATA INJECTION ATTACKS . . . . .	101
6.1	Introduction . . . . .	101
6.2	LFC Model . . . . .	106
6.3	Anomaly Detection . . . . .	108
6.3.1	ANN observer . . . . .	108
6.3.2	ANN update law . . . . .	109
6.3.3	Luenberger Observer . . . . .	110
6.4	Controller Design . . . . .	111
6.4.1	Resilient Controller . . . . .	111
6.5	Stability Analysis of the Controller . . . . .	113
6.6	Numerical Simulation Result . . . . .	117
6.6.1	Scenario I: Single non-periodic FDI attack . . . . .	118

6.6.2	Scenario II: Single periodic FDI attack . . . . .	120
6.6.3	Simultaneous FDI attacks . . . . .	122
6.6.4	Discussion . . . . .	123
6.7	Conclusion . . . . .	125
7.	CONCLUSION AND FUTURE WORKS . . . . .	127
7.1	Conclusion . . . . .	127
7.2	Future Works . . . . .	129
7.2.1	Improving FDI Accuracy . . . . .	129
7.2.2	Improving the FTC system . . . . .	130
7.2.3	Applications . . . . .	130
	BIBLIOGRAPHY . . . . .	131
	VITA . . . . .	154

## LIST OF TABLES

TABLE	PAGE
2.1 Summarizing the advantages and disadvantages of the model-based FDI approaches. . . . .	22
2.2 Summarizing the advantages and disadvantages of the Knowledge-based FDI approaches. . . . .	28
4.1 RMSE in the presence of a fault in aileron. . . . .	71
4.2 RMSE in the presence of a fault in the elevator. . . . .	74
4.3 RMSE in presence of fault in rudder. . . . .	76
6.1 Analytical analysis of the proposed approach in detection and compensation of FDI-attack in the LFC system. . . . .	123

## LIST OF FIGURES

FIGURE	PAGE
1.1 Potential faults in a control system. . . . .	3
1.2 The graphical description of abrupt, incipient, and intermittent faults. . . . .	5
1.3 Passive FTC Structure: This kind of controller can be designed by considering redundant controller/actuator/plant/sensor and in the presence of fault will switch to the redundant component. . . . .	8
1.4 General Structure of active FTC systems. . . . .	9
2.1 General structure of fault detection and isolation (FDI). . . . .	15
2.2 Classification of the FDI approaches based on their methodology. (The abbreviations: KF (Kalman Filter), EKF (Extended Kalman Filter), UKF (Unscented Kalman Filter), SMO (Sliding Mode Observer), PCA (Principal Component Analysis), ICA (Independent Component Analysis), PLS (Partial Least Square), SVM (Support Vector Machine), ANN (Artificial Neural Networks) . . . . .	16
2.3 General structure of Kalman filter-based fault detection [1]. . . . .	17
2.4 General structure of knowledge-based FDI approaches. . . . .	23
2.5 Fuzzy Logic (FL) based fault detection and isolation (FDI). . . . .	27
2.6 General structure of the combined ANN and model-based approach. . . . .	28
2.7 The general structure of the Switching-based active FTC system. . . . .	31
2.8 The general structure of the analytical feedback compensation active FTC system. . . . .	32
3.1 Block diagram of the updating process of the ANN with the EKF. . . . .	40
3.2 Block Diagram of the proposed FDI for actuators in nonlinear systems. . . . .	46
3.3 Block Diagram of the proposed FDI for actuators in nonlinear systems. . . . .	47
3.4 Block Diagram of the proposed Active FTC for actuator fault in nonlinear systems. . . . .	49
4.1 The aircraft coordinate system [2] . . . . .	59
4.2 The proposed united framework for fault detection and compensation (active FTC) diagram for an aircraft. . . . .	68
4.3 Fault detection using NNAS. . . . .	70

4.4	Attitude tracking control of the aircraft in presence of fault in the aileron actuator. . . . .	72
4.5	Actuator deflections in the presence of a fault in the aileron actuator. . . . .	73
4.6	Attitude tracking control of the aircraft in presence of fault in the elevator actuator. . . . .	74
4.7	Actuator deflections in presence of fault in the elevator. . . . .	75
4.8	Attitude tracking control of the aircraft in the presence of fault in the rudder actuator. . . . .	77
4.9	Actuator deflections in presence of fault in the rudder. . . . .	78
5.1	The diagram of the operation and air pressure control of the PEMFC. . . . .	87
5.2	Block diagram of the proposed active FTC controller for PEMFC. . . . .	94
5.3	The load profile of connected to the PEMFC. . . . .	96
5.4	Fault detection in actuators of PEMFC. . . . .	97
5.5	Fault effect on the actuators. . . . .	98
5.6	Pressure control in the presence of a fault in the actuators. . . . .	99
5.7	Fault effect on the actuators. . . . .	100
5.8	Pressure control in the presence of a fault in the actuators. . . . .	100
6.1	Overall diagram of the proposed control system. . . . .	112
6.2	The performance of the proposed AD system in the detection of the scenario I. . . . .	120
6.3	A comparison between the states of LFC system controlled with the proposed resilient controller and LQR controller in the presence of the attack in the first scenario. . . . .	121
6.4	The performance comparison of the proposed resilient control system with LQR controller in presence of the attack in the first scenario. . . . .	122
6.5	The performance of the proposed AD system in the detection of a single periodic FDI-attack in the second scenario. . . . .	123
6.6	The performance comparison of the proposed resilient control system with LQR controller in presence of a single periodic FDI-attack in the second scenario. . . . .	124

6.7	The performance of the proposed AD system in the detection of two simultaneous attack. . . . .	125
6.8	The performance comparison of the proposed resilient control system with LQR controller in presence of simultaneous FDI attacks on third and eighth states of the LFC system. . . . .	126

## NOMENCLATURE

### CHAPTER 1

ANN artificial neural network

DoF degree of freedom

EKF extended Kalman filter

FDI fault detection and isolation

FTC fault tolerant controller

LFC load frequency control

PEMFC proton exchange membrane fuel cells

SMC Sliding Mode Control

UAV unmanned aerial vehicle

### CHAPTER 2

FL fuzzy logic

HKF hybrid Kalman filter

ICA independent component analysis

IMU inertial measurement unit

KF Kalman Filter

LDTV linear discrete time-varying

LMI linear matrix inequalities

LPV linear parameter varying

LQG linear quadratic Gaussian

LTI linear time-invariant

PCA principal component analysis

PLS partial least square

PWM-VSI pulse-width modulation voltage source inverter

SMO sliding mode observer

SVM Support Vector Machine

T-S Takagi-Sugeno

UIO unknown input observer

UKF unscented Kalman filter

CHAPTER 3

$\eta_i(k)$  ANN learning constant

$\sigma(\bullet)$  The ANN activation function

$\theta_i(k)$  ANN update parameter

$f_a(x, t)$  fault in the actuator

$f_s(x, t)$  fault in the sensor

$K_i(k)$  Kalman filter gain

$M(t)$  The ANN observer

$P_i(k)$  covariance matrix of state estimation error

$R_i(k)$  noise estimated covariance matrix

$W, V$  ANN weight matrices that joint the first layer to the second layer

DI detection interval

NNAS neural network adaptive structure

PI proportional-integral

WNN wavelet neural network

#### CHAPTER 4

$\alpha$  angle of attack (AoA), [rad] or [deg]

$\beta$  sideslip angle, [rad] or [deg]

$\delta_e, \delta_a, \delta_r$  deflection of elevator, aileron and rudder, [rad] or [deg]

$\rho$  air density, [ $kg/m^3$ ]

$b$  wing span and wing mean aerodynamic chord, [ $m$ ]

$C_l, C_m, C_n$  aerodynamic moment coefficients

$C_L, C_D$  lift and drag coefficients

$C_x, C_y, C_z$  aerodynamic force coefficients

$C_{D_0}$  zero-lift drag coefficient

$C_{L_\alpha}$  lift-curve slope, [/rad]

$D$  drag, [ $N$ ]

$g$	acceleration due to gravity, $[m/s^2]$
$H$	altitude, $[m]$
$I_x, I_y, I_z$	moments of inertia, $[kg\ m^2]$
$L$	lift, $[N]$
$M$	mass, $[kg]$
$p, q, r$	components of airplane angular velocity about $x, y, z$ body axes, $[rad/s]$
$S$	wing area, $[m^2]$
$T$	thrust, $[N]$
$v$	velocity, $[m/s]$

## CHAPTER 6

$\alpha$	coefficient of charge transfer
$\phi_a$	Humidity on the anode side
$\phi_c$	Humidity on the cathode side
$F$	Faraday constant $[C/mole]$
$I_{fc}$	Current density of the fuel cell
$k_a$	Anode conversion factor
$k_c$	Cathode conversion factor
$N$	Cell number
$P_{vs}$	Saturation pressure $[kPa]$

$R$  Universal gas constant [ $J/mol - k$ ]

$r$  Electrical resistance [ $kUcm^2$ ]

$T$  Fuel cell temperature [ $K$ ]

$u_{H_2}$  Pressure valve of Hydrogen gas

$u_{O_2}$  Pressure valve of Oxygen gas

$V_0$  Open cell voltage

$V_a$  Anode volume [ $m^3$ ]

$V_c$  Cathode volume [ $m^3$ ]

## CHAPTER 7

$\Delta f^i$  frequency deviation

$\Delta P_g^i$  generator power deviation

$\Delta P_l$  load deviation

$\Delta P_{pf}^i$  power flow of the tie-line

$\Delta P_{tu}^i$  turbine valve position

$\mu_i$  The  $i^{th}$  power areas damping coefficient

$\omega_i$  The  $i^{th}$  power areas speed droop coefficient

$d(t)$  bounded disturbance

$e^i$  control error

$J_i$  The  $i^{th}$  power areas moment of inertia of generator

- $L$  The gain of the Luenberger observer
- $N$  number of interconnected power areas
- $T_{g,i}$  The  $i^{th}$  power areas governor time constant
- $T_{tu,i}$  The  $i^{th}$  power areas turbine time constant
- AD anomaly detection
- DPS distributed power systems
- WLS weighted least square

# CHAPTER 1

## INTRODUCTION

### 1.1 Introduction

In this chapter, the basic concepts of fault, failure, fault detection and isolation (FDI), and fault tolerant controller (FTC) are illustrated which will be helpful to differentiate them with uncertainty, disturbances, observer, and robust controller. Furthermore, faults and failure are categorized based on their cause, severity, and location. In addition, to demonstrate the importance of a reliable controller, some recent incidents related to the faults and failure in the controllers are reviewed.

The rest of this chapter is organized as follows: Section 2 describes the fault and the failure problem, and discusses their effects on the control system. Section 3 illustrates the FTC concept and classifies them into two groups based on their need of FDI in their design. Section 4 discusses the motivations for doing this research work, and the contributions are summarized. Finally, in Section 5, the road-map of this dissertation is presented.

### 1.2 Problem Statement

Faults and failures in the components of a control system can endanger the system stability and degrade its performance. Fault in a dynamical system can be described as a deviation of the system structure or system parameters from a nominal situation [3]. The overall effect of a single fault in a system can be varied from performance degradation to a total failure [4]. It is worthwhile to mention the difference between faults, and system uncertainties and external disturbances. The faults

are those elements which should be detected and whose effects should be removed by remedial actions. Disturbances and model uncertainties are nuisances, which are known to exist but whose effects on the system performance are handled by appropriate measures like filtering or robust design. In theory, it has been demonstrated that controllers can be designed to attenuate disturbances and tolerate model uncertainties up to a certain size while faults are more severe changes, whose effects on the plant behavior cannot be surpassed by a fixed controller. The difference between fault and failures should also be illustrated. A fault causes a change in the characteristics of a component such that the mode of operation or performance of the component is changed in an undesired way. Hence, the required specifications for the system performance are no longer met. In general, a fault can be worked around by fault-tolerant control so the faulty system remains operational. In contrast to this, the notion of a failure describes the inability of a system or a component to accomplish its function. The system or component has to be shut off because the failure is an irrecoverable event. Therefore, redundancy is the main solution in the presence of a failure in the system. Fault, based on its location, can be classified to sensor, actuator, and plant (component or parameter) faults [3].

In general, most of the classical control techniques assume that all the components in the system work correctly and the controller is designed based on this assumption. Hence, the occurrence of faults in the system component would send incorrect information to the controller, and subsequently, the controller will be misled based on the received false data. Figure 1.1 shows possible faults in a control system. As can be seen in Fig. 1.1, faults based on their component type can be classified in three categories:

**Plant Faults:** These faults change the dynamic I/O properties of the system.

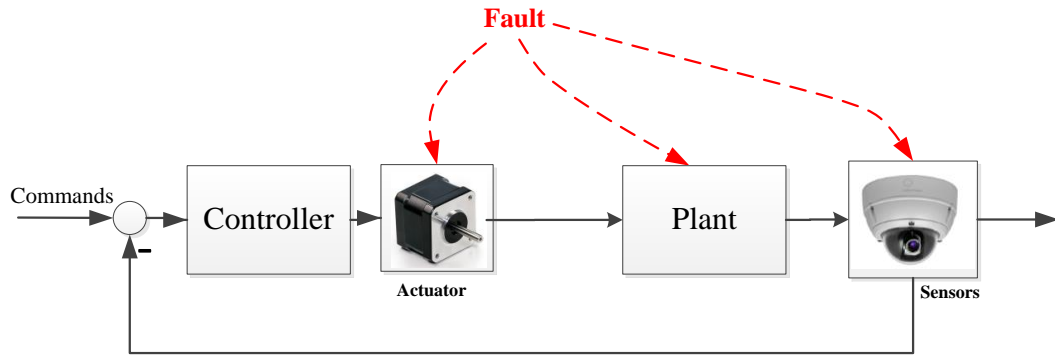


Figure 1.1: Potential faults in a control system.

**Sensor Faults:** The plant properties are not affected, but the sensor readings have substantial errors.

**Actuator Faults:** The plant properties are not affected, but the influence of the controller on the plant is interrupted or modified.

Faults and failures in a control system may occur due to various reasons, such as

- *Interruptions in communication between the actuator/sensor and the control unit* due to severe vibration, improper connections, metal flakes separating, and short circuit.
- *Noise effect on the actuator/sensor* due to environmental noise like a magnetic field.
- *Denial of service for a period of time* due to processor speed and network bandwidth [5,6].
- *A fall in a supply voltage/current of the electrical actuator/sensor* since they normally need a separated power supply [7].
- *False data injection* by a malicious intruder. In this kind of fault, an attacker penetrates to the system communication and injects false data to actuators/sensors to mislead the control system [8–11].

- *Floating actuator* (control surface moves freely without providing any moment) due to loss of hydraulic fluid [12, 13]. Float actuator failure has been reported as the main cause of flight incidents such as Flight 123 (B-747, Japan 1985) [14], and DHL A300B4 (A300, Baghdad, 2003) [13].

- *Actuator runaway/hardover* where the control surface moves at its maximum rate limit and reaches its saturation limit. The actuator runaway can occur due to failure in an electronic component which leads to sending a random large signal to the actuators causing the actuator to be deflected at its maximum rate to its maximum deflection. This kind of failure has been reported as the main reason for several aircraft crashes such as those of Flight 85 (B-747, Alaska, 2002) [15] (where the lower rudder runaway led to full left deflection and caused the excessive roll of the aircraft).

- *Actuator lock/stuck* can be caused by a mechanical jam due to lack of lubrication or being locked by ice for example. This type of failure led to flight incidents such as Flight 1080 (Lockheed L-1011, San Diego, 1977) [15], and flight 96 (DC-10, Ontario, 1972) [15].

Faults can be categorized based on their severity as well. In this study, we categorized faults into three major groups:

- *Abrupt Faults*: Abrupt faults can be defined as changes in parameter values, which are faster than the nominal dynamic process. Since tracking fast changes is a difficult process based on residuals, the ability to detect these abrupt changes is a great challenge for most of the fault detection algorithms [3]. Reference [16] considered the occurrence of three types of abrupt faults, severe vibrations, metal flakes separating, and short circuit.

- *Incipient Faults*: The problem with incipient faults is their small effects on the residuals, which could be hidden from the detection system. The sources of these

faults are sensor/actuator inaccuracy or partial failure.

- *Intermittent Fault*: This kind of fault is a malfunction that occurs at irregular intervals. This kind of fault, common in most systems, can be caused by various contributing factors, i.e., improper connection of electrical wires to the sensors, actuators, etc. The complexity of the system increases the chance of the occurrence of intermittent faults. Due to the inconsistent nature of the intermittent faults, their detection is a great challenge for most of the detection algorithms. Figure 1.2 presents a graphical description of abrupt, incipient, and intermittent faults in the system.

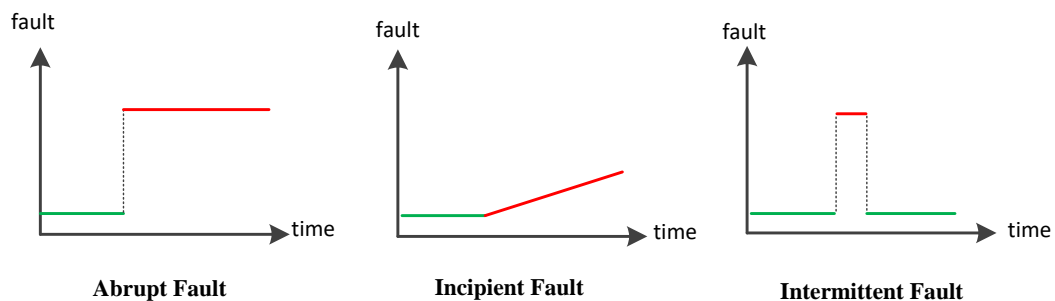


Figure 1.2: The graphical description of abrupt, incipient , and intermittent faults.

### 1.3 Definition of Fault-Tolerant Controller

To improve the safety and reliability of control systems against fault and failures, FTC approaches are introduced in recent decades. A control system that can automatically compensate for fault (and sometimes failures) effect in the system components while maintaining the system stability along with the desired level of overall performance is called an FTC system [13, 17–19]. Generally, based on the dependency on the fault information, FTC systems can be categorized into two main classes: passive FTC and active FTC. Passive FTC is an FTC system that does not

rely on faulty information to control the system and are closely related to robust control where a fixed controller is designed to be robust against a predefined fault in the system [4, 13]. In general, redundancy is integrated into the passive fault-tolerant control design to make them resilient against faults [18].

In contrast with passive FTC systems, active FTC systems perform based on the occurred fault in the system. In such control systems, a fault detection and isolation (FDI) unit is used to find the fault location and measure its size; then, a supervisory controller decides how to modify the control structure and parameters to compensate for the occurred fault in the system. Such modification can be varied from control reconfiguration [20, 21] to managing redundancies [22], and analytical redundancy [23–29]. Both active and passive approaches use different techniques for the same purpose, however, due to their difference in their design approach, each approach may result in some unique properties.

In the following, a brief illustration of the passive FTC, and active FTC are presented.

### **1.3.1 Passive FTC**

This subsection reviews the recent research works in the field of passive FTC theory. Passive FTC systems do not rely on the fault information, and their design is directly integrated with the concept of redundancy. The concept of hardware redundancy in passive FTC systems can be defined as the application of identical components with the same input signal so that the duplicated output signal can be compared with the main component to do fault detection using various methods such as majority voting and limits checking [3]. As can be seen in Fig. 1.3, in passive FTC design,

redundancy can be considered in the controller, actuators, plant components, and sensors that the FTC system can switch to them in the presence of a fault in the system.

Several approaches have been used in designing passive FTC varies from sliding mode control (SMC) approach [30–32] to  $H_\infty$  [33–35], Linear-Quadratic control [36], fuzzy logic control [37, 38], Lyapunov-based control [39], and control allocation [40–42]. Such control strategies are commonly less complicated and are popular due to their simplicity in design and application, less lag between fault occurrence and accommodation, and their low computation load [4, 18, 43].

The main challenges of passive FTC can be summarized as

- 1) The extreme dependency on hardware redundancy: despite the reliability of hardware redundancy, they are expensive, and increase the needed space and the weight of the product. It is obvious that the key components need redundancy to avoid breakdown, but applying redundancy for the whole system would be costly, and difficult to be applied considering the weight and space limits.
- 2) Passive FTC strategies rely on the assumption that the system will maintain its asymptotic stability of the closed-loop under specified fault/failure scenarios. However, this assumption may not be sufficient to prevent system break down in the presence of a large number and unforeseen faults.
- 3) Due to the fact that in passive FTC design the normal and fault/failure conditions should be considered simultaneously, in the performance aspect, they are more conservative compared to active FTC design. In other word, passive FTC systems focus on the robustness of the system considering all the scenarios rather than the optimal performance for each scenario, i.e., in order to guarantee the stability of the system in the presence of a fault, the settling time of the controller would be increased even in a normal situation.

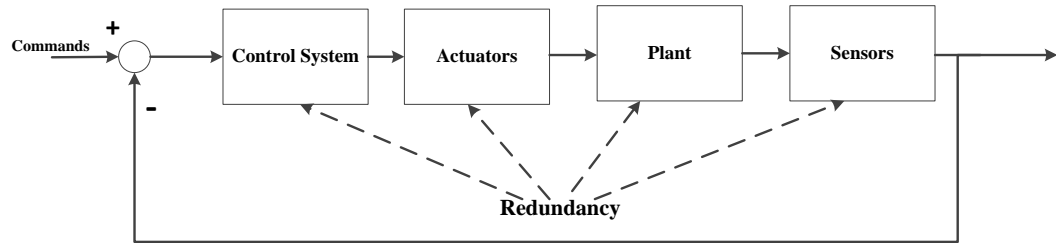


Figure 1.3: Passive FTC Structure: This kind of controller can be designed by considering redundant controller/actuator/plant/sensor and in the presence of fault will switch to the redundant component.

### 1.3.2 Active FTC

In contrast with passive FTC systems, active FTC systems react to each fault differently. This reaction is based on the control approach used in the active FTC design and information received from the detection system. Generally, active FTC design has three main steps: 1) Detection, 2) Supervision, 3) Control. Figure 1.4 shows the three main steps and their roles in designing active FTC systems.

Generally, in designing an efficient active FTC system, three major factor should be considered: First, the detection unit should be accurate. False fault alarm and inaccurate fault measurement have a direct impact on the performance of the active FTC system. This inaccuracy will lead to the wrong reaction to the fault and would even endanger the system stability. Second, the designed active FTC should be robust against the imperfect fault detection information. Third, the time spent for fault recovery should be less than the available time for recovery. In other words, the control-reconfiguration/fault-compensation should be fast enough to guarantee the system stability and performance.

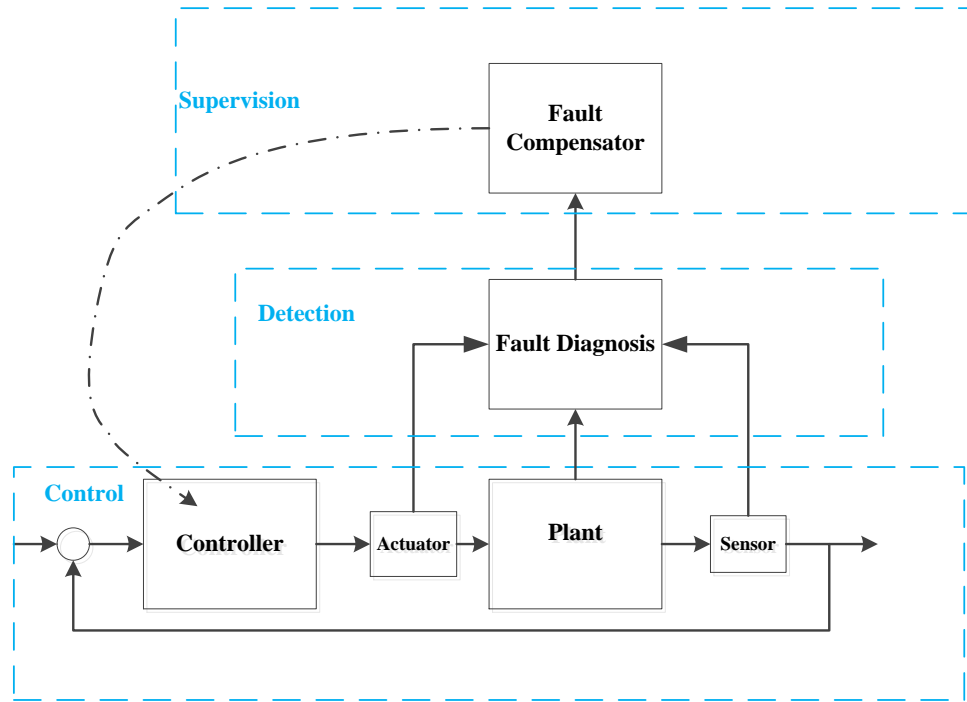


Figure 1.4: General Structure of active FTC systems.

## 1.4 Motivations, and Summary of Contributions

Fault tolerant control is one of the most attractive topics in the field of control theory which received a great deal of attention among researchers. The ongoing achievements in this field of control and the increasing need to develop a reliable control system which can tolerate faults and failure are the main reasons that motivated us to work in this field of control theory.

Although the valuable efforts have been made in the last decades to provide comprehensive FTC and FDI approaches, most of the works are only based on hardware-redundancy, while analytical redundancy which has received a great deal of attention in recent years has not been significantly investigated. In addition, most of the works investigated FDI and FTC separately and the link between active FTC and FDI to

obtain a united active FTC system was not technically investigated. These reasons motivated us to work on this topic. In this dissertation, the latest achievements in the field of fault tolerant control system are reviewed, and their advantages and disadvantages are investigated, then a novel FDI technique is introduced which can detect fault and failures in real time with relatively higher accuracy than conventional methods. This FDI technique consists of a model-based observer and an adaptive artificial neural network (ANN) in which its learning coefficients are updated by the extended Kalman filter (EKF). The combination of the model-based observer and ANN observer helped to reduce the uncertainties in the model-based observer and at the same time reduced the computation load on the ANN in comparison with the conventional ANN detection methods. We demonstrated that the application of EKF algorithm in tuning ANN weights helps to improve the ANN accuracy and reduces its response time. In the next step, we introduced a new active FTC based on our introduced FDI system. The proposed active FTC can detect and compensate for the occurred fault based on the information received from the FDI system. To the best of our knowledge, the problem of designing a united framework for FTC which uses FDI information has not been solved. The proposed active FTC system is evaluated through numerical simulations, and mathematical analysis. Based on the proposed active FTC method, new controllers for different complex systems are designed, e.g., unmanned aerial vehicle (UAV), load frequency control (LFC) system, and proton exchange membrane fuel cells (PEMFC) system, and their advantages are demonstrated.

## 1.5 Dissertation Road-map

The five main research themes of this dissertation can be described as follows:

✓ Introducing a novel neural adaptive observer-based sensor and actuator fault detection and isolation (FDI) in nonlinear systems.

✓ Active fault tolerant control (FTC) based on neural adaptive observer for nonlinear systems.

✓ Active FTC design for UAV.

✓ Active FTC Design for LFC system.

✓ Active FTC Design for PEMFC system.

Accordingly, this dissertation is structured as follows:

**Chapter 2** investigates the state of art FDI and FTC approaches. In this chapter, the advantages and disadvantages of the different FDI and FTC approaches are reviewed and solutions to improve their performance are suggested.

**Chapter 3** introduces the proposed FDI and active FTC design, and their design procedures are illustrated. Furthermore, the stability and efficiency of the proposed designs for the nonlinear affine systems are mathematically proven.

**Chapter 4** presents a new active FTC design for an UAV system based on the approach introduced in Chapter 3. The proposed design is implemented on nonlinear six-degree of freedom (six-DoF) model of an aircraft and the advantages of the

proposed design are demonstrated through numerical simulations.

**Chapter 5** proposes a new active FTC design for PEMFC system based on the methodology described in Chapter 3. The effectiveness of the proposed design is evaluated through numerical simulation.

**Chapter 6** introduces a new resilient control design for LFC system based on the results achieved in Chapter 3. The proposed design is evaluated through numerical simulation and the effectiveness of the proposed design against false data injection attacks is demonstrated.

**Chapter 7** concludes the dissertation outcomes and discusses the findings and implications for potential future research.

## CHAPTER 2

### LITERATURE REVIEW AND DESIGN FUNDAMENTALS

#### 2.1 Introduction

In the previous chapter, the definition of fault, failure, fault detection and isolation (FDI), and fault tolerant control (FTC) were discussed and the reasons for designing a reliable controller was investigated. As it was discussed in the previous chapter, the performance of the active FTC system relies on the accuracy of the FDI unit used in its design structure; thus, an accurate FDI design with capability of online fault detection and isolation is a must for the active FTC design. This chapter reviews the state of the art FDI and FTC techniques, and investigates their advantages and disadvantages. Furthermore, the solutions to improve their performances are suggested.

The rest of this chapter is organized as follows: in Section 2, FDI approaches are reviewed and classified based on their design methodology. Section 3 reviews the FTC approaches and classify them based on the methodology used in their design for fault accommodation.

#### 2.2 Fault Detection and Isolation

Although the terms “fault isolation” and “fault detection” are sometimes used synonymously, fault detection means determining that a problem has occurred, whereas fault isolation pinpoints the size and location of the fault [44].

The first step in designing FDI is to design an observer to estimate the system states and output. For simplicity, consider a linearized state-space model of a system as

follows

$$\begin{aligned}\dot{x}(t) &= Ax(t) + Bu(t) + f_a(t) + f_c(t) + d(t) \\ y(t) &= Cx(t) + f_s(t) + D(t)\end{aligned}\tag{2.1}$$

where  $x(t) \in R^n$  is the system states,  $u \in R^m$  is the control input,  $f_a \in R^{l_a}$ ,  $f_c \in R^{l_c}$ , and  $f_s \in R^{l_s}$  are actuator, component, and sensor faults, respectively.  $A \in R^{n \times n}$ ,  $B \in R^{n \times m}$ , and  $C \in R^{n \times m}$  are the matrices of the state-space system.  $d(t)$  and  $D(t)$  are unknown disturbances and uncertainties in the system states and the output. The observer for the system described in (2.1) can be defined as

$$\begin{aligned}\hat{\dot{x}}(t) &= A\hat{x}(t) + B\hat{u}(t) + He(t) \\ e(t) &= y(t) - C\hat{x}(t)\end{aligned}\tag{2.2}$$

where  $\hat{x}(t)$ , and  $\hat{u}(t)$  are the estimates of system states and control input, and  $H$  is the observer gain to be tuned by the designer to reduce the error or residual ( $e(t)$ ) in the system. In other words, the residual shows the inconsistency between the measured data and the expected data and is obtained through a recursive estimation process as follows

$$\text{New Prediction} = \text{Predication} + \text{Gain} \times \text{Residual}$$

This well-known framework is the generalized likelihood ratio approach that was introduced by Willsky and Jones [45] and have been used with different observer approaches for estimation of the system states and then fault detection. Based on this framework, a fault detection will be designed which alarms if the residuals exceed a predefined threshold. Figure 2.1 shows the general structure of the FDI system.

In this study, FDI approaches are classified based on the observer design in three main categories: model-based approaches, knowledge-based approaches, and combined model-knowledge based approaches. Figure 2.2 shows the classification of FDI

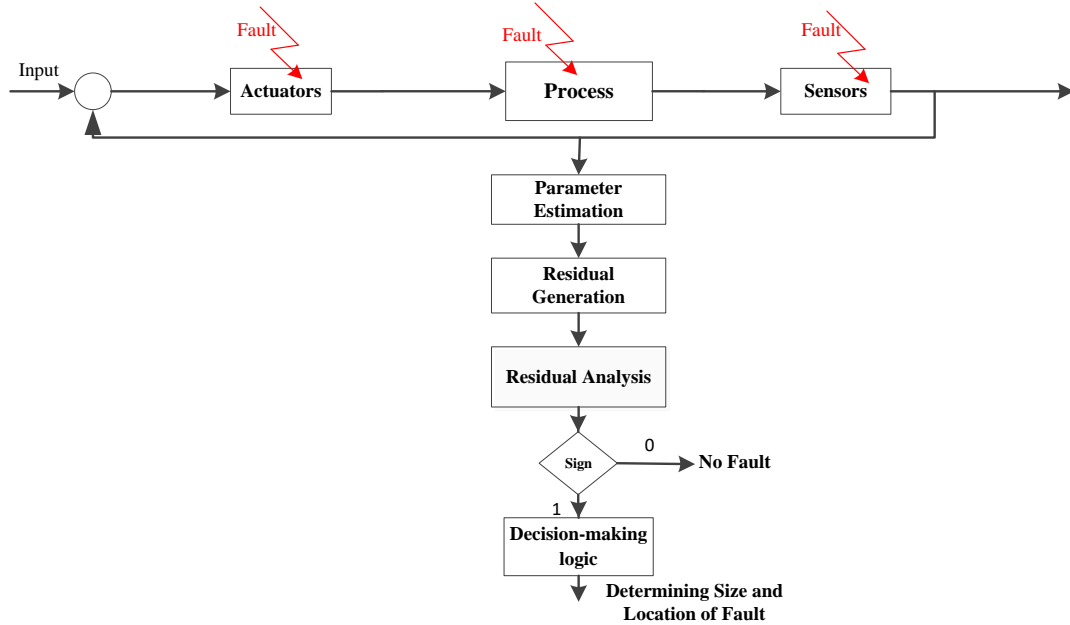


Figure 2.1: General structure of fault detection and isolation (FDI).

approaches based on the technique used in their design. It should be noted that the combined model-knowledge based approaches can be varied as any combination of the model-based and knowledge-based approaches.

### 2.2.1 Model based FDI

Model-based FDI is one of the oldest strategies in fault diagnosis which was introduced in 1971 [46]. Detailed investigation of model-based methods can be found in well-written books [47, 48] and survey papers [49–51]. In model-based techniques, the mathematical model of the operation system (plant) is required. This model can be obtained through physical approaches or system identification methods; then, an observer will be designed based on this model to estimate the system output and monitor the consistency between the estimated output and the practical system output. Fault can be detected and isolated by subtracting the system output from

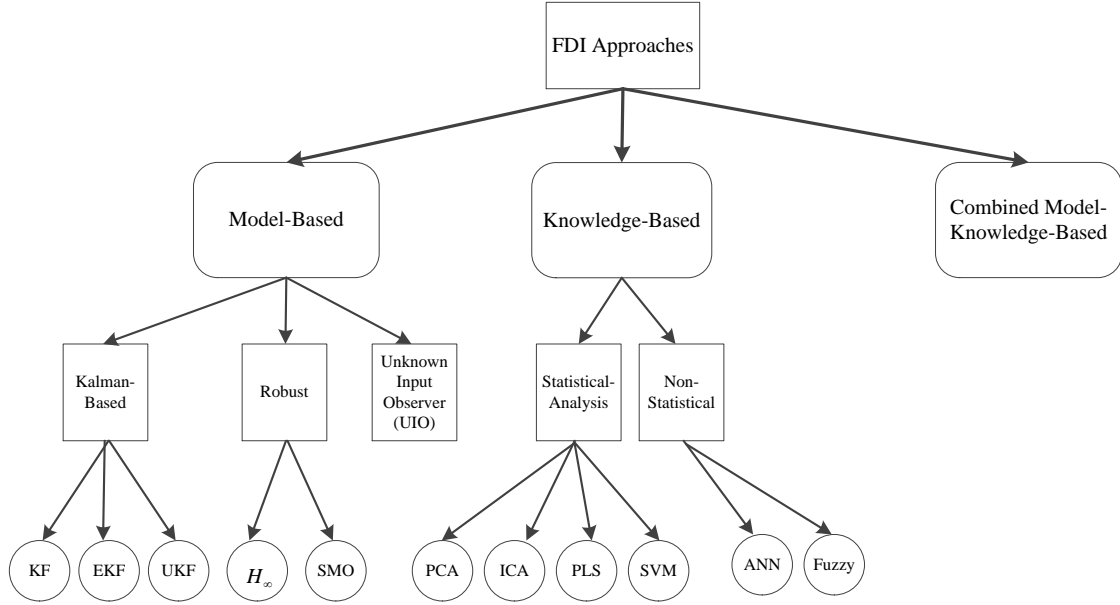


Figure 2.2: Classification of the FDI approaches based on their methodology. (The abbreviations: KF (Kalman Filter), EKF (Extended Kalman Filter), UKF (Unscented Kalman Filter), SMO (Sliding Mode Observer), PCA (Principal Component Analysis), ICA (Independent Component Analysis), PLS (Partial Least Square), SVM (Support Vector Machine), ANN (Artificial Neural Networks)

the predicted output. Different model-based approaches have been used to design the observer such as Kalman filter [52–57],  $H_\infty$  [58–62], and sliding mode observer (SMO) [63–65].

### 2.2.1.1 Kalman Filter-based

Kalman filter observers are efficient recursive filters which estimate internal states of the linear dynamic system from a series of noisy measurements based on minimization of the mean square variance of the estimation error. This minimization of error is based on the linear quadratic Gaussian (LQG) optimization problem. Mannandhar et al. used a Kalman filter to estimate the system states and then a  $\chi^2$  detector was used for fault alarm in the presence of a fault and false data injection attack in

the system [52]. Other statistical tools can also be used for alarming the system if a particular fault occurs, e.g., generalized likelihood [45], multiple hypothesis test [66], and cumulative sum algorithms [67]. Figure 2.3 shows the general structure of the Kalman filter observer in designing the FDI system.

Kalman filters are commonly used for linear systems, and it can obtain an unbiased

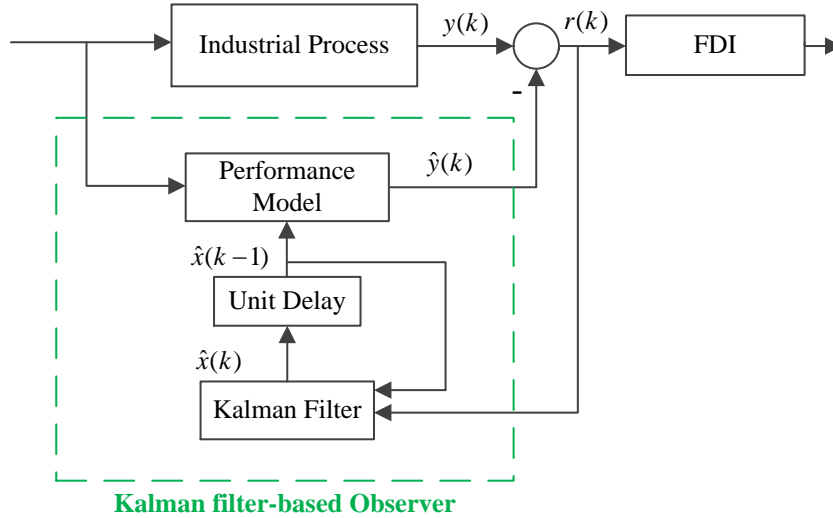


Figure 2.3: General structure of Kalman filter-based fault detection [1].

minimum estimation error variance if only the noise in their measurements satisfies the Gaussian assumption. To overcome these deficiencies of the Kalman filters, they have been modified, e.g., extended Kalman filter (EKF) [55, 56], unscented Kalman filter (UKF) [57], and Hybrid Kalman filter (HKF) [53].

One solution to apply Kalman filter to nonlinear system is to linearize the system around its state using Taylor expansion series and modify the filter to use this linearized version of the system as a model which is called EKF [68]. An adaptive two-stage EKF with covariance matrix adoption was designed to detect faults in an inertial measurement unit (IMU) sensors of an aircraft [55]. In [56], adaptive

EKF was used for FDI in a series of the battery pack to prevent overcharge and over-discharge. In their approach, the states of each battery cell were estimated using EKF, and they identified a fault in the system by comparison of the measured values with the estimated values.

However, the computation burden on EKF is heavier than the Kalman filter, and sometimes this linearization is not accurate which subsequently converges to the wrong solution. In order to tackle these deficiencies, instead of linearization of the nonlinear system, an alternative solution was introduced which is unscented transformation. The unscented transformation is a deterministic sampling technique that picks a minimal set of sample point (called sigma points) around the mean. Then, by propagation of the sigma points through the nonlinear functions, a new mean and covariance estimation will be formed which is called UKF [69]. In addition, UKF removes the need for direct calculation of Jacobian and obtains it through sigma points propagation without the need for analytical differentiation; this will reduce the computational burden for complex functions. However, similar to the EKF, this filter may become unstable in some highly nonlinear systems and converges to the wrong solution. In [57], UKF was used to detect faults in the reaction wheels of a spacecraft where particle swarm optimization was used off-line for tuning the initial parameters of the UKF. Pourbabae et al. introduced a multiple-model (MM) HKF approach for FDI which incorporates a nonlinear mathematical model of the system with a number of piecewise linear models [53].

### **2.2.1.2 Unknown Input Observers**

Unknown input observer (UIO) is a type of the Luenberger observer which is primarily used for state estimation in linear systems. The major advantage of this kind of observer is its ability in the complete decoupling of the estimated states from the

unknown inputs under certain conditions. The reason that this kind of observers is called UIO is the fact that the state estimation error is free from any unknown inputs [48].

Recently, standard UIO approaches have been developed to be applied to the nonlinear systems using linear parameter varying (LPV) process. These developments can be categorized in two aspects: 1) using linear matrix inequalities (LMI) technique to obtain required conditions of UIO observers for LPV systems [70–74], 2) integration with other robust control techniques to improve FDI performance [75]. For example, an  $H_\infty$  filter was integrated to UIO to detect a failure in inertial measurement unit (IMU) of a robot manipulator [75]. The  $H_\infty$  filtering helped to guarantee the boundedness of the estimation error against input noise.

### 2.2.1.3 Robust Fault Detection

In the FDI process, the residual signals should be robust to uncertainties while being sensitive to faults to have an accurate fault detection. To this aim, robust control techniques were combined with model-based observers to improve the robustness of the FDI. Among robust approaches,  $H_\infty$  and sliding mode have received a great deal of attention in designing robust FDI systems. In [58,60,62],  $H_\infty$  norm has been used to reflect the maximum influence of disturbances, and the residual generation in FDI process was formulated as the  $H_\infty$  optimization problem. In addition, the norms  $H_\infty$ ,  $H_-$ , and  $H_2$  can be used to measure the sensitivity of the residuals to fault occurrence, and then, between the sensitivity to fault and robustness to disturbance an optimization problem can be defined for the performance indices of  $H_\infty/H_\infty$ ,  $H_-/H_\infty$ , and  $H_2/H_\infty$ . Based on this theory, the FDI design can be converted to a multi-objective optimization problem [61,76,77].

It should be mentioned that the online implementation of the above optimization

problem depends on the complexity of its Riccati equation which has a direct relation to computation time. Recursive algorithms have been proposed to simplify the online implementation and reduced computational load. One of these recursive algorithms is Kerin space technique which is a special type of indefinite-matrix space and can share many properties with Hilbert space and at the same time preserving the required characteristics of the  $H_2$  and  $H_\infty$ . Particularly, for estimation problem (Kalman-like filters), it allows the application of recursive algorithms to solve  $H_2$  and  $H_\infty$  problems [78]. Due to these advantages, the Kerin space have been used broadly in designing optimal FDI based on different recursive algorithm [79–83]

The sliding mode observer (SMO) has been widely used for state estimation of uncertain and nonlinear systems in recent decades. This wide application is because of SMO robustness to uncertainties and its capability of reconstructing uncertainties based on the concept of the equivalent injection of the exogenous input [84]. In this concept, SMO observers estimate the system states and output based on an exogenous input which forces the estimation error to be converged to zero in finite time steps [65,84]. Walcott and Zak introduced one of the first Lyapunov-based SMO for dynamic systems with bounded disturbances [85] and developed to be applied to a more general class of nonlinear systems in [86,87]. Drakunov and Utkin introduced the first SMO observer based on the idea of equivalent control concept [88] which was later applied to a class of nonlinear system with triangular input form [89]. The sliding mode term was incorporated in high-gain observer (HGO) to design a robust nonlinear observer for a class of nonlinear Lipschitz system [90], where the unknown disturbances can be identified by sliding surfaces.

The implicit or explicit use of differentiation in the SMO process makes them relatively restricted to one degree. To tackle this restriction, the high order sliding

mode observers were introduced to remove the relative degree restriction and obtain a better FDI accuracy [84, 91–94]. The application of sliding mode observers have been widely investigated for linear time-invariant (LTI) systems, and the required conditions for SMO were defined as matching and minimum phase conditions [95]. However, satisfying these two conditions is difficult when it comes to FDI for linear discrete time-varying (LDTV) systems, hence, high order SMO came as a solution to relax these restrictions [84]. Based on these achievements, different SMO approaches have been modified for FDI in linear and nonlinear systems [93, 94].

The main advantage of the SMO observer is their strong robustness to bounded robustness. However, this strong robustness make them insensitive to incipient faults when they have small size during the initial phase; consequently, the system might be vulnerable to the incipient fault. To tackle this problem, in [96, 97], a Luenberger observer was integrated to SMO to improve its ability in the detection of an incipient fault in sensors. Incorporating adaptive thresholds in the residual analysis is another way to improve the performance of SMO [63].

Overall, the dependency of the model-based FDI approaches to the accuracy of the dynamic model can be considered as their main weakness, other than that, the summarized advantages and disadvantages of the model-based FDI techniques are presented in Table 2.1.

### **2.2.2 Knowledge-based Approaches**

On the contrary of model-based approaches which require a prior known model of the system, knowledge-based approaches are not dependent on the system model and require a large volume of historical data of the system performance. Various

Table 2.1: Summarizing the advantages and disadvantages of the model-based FDI approaches.

Approach	Advantage	Disadvantage
KF	Low computation load and guaranteed convergence for linear systems with noise	Cannot be applied to nonlinear systems or linear systems without Gaussian distribution
EKF	Can be applied to nonlinear system. Robustness against the unmodeled dynamics, model uncertainties, and disturbances.	Heavier computation load than KF, and can be only implemented on systems with Gaussian distribution. Errors related to the linearization of EKF may reduce the estimation accuracy or can even result in filter divergence.
UKF	Can be applied to nonlinear systems and lower computation load than EKF	Similar to EKF may be unstable to highly nonlinear system
UIO	Its ability in the complete decoupling of the estimated states from the unknown inputs under certain conditions	Cannot be applied to highly nonlinear systems
$H_\infty$	Being robust against uncertainties and disturbances	Vulnerable to incipient faults. Cannot be applied to highly nonlinear systems
SMO	Being robust against uncertainties and disturbances	Vulnerable to incipient fault

artificial intelligence methods have been applied for the detection of a fault in the current historical data set of the industrial systems. Figure 2.4 shows the overall block diagram of a knowledge-based FDI algorithm. Most of knowledge-based FDI approaches are formulated to solve the diagnostic problem as a pattern recognition problem. Therefore, the FDI problem can be solved either by using statistical or non-statistical techniques. Thus, we classified the knowledge-based FDI approaches to statistical-analysis-FDI and non-statistical-analysis-FDI.

### 2.2.2.1 Statistical-Analysis-FDI

In statistical FDI framework, most of the methods are based on the principal component analysis (PCA), Independent component analysis (ICA), partial least squares (PLS), statistical pattern classifiers, and support vector machine (SVM) algorithms. These algorithms require a large amount of historical data of the system performance

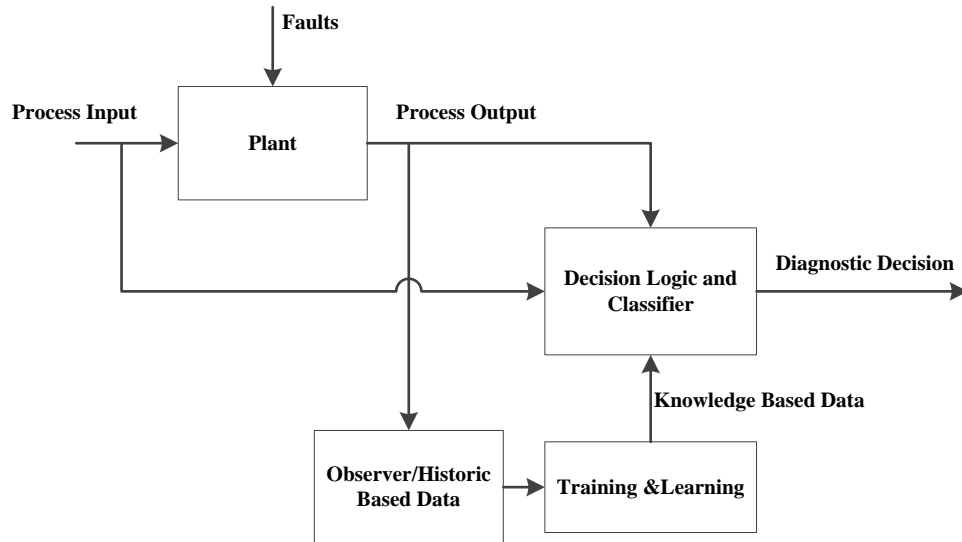


Figure 2.4: General structure of knowledge-based FDI approaches.

to be trained for FDI application.

PCA is one of the most popular monitoring technique, which is used to find factors with a much lower dimension than the original data set, hence the main variations in the original data set can be correctly noticed [98]. FDI design based on PCA methods have been successfully applied to complex systems, e.g., diagnosing faults in diesel engines [99], rolling bearing [100], electrical power drive [101], and power inverters [102]. However, the fact that PCA can be only applied to Gaussian distribution data limits their application for application in non-Gaussian distribution.

PLS is another statistical tool for FDI in industrial systems. Recent achievements in the implementation PLS-based FDI can be found on [103–107]. In [103], dynamic PLS algorithm was used for dynamic modeling which was able to capture

dynamic correlation between the measurement block and the quality data block; then, for FDI purpose, a total PLS (T-PLS) was introduced to further decomposition of the obtained PLS structure. The proposed T-PLS method was able to detect quality-related anomalies in the system process. Ding et al. introduced an improved PLS-based FDI scheme based on the key performance indicator [104]. In comparison with standard PLS, their approach significantly reduced the computation load. An FDI based on a combination of PLS method and pseudo-sample projection for the complex nonlinear system was presented in [105]. Further investigation to improve PLS-based FDI method were presented in [106, 107].

In statistical-based approaches, ICA has a key role in real-time monitoring due to its ability to not restricting latent variables in following a Gaussian distribution. In [108], a kernel-ICA-based FDI was introduced for non-Gaussian nonlinear systems. ICA has been successfully implemented for designing FDI in industrial processes, e.g., rolling-element bearing [109], induction motor [110]. Recently, an FDI design based on a combination of ICA and PCA was introduced in [111]. In their approach, because PCA cannot deal with non-Gaussian process, ICA was used for monitoring the non-Gaussian part of the process, and PCA was used for monitoring the Gaussian part. Then, a Bayesian network classifier was used to detect the fault in the system.

Among statistical-based FDI techniques, SVM is relatively new and due to its ability to work with large and low input features, has the potential to achieve more generalization. Another advantage of the SVM is its ability with working with both Gaussian distribution and non-Gaussian distribution data. In [112], most of the SVM schemes in designing FDI dated to 2006 were reviewed. Recent studies of

the SVM-based FDI can be found in [113–118]. In [113], an SVM-based FDI was developed by integrating of a kernel function with cross-validation. They showed that their proposed FDI algorithm has more accuracy than conventional PLS algorithms. In [114], a genetic algorithm was used to tune the SVM parameters to improve the FDI performance. Yi and Etemadi introduced an FDI design for a photovoltaic system based on multi-resolution signal decomposition and two-stage SVM [115]. In their design, the multi-resolution signal decomposition algorithm was used for feature extraction, and the two-stage SVM was used for decision making. Various applications of the SVM for FDI design have been investigated, e.g., wireless network sensor [116], ultrasonic flow meters [117], and ship propulsion system [118].

#### **2.2.2.2 Non-Statistical-Analysis-FDI**

Artificial neural network (ANN) is a powerful tool for the approximation of nonlinear systems and adaptive learning. Due to this ability, the ANN is the most popular non-statistical data-driven tool for designing FDI systems. Based on the learning strategy, the ANN can be classified into supervised FDI and unsupervised FDI. The unsupervised learning ANN uses the historical data to obtain the knowledge of emulating of the normal behavior of the system, which will be used to compare with the behavior of the real-time process to check if any deviation from the expected behavior occurs or not. The supervised learning ANN has the knowledge of the normal condition and faulty condition which will be used for FDI in a real-time process. ANN-based FDI have been applied for various application, e.g., combustion engine [119], railway track circuits [120], wind turbine drive-train [121], and microgrid system [122, 123].

Fuzzy logic (FL) is another non-statistic approach which can be used for FDI. In FL-based FDI, space features are partitioned into fuzzy sets, and then, fuzzy rules are designed based on the human reasoning to analyze the system behavior. Figure 2.5 shows the overall block diagram of an FL based FDI system.

The FL has been successfully implemented for designing the FDI system. For example, in [124], an FL-based FDI design is introduced for the detection of intermittent loss of firing pulses in the inverter power switches pulse-width modulation voltage source inverter (PWM-VSI). In this design, the fault modes of the current analysis of the PWM-VSI were used to extract fuzzy approximation model. Among various FL approximation models, the Takagi-Sugeno (T-S) is the most efficient method which received a great deal of attention [125–128]. Particularly, in [125–127], a T-S dynamic modeling technique was used to design the FDI system for general nonlinear processes. To this end, a universal T-S fuzzy observer-based residual generator was created by using fuzzy Lyapunov functions, then, it was integrated to an embedded dynamic threshold to be applied for real-time FDI in an industrial process. Luo et al. introduced a T-S approach for FDI in a class of network fuzzy systems with multiplicative noises on measurement and states [128]. In their design, the T-S FL FDI was constructed to generate the residual signal, and an adjustable threshold was defined for efficient detection of the fault.

The summarized advantages and disadvantages of the reviewed knowledge-based FDI strategies are presented in Table 2.2.

### **2.2.3 Combined Model-Knowledge based Approach**

Model-based and knowledge-based approaches have their distinguished advantages and various restrictions. Particularly, model-based FDI approaches can diagnose

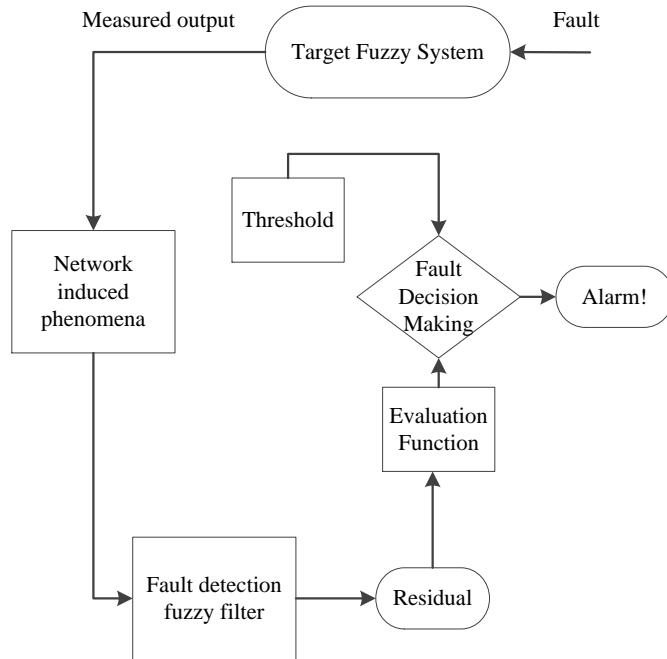


Figure 2.5: Fuzzy Logic (FL) based fault detection and isolation (FDI).

the fault with the minimum computation load which makes them suitable for the real-time application. However, the accuracy of the detection depends on the accuracy of the mathematical model of the system. On the other hand, knowledge-based approaches are not dependent on the system model which make them suitable for complex industrial systems that their models are unavailable or difficult to obtain. However, knowledge-based approaches need a large amount of data for training and suffer from the high computational load, and they may not be able to detect undefined fault types. To leverage the advantages of these two types of FDI approaches and reduce their inaccuracy and computational load, a combination of these two methods was suggested. Talebi et al. introduced an integrated recurrent ANN and nonlinear observer to design an FDI system for sensor and actuator faults in a satellite [129]. The general structure of a combination of the model-based and

Table 2.2: Summarizing the advantages and disadvantages of the Knowledge-based FDI approaches.

Approach	Advantage	Disadvantage
PCA	reducing the dimensionality of data, while keeping as much variation as possible	can be only applied to Gaussian distribution data
ICA	Can be applied to non-Gaussian distribution	The historical data must be statistically independent and must have non-Gaussian distributions
SVM	Ability with working with both of Gaussian distribution and non-Gaussian distribution	dependency to the kernel selection
ANN	Ability with working with both of Gaussian distribution and non-Gaussian distribution	Need of huge historical data of the system performance
Fuzzy	Being robust against uncertainties and disturbances. This observer is only sensitive to the fault signal, and other parameter variations and uncertainties cannot deteriorate the FD performance	Vulnerable to the incipient fault. Obtaining the fuzzy if-then rules needs extensive expert knowledge of the system.

ANN-based FDI strategy is presented in Fig.2.6.

A combination of the SVM and model-based observer were introduced to design

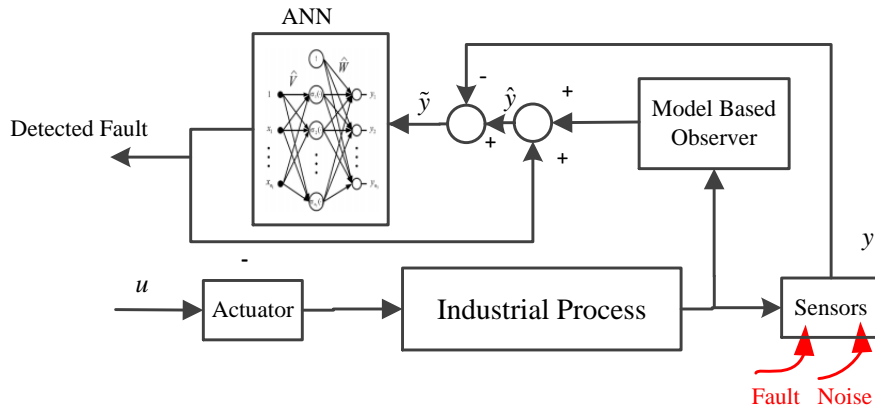


Figure 2.6: General structure of the combined ANN and model-based approach.

FDI for chemical reactors by Sheibat et al. [130]. They found out using the only

SVM for FDI would have difficulty to detect faults due to the highly nonlinear behavior of the system and transitional dynamics. Thus, they used a model-based observer based on a simplified initial model and the SVM was used to correct the uncertainties and nonlinearities of the system behavior. Their proposed approach showed effectiveness in detection and isolation of the faults. Based on the design procedure and criteria, different combinations of model and knowledge-based approaches can be applied to achieve an effective FDI, e.g., PLS and inverse dynamic model observer [131], and hidden Markov model-based and ICA approach [132].

### **2.3 Active Fault Tolerant Control**

Fault tolerant control (FTC) techniques can be divided into two main categories: active and passive [133, 134]. Active FTC uses detection techniques to find the fault, then, a supervisory system will decide how to modify the control structure and parameters to compensate for the effect of the faults in the system [18]. But, in passive FTC, a robust compensator is used to reduce the fault effects in the system or at least stabilize the system in the presence of fault in the system.

Passive fault tolerant controllers have been used widely in the literature due to their simplicity, low computation load, and robustness in small failures [31, 34, 35, 38, 135]. Various approaches have been used in designing passive FTC systems, from sliding mode control approaches [31] to fuzzy control [38] and  $H_\infty$  approaches [34, 35]. Despite the advantages of passive FTC techniques, they suffer from several limitations [136]. First, they commonly employ hardware redundancy which increases the cost and weight of the aircraft. Second, the controller design is based on conservative principles that limit the agility of the controller, i.e., in order to keep the system stable in the presence of a fault, the settling time of the controller would be increased.

Third, passive FTCs are designed to tolerate small fault while they might be vulnerable in the presence of sudden and severe faults in the system. For these reasons, active FTC system received a great attention among the researchers [30, 137–144].

Active FTC approaches are mainly categorized based on the FDI unit used in their design. However, the strategy used for the compensation of fault might be different. Here, a brief review of different fault compensation approaches used in active FTC design is presented.

### **2.3.1 Switching-Based Active FTC**

This kind of the controller relies on a set of predefined candidate controllers and the system switches among them based on the fault type and severity. Figure 2.7 shows the overall block diagram of a switching-based active FTC system. An important factor in designing a switching based controller is the dwell time [145]. The dwell time is the lower band on the length of the time interval between the consecutive switching instances. It should be noted that the upper-bound is the detection interval (DI) which is the length of time which the controller performance does not change after the fault occurrence. Allerhand and Shaked introduced an active FTC technique considering the dowering time among switches which guarantees the stability of the system by solving linear matrix inequalities [146]. In [147], a switching-based controller without any extra models or filters is developed. In their design approach, the bounds of the state were guaranteed during the switching delays.

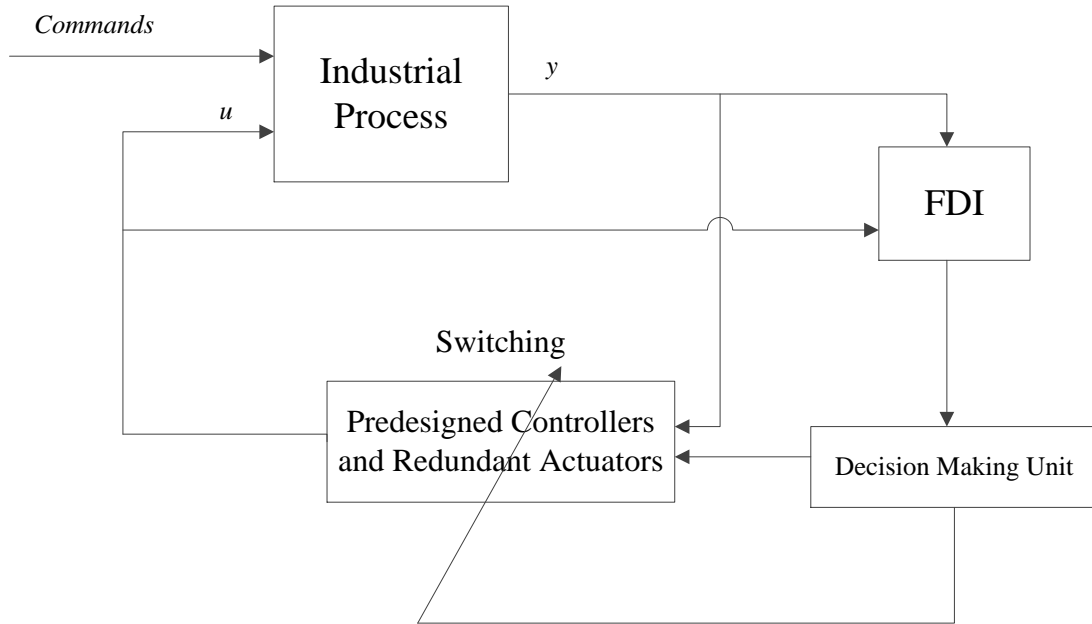


Figure 2.7: The general structure of the Switching-based active FTC system.

### 2.3.2 Hierarchical Structure Active FTC

Hierarchical structures are applied in the integration of FDI and FTC in active FTC systems. In this strategy, after detection and isolation of the fault in the system, the controller can be reconfigured either by adaptive control strategies [148,149], or receding horizon control [150].

### 2.3.3 Safe Parking Active FTC

The concept of “safe parking” was firstly introduced by Gandhi and Mhaskar [151]. This concept is based on the idea of maintaining the system at a proper temporary equilibrium (safe parking) point in the presence of fault until the active controller pushes the states of the system to a nominal equilibrium point. Later, this work was

further developed to choose a “safe parking” point using the FDI information [152]. Similarly, Paolo and Lafotune used this concept to propose a “safe controllability” method [153].

### 2.3.4 Analytical Feedback Compensation Active FTC

Analytical feedback compensation strategies are based on the real-time fault detection and isolation. These approaches need very accurate FDI information with minimum delay. The overall structure of the analytical feedback compensation method for active FTC design is depicted on Fig. 2.8.

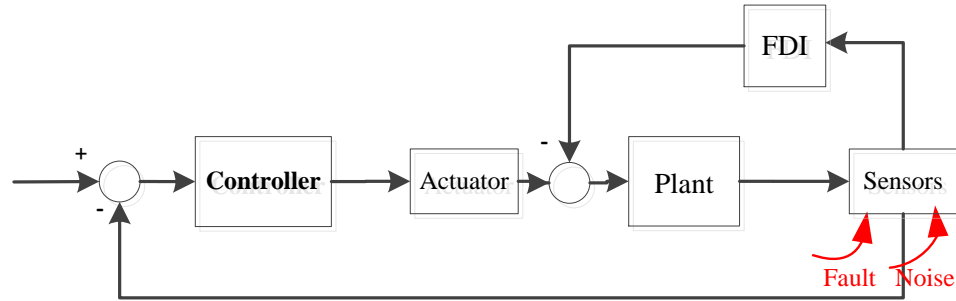


Figure 2.8: The general structure of the analytical feedback compensation active FTC system.

In [154], an online recursive identification method was used for FDI and was integrated to a PID controller through a feedback signal to compensate the fault in the system analytically. An active FTC system for a multi-agent leader-following system based on wavelet neural network (WNN) was designed [155]. In their work, a robust leader-follower controller based on graph theory was designed for the multi-agent system, then, the WNN-based FDI was used to compensate for the fault in the actuators through a feedback structure.

In [156], an integral-type robust sliding mode controller was designed based on

the feedback data from the iterative learning FDI unit which could map analytical redundancy in an optimal manner.

### **2.3.5 Hybrid FTC**

Hybrid FTC systems are introduced to leverage the advantages of passive and active FTC at the same time [140]. Based on this idea, the passive controller is used as a safe controller until a reliable controller based on the information received from FDI unit is achieved. Based on this concept, the controller has more amount of time to obtain accurate fault information, and optimal control reconfiguration can be performed without the concerns about system safety.

### 3.1 Introduction

Active fault tolerant control (FTC) techniques perform based on the received data from the fault detection and isolate (FDI) unit. These controllers have advantages over the passive FTC due to their intelligent reaction to faults, which leads to minimizing the effect on the faultless part of the control system.

In this chapter, we introduced a novel active FTC system design for nonlinear affine systems which can detect the fault and compensate for its effect without the need of control reconfiguration. The proposed active FTC design consists of a new ANN-based FDI system, a feedback linearization controller, and a new feedback structure which compensates the occurred fault based on the information received from the FDI system. The proposed FDI system uses an extended Kalman Filter (EKF) algorithm to update ANN weights to improve the accuracy and response time of the ANN-based fault detection system. The convergence of the update process of the ANN using EKF and the stability of the proposed FDI system is mathematically proven using the nonlinear Lyapunov functions. Based on the proposed FDI system, a novel active FTC design is introduced in the next step, and its mathematical stability is demonstrated using the nonlinear Lyapunov functions. To the best of our knowledge, the problem of designing a united framework for FTC which uses FDI information has not been solved before this study. The main contributions of this work can be summarized as 1) a new FDI design for nonlinear affine system is introduced, 2) a novel nonlinear active FTC design for nonlinear affine systems is developed, 3) the proposed design helps to detect and isolate abrupt faults without the need of control reconfiguration which is a challenge for other FTC designs.

The rest of this chapter is organized as follows. Section 2 provides the design procedure and the stability proof of the proposed FDI system, while Sections 3 and 4 illustrate the FDI design for actuators and sensors, respectively. In Section 5 the proposed FTC design is presented, and its mathematical stability is investigated.

## 3.2 Proposed FDI Method

In this section, our proposed strategy for FDI in general nonlinear systems is illustrated. The proposed strategy is a combination of the model-based and knowledge-based approaches to leverage the advantages of both types of strategies.

Consider a nonlinear system described by

$$\begin{aligned}\dot{x}(t) &= f(x(t)) + g(x(t))u(t) + D(x, t) + f_a(x, t) \\ y(t) &= h(x(t)) + f_s(x, t)\end{aligned}\tag{3.1}$$

where  $u(t) \in R^m$  is the input vector,  $y(t) \in R^r$  is the output vector,  $x(t) \in R^n$  is the state vector,  $f : R^n \rightarrow R^n$  is the state function,  $g : R^n \rightarrow R^{n \times m}$  is the input function,  $D \in R^n$  is the system's uncertainties and disturbances,  $h : R^n \rightarrow R^r$  is the output function, and  $f_s(x, t)$  and  $f_a(x, t)$  are the sensor fault and actuator fault vectors, respectively, whose elements describe the faults in the system. Due to the fact that nonlinear models have some level of uncertainty, using only a nonlinear model-based observer cannot accurately determine the faults in Equation (3.1); thus, an extra term is needed to find the  $f_s(x, t)$  and  $f_a(x, t)$ . In this dissertation, a neural network adaptive structure (NNAS) is used to detect the faults in sensors and actuators. The nonlinear model-based observer provides the expected output, while the NNAS detects and identifies the fault using the actual output and the expected output. In order to have a stable NNAS, several assumptions are considered :

**Assumption 1:** All of the state variables in  $x(t)$  are measurable.

**Assumption 2:** An upper bound for the plant uncertainties  $D(x, t)$  is assumed ( $\|D(x, t)\| \leq \chi_{max}$ ). This assumption can be achieved by using a nonlinear model with a sufficient level of accuracy.

**Assumption 3:** The state function  $f(x(t))$  can be differentiated at  $\hat{x}(t)$

$$A(t) = \left. \frac{\partial f(x(t))}{\partial x(t)} \right|_{x(t)=\hat{x}(t)}$$

where  $A(t)$  is an  $n \times n$  matrix.

The Taylor series expansion of  $f(x(t))$  at  $\hat{x}(t)$  can be represented as

$$f(x(t)) - f(\hat{x}(t)) = A(t)\tilde{x}(t) + \Theta(\hat{x}(t), x(t))$$

where  $\Theta(\hat{x}(t), x(t)) = o(\|\tilde{x}(t)\|^2)$  contains the higher order terms of the state estimation error. Here,  $\tilde{x}(t) = x(t) - \hat{x}(t)$ .

**Assumption 4:** The control input function  $g(x(t))$  and  $\Theta(x(t), \hat{x}(t))$  satisfy the Lipschitz condition, i.e.,

$$\begin{aligned} \|g(x(t)) - g(\hat{x}(t))\| &\leq L_g \|\tilde{x}(t)\| \\ \|\Theta(\hat{x}(t), x(t))\| &\leq L_\Theta \|\tilde{x}(t)\| \end{aligned}$$

with the Lipschitz constants  $L_g$  and  $L_\Theta$ , respectively. Here, we assume the detection system is accurate and the detection error is bounded by  $L_g$  and  $L_\Theta$ . The validity of this assumption will be proven in the following subsection.

**Assumption 5:** The control input vector of the system is bounded by  $L_u$  and the fault,  $F(t)$ , is bounded by  $L_F$ , i.e.,

$$\begin{aligned} \|u(t)\| &\leq L_u \\ \|F(t)\| &\leq L_F \end{aligned}$$

Here, the actuation output and the occurred fault are considered to be bounded.

With the above assumptions, NNAS stability can be guaranteed, and its proof is discussed in the following.

### 3.2.1 NNAS

The proposed FDI technique is a neural network (NN)-based detection design in which its learning weights are updated online through the EKF algorithm. This FDI strategy is adopted due to its accurate and fast detection ability. In the following, the proposed NNAS is presented.

Faults in a system may be nonlinear and unpredictable; hence, ANN can be a suitable candidate for their estimation. Unlike the direct ANN modeling procedures that uses an ANN to simulate the system behavior [157, 158], the NNAS detects faults based on the output of the nonlinear observer

$$\begin{aligned}\dot{\hat{x}} &= f(\hat{x}(t)) + g(\hat{x}(t))u(t) + M_i(t) \\ \hat{y} &= h(\hat{x}(t))\end{aligned}\tag{3.2}$$

where  $\hat{x}(t)$  is the state vector of the nonlinear observer and  $M(t)$  is the neural network observer that defined as [159]:

$$M_i(t) = W_i(t)\sigma(V_i(t)\delta_i(t))\tag{3.3}$$

where  $M_i(t)$  is the  $i$ th vector of  $M(t)$  for  $i = 1, \dots, n$ .  $W_i(t)$  and  $V_i(t) = [V_{i,1}(t), \dots, V_{i,m+n}(t)]$  are the weights associate with the  $i$ th output of the NNAS at time  $t$ . Here,  $\delta_i(t)$  can be defined as  $\delta_i(t) = [M_i(t - \tau), \dots, M_i(t - m\tau), e_i(t - \tau), \dots, e_i(t - n\tau)]^T$ . Here,  $\tau$  indicates the sampling period or the step size of the observer;  $e_i(t) = y_i(t) - \hat{y}_i(t)$ , and  $\sigma(\cdot)$  is a *tanh* activation function which is selected due to its gradient strength.

$$\sigma(x) = (1 - e^{-x})/(1 + e^{-x})\tag{3.4}$$

In terms of the  $i$ th element  $M_i(t)$  of  $M(t)$  for  $i=1,\dots,n$ , the NN observer can be represented as

$$M_i(t) = W_i(t)\sigma(Z_i(t)) \quad (3.5)$$

where

$$Z_i(t) = \sum_{j=1}^m V_{i,j}(t)M_i(t - j\tau) + \sum_{j=1}^n V_{i,m+j}(t)e_i(t - j\tau) \quad (3.6)$$

The input of the observer  $M(t)$  is recursively updated with the previous  $m$  samples of the observer inputs for  $j = 1, 2, \dots, m$ , and also previous  $n$  samples of the system output error  $e_i(t - j\tau)$  for  $j = 1, 2, \dots, n$ . Here,  $m$  and  $n$  are chosen based on the needed accuracy and training time in the system. Large values of  $m$  and  $n$  guaranty the convergence of the training and the accuracy of the ANN; however, large values of them may increase the computation time and add unnecessary delays by increasing the training duration [159]. Thus, to have a real-time and accurate fault detection,  $m$  and  $n$  should be chosen based on the needed accuracy and the system bandwidth.

Subtracting the observer Equation (3.2) from the nonlinear system Equation (3.1), the error of the state estimation for the actuator can be obtained as follows:

$$\dot{\tilde{x}}(t) = A(t)\tilde{x}(t) + \Theta(\hat{x}, x) + (g(x) - g(\hat{x}))u(t) + f_a(x, t) - M(t) + D(x, t) \quad (3.7)$$

According to Assumption 3,  $A(t)$  is an  $n \times n$  matrix defined as  $A(t) = \frac{\partial f}{\partial x}|_{x=\hat{x}}$ , and  $f(x) - f(\hat{x}) = A(x)\tilde{x}(t) + \Theta(\hat{x}, x)$ .

Likewise, the error of the estimation for the sensor can be obtained by the following formula

$$\tilde{y} = y(t) - \hat{y} = h(x(t)) - h(\hat{x}(t)) + f_s(x, t) - M(t) \quad (3.8)$$

### 3.2.2 Neural network weight update law

In order to achieve real-time performance, the NN weights should be tuned effectively [160]. In this study, an adaptive tuning algorithm based on EKF is introduced. The EKF helps to update the NN weighting parameters online, so that fast convergence rate of the NN learning will be guaranteed. Through the updating process, if we consider the  $i$ th element of NNAS, then the EKF updating parameter can be described by [159]:

$$\theta_i(k) = [W_i(k), V_{i,1}(k), \dots, V_{i,m+n}(k)]^T \quad (3.9)$$

where  $k$  is the  $k$ th sampling instant, and  $t = k\tau$ . The parameters will be calculated in each sampling time with the following rules [159].

$$\begin{aligned} \theta_i(k) &= \theta_i(k-1) + \eta_i K_i(k) [y_i(k) - \hat{y}_i(k)] \\ K_i(k) &= P_i(k) H_i(k) [H_i(k)^T P_i(k) H_i(k) + R_i(k)]^{-1} \\ P_i(k+1) &= P_i(k) - K_i(k) H_i(k)^T P_i(k) \end{aligned} \quad (3.10)$$

where  $\eta_i$  is the learning coefficient,  $P_i(k)$  is the covariance matrix of the state estimation error,  $K_i(k)$  is the Kalman gain, and  $R_i(k)$  is the covariance matrix of the estimated noise, which is computed recursively by [161]:

$$R_i(k) = R_i(k-1) + [e_i^T(k) e_i(k) - R_i(k-1)] / k \quad (3.11)$$

Here,  $H_i(k)$  is the derivative of  $e_i(k)$  with respect to  $\theta_i(k)$ . Based on the observer input in Equation (3.5),  $H_i(k)$  can be calculated as follow:

$$\begin{aligned} H_i(k) &= \frac{\partial e_i(k)}{\partial \theta_i} \Big|_{\theta_i = \theta_i(k-1)} \\ &= \begin{cases} \sigma(Z_i(k)), & \theta_i = W_i \\ W_i(k) M_i(k-j) \sigma(Z_i(k)), & \theta_i = V_{i,j} \\ W_i(k) e_i(k-j) \sigma(Z_i(k)), & \theta_i = V_{i,m+j} \end{cases} \end{aligned} \quad (3.12)$$

Figure 3.1 shows the overall structure of the proposed NNAS method.

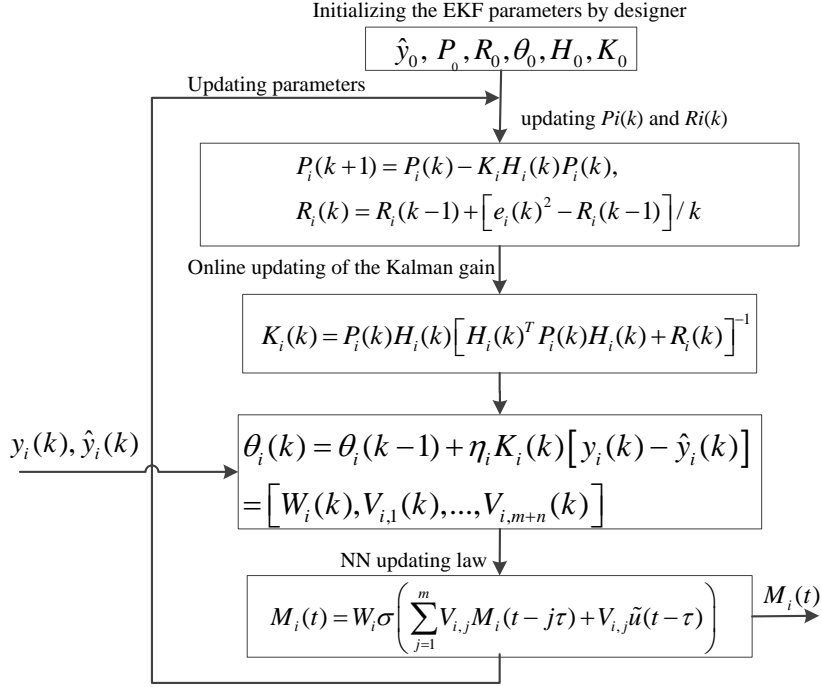


Figure 3.1: Block diagram of the updating process of the ANN with the EKF.

### 3.2.3 Stability Analysis of ANN Updating Based on EKF

In order to guarantee the convergence and stability of the EKF law for updating NNAS, the following assumption is made.

**Assumption 6:** For single input, single output (SISO) systems, the noise estimated variance,  $R_i(k)$ , satisfies the following condition

$$0 < R_i(k) \ll H_i(k)^T P_i(k) H_i(k) \quad (3.13)$$

**Theorem 2.1:** The EKF algorithm can update the NNAS parameters described in Equation (3.5) if the learning coefficient satisfies the following rule

$$0 < \eta_i < 2 + \frac{2R_i(k)}{\|H_i(k)\| \lambda_{max}(P_i(k))} \quad (3.14)$$

then, the updating process is convergent.

**Proof:** According to the assumption, if (3.14) is satisfied, then

$$0 < \eta_i < 2 + \frac{2R_i}{H_i^T P_i H_i} = 2 \frac{H_i^T P_i H_i + R_i}{H_i^T P_i H_i} \quad (3.15)$$

Therefore,

$$0 < \eta_i H_i^T P_i H_i [H_i^T P_i H_i + R_i]^{-1} < 2 \quad (3.16)$$

By defining  $K_i(k) = P_i H_i [H_i^T P_i H_i + R_i]^{-1}$ , we have:

$$0 < \eta_i H_i(k)^T K_i(k) < 2 \quad (3.17)$$

The Lyapunov function considered is

$$V(k) = \frac{1}{2} e_i(k)^2 \quad (3.18)$$

while the difference of  $V(k)$  can be obtained as

$$\Delta V(k) = V(k+1) - V(k) = \Delta e_i(k) \left( e_i(k) + \frac{1}{2} \Delta e_i(k) \right) \quad (3.19)$$

where the error difference,  $\Delta e_i(k)$ , is approximated by

$$\Delta e_i(k) = - \left( \frac{\partial e_i(k)}{\partial \theta_i(k)} \right)^T \Delta \theta_i(k) = -\eta_i H_i(k)^T K_i(k) e_i(k) \quad (3.20)$$

So,  $\Delta V(k)$  is equal to

$$\Delta V(k) = \Delta e_i(k) \left( e_i(k) + \frac{1}{2} \Delta e_i(k) \right) = -\eta_i H_i(k)^T K_i(k) \left( 1 - \frac{1}{2} \eta_i H_i(k)^T K_i(k) \right) e_i(k)^2 \quad (3.21)$$

If the condition in (3.15) is satisfied, then according to Equations (3.17) and (3.20),  $\Delta V(k) < 0$ . Hence, the updating operation will be convergent.

**Remark 2.1:** In order to guarantee the condition in the assumption, it is common practice to choose a large identity matrix for the initial value of  $P_i(k)$ , so it can be assured that  $R_i(k) \ll H_i(k)^T P_i(k) H_i(k)$ .

### 3.2.4 The Overall Stability of The NNAS

The stability of the NNAS input,  $M_i(t)$ , is investigated next. The value of  $M_i(t)$  is updated at each sample time and defined by

$$M_i(k+1) = W_i \sigma \left( \sum_{j=1}^m V_{i,j} M_i(k-j+1) + B_i(k) \right) \quad (3.22)$$

where  $B_i(k) = \sum_{j=1}^n V_{i,m+j} e_i(k-j+1)$  is the bias. By defining  $z(k)$  as  $z(k) = [z_1(k), \dots, z_m(k)]^T$ , where  $z_j(k) = M_i(k-j+1)$ , for  $j = 1, \dots, m$ , a new state vector of the observer input will be obtained. Then, the NNAS input can be written as:

$$z_m(k+1) = W_i \sigma \left( \sum_{j=1}^m V_{i,j} z_j(k) + B_i(k) \right) \quad (3.23)$$

The stability of  $z_m(k)$  is clear because  $z_j(k)$  is bounded, i.e.,  $(z_j(k) \leq \pm W)$ , due to the bounded nature of  $\sigma(\bullet)$ . Consider the equilibrium point of Equation (3.23) as  $z^* = [z_1^*, \dots, z_m^*]$ . Based on the recursive property of the state  $z$ , and the fact that at the equilibrium point  $z(k+1) = z(k) = z^*$ , the equilibrium point of the state equation can be represented as

$$z_m^* = W_i \sigma \left( \sum_{j=1}^m V_{i,j} z_j^* + B_i(k) \right) \quad (3.24)$$

where  $z_1^* = z_2^* = \dots = z_m^*$ .

The stability of the equilibrium point of (3.23) can be proved by the following theorem.

**Theorem 2.2:** If the absolute value of  $W_i \Delta \sum_{j=1}^m V_{i,j}$  is less than one, then the equilibrium point  $z^*$  in (3.24) is asymptotically stable, where  $\Delta$  is described by

$$\Delta = \frac{1}{2} \left[ 1 - \sigma^2 \left( \sum_{j=1}^m V_{i,j} z_p^* + B_i(k) \right) \right] \quad (3.25)$$

**Proof:**  $z_m(k+1)$  can be approximated around the equilibrium point  $z_m^*$  by Taylor series expansion as

$$\begin{aligned} z_m(k+1) &= W_i \sigma \left( \sum_{j=1}^m V_{i,j} z_j(k) + B_i(k) \right) = \\ &W_i \sigma \left( \sum_{j=1}^m V_{i,j} z_m^* + B_i(k) \right) + W_i \Delta \sum_{j=1}^m V_{i,j} (z_m(k) - z_m^*) \end{aligned} \quad (3.26)$$

where  $W_i \Delta \sum_{j=1}^m V_{i,j}$  is the first-order derivative of  $z_m(k+1)$  at the equilibrium point  $z_m^*$ , and  $0 < \Delta < \frac{1}{2}$ . Thus, the equilibrium point  $z_m^*$  is asymptotically stable if  $|W_i \Delta \sum_{j=1}^m V_{i,j}| < 1$ . Hence, *Theorem 2.2* is proved.

**Remark 2.2:** In a faultless system with an ideal observer,  $e_i(k)$  is equal to zero. Consequently,  $M_i(k)$  becomes independent, and *Theorem 2.2* is directly applicable to this case. On the other hand, in a faulty system,  $B_i(k)$  in (3.22) will be nonzero ( $e_i(k) \neq 0$ ). Thus, to satisfy *Theorem 2.2*, the value of  $W_i \Delta \sum_{j=1}^m V_{i,j}$  must be adjusted to make the system stable. Hence, the stability of both of the faultless and the faulty systems can be proved by  $W_i \Delta \sum_{j=1}^m V_{i,j}$ . When there is no fault in the system,  $M_i(k)$  converges to a zero equilibrium point, otherwise,  $M_i(k)$  converges to a nonzero equilibrium point, i.e., values of fault in sensor  $f_s(k)$  or actuator  $f_a(k)$ . The stability of the nonlinear NNAS-based FD system is proved using the following theorem.

**Theorem 2.3:** Consider the nonlinear system described in (3.1), and the NNAS described in (3.3). According to Assumptions 1-5, if the condition in Equation (3.27) is satisfied, then the error of the state estimation  $\tilde{x}(t)$  is bounded, i.e.,

$$\lambda_{\min}(Q) > 2L_{\Theta}\beta + 2L_g L_u \beta + \delta_m \quad (3.27)$$

where  $\delta_m = \sqrt{\sum_{j=1}^n \delta_j^2}$  and  $f_{sj} - M_j(k)$  is the detection error which yields  $\|f_s - M(k)\| < \sqrt{\sum_{j=1}^n \delta_j^2} = \delta_m$ .

**Proof:** In order to prove the stability of the estimation error  $\tilde{x}(t)$ , a Lyapunov function is defined as

$$V(\tilde{x}(t), t) = \tilde{x}^T(t)\Phi(t)\tilde{x}(t) \quad (3.28)$$

where  $\Phi(t)$  is a positive definite matrix, and  $\tilde{x}(t) = x(t) - \hat{x}(t)$ . The derivative of this Lyapunov function with respect to  $t$  can be obtained as follows:

$$\dot{V}(t) = \dot{\tilde{x}}(t)^T\Phi(t)\tilde{x}(t) + \tilde{x}(t)^T\dot{\Phi}(t)\tilde{x}(t) + \tilde{x}(t)^T\Phi(t)\dot{\tilde{x}}(t) \quad (3.29)$$

By substituting the state error equation (3.7) into (3.29), and according to the result from the proof of convergence of the parameter updating process, we have:

$$\begin{aligned} \dot{V}(t) &= \tilde{x}(t)^T \left( A(t)^T\Phi(t) + \Phi(t)A(t) + \dot{\Phi}(t) \right) \tilde{x}(t) + 2\tilde{x}(t)^T\Phi(t)\Theta(x, \hat{x}) \\ &\quad + 2\tilde{x}(t)^T\Phi(t) \left( g(x(t)) - g(\hat{x}(t)) \right) u(t) + 2\tilde{x}(t)^T\Phi(t) \left( f_s - M(t) \right) \\ &\leq -\lambda_{\min}(Q)\|\tilde{x}(t)\|^2 + 2L_\Theta\|\Phi(t)\|\|\tilde{x}(t)\|^2 + 2L_gL_u\|e(t)\|^2\|\Phi(t)\| + 2\|\tilde{x}(t)\|^2\|\Phi(t)\|\delta_m \\ &\leq -\lambda_{\min}(Q)\|\tilde{x}(t)\|^2 + 2L_\Theta\|\Phi(t)\|\|\tilde{x}(t)\|^2 + 2L_gL_u\|\tilde{x}(t)\|^2\|\Phi(t)\| + \delta_m \left( \|\tilde{x}(t)\|^2 + \|\Phi(t)\|^2 \right) \\ &\leq \left( -\lambda_{\min}(Q) + 2L_\Theta\beta + 2L_gL_u\beta + \delta_m \right) + \delta_m\beta^2 \end{aligned} \quad (3.30)$$

where  $\beta$  is a positive bounded real value. Therefore, if the equation (3.27) is satisfied, then

$$\dot{V}(t) \leq -\gamma\|\tilde{x}(t)\|^2 + \delta_m\beta^2 \quad (3.31)$$

where  $\gamma = \lambda_{\min}(Q) - 2L_\Theta\beta - 2L_gL_u\beta - \delta_m$ .

The above inequality guarantees that  $\dot{V}(t) < 0$  when  $\|\tilde{x}\| > \sqrt{\frac{\delta_m\beta^2}{\gamma}}$ . Since  $\delta_m$ ,  $\beta$ , and  $\gamma$  are bounded and positive variables, when  $k \rightarrow \infty$ , the estimation error will converge to a sufficiently small bound; subsequently, the condition (3.27) is adequate for guaranteeing the stability of the state estimation error  $\tilde{x}(t)$ .

### 3.3 Actuator FDI Design

Here, the design procedure of the proposed actuator FDI using NNAS will be explained. Reminding Equation (3.1), a nonlinear system described by

$$\begin{aligned}\dot{x}(t) &= f(x(t)) + g(x(t))u(t) + D(x, t) + f_a(x, t) \\ y(t) &= h(x(t)) + f_s(t)\end{aligned}\tag{3.32}$$

where  $f_a(x, t)$  is the fault which occurs in the actuator, and  $f_s(t)$  is the sensor fault. Considering Equations (3.32), the FDI design for the actuators an affine nonlinear system can be presented by

$$\begin{aligned}\hat{u} &= g(x)^{-1}(\dot{x}(t) - f(x(t))) \\ \tilde{u} &= u - (\hat{u} + M_i(t))\end{aligned}\tag{3.33}$$

where  $\hat{u}$  in Equation (3.33) represents the nonlinear observer model of the actuator,  $\tilde{u}$  is the FDI error which is used as an NN input in  $\delta_i(t)$ , and  $M_i(t)$  which is updated at each sample time can be described with the following equation.

$$M_i(k+1) = W_i \sigma \left( \sum_{j=1}^m V_{i,j} M_i(k-j+1) + B_i(k) \right)\tag{3.34}$$

where  $B_i(k) = \sum_{j=1}^n V_{i,m+j} e_i(k-j+1)$ .

Figure 3.2 shows the block diagram of the proposed procedure for FDI design of actuators in a nonlinear system.

### 3.4 Sensor FDI Design

Similar to actuator FDI design which was described in the previous subsection, a neural adaptive observer for sensor fault detection in a general affine nonlinear system (described in Equation (3.32)) can be presented as:





adaptive fault compensation feedback controller.

### 3.5.1 Nonlinear Feedback Linearization Controller

Feedback linearization technique eliminates the need for gain scheduling by inversion and cancellation of the inherent dynamics and replacement of a set of desired dynamics in the control loop. Consider the nonlinear system described in Equation 3.37, the feedback linearization controller for this system can be obtained

$$u = g^{-1}(x(t)) \left( \dot{x}_d(t) - f(x(t)) \right) \quad (3.38)$$

where  $\dot{x}_d(t)$  is the derivative of the desired states that can be controlled through a linear stabilizer controller, i.e., a proportional-integral (PI) controller. It should be noted that by choosing sufficiently large gains in the stabilizer controller, the stability of  $g(x)$  and its inverse matrix will be guaranteed [162]. The PI controller can be obtained by defining a new controller input as follows:

$$\nu = \dot{x}_d(t) - k_1 e - k_2 \int e dt \quad (3.39)$$

where  $e = x - x_d$ ,  $k_1$  is the proportional control gain and  $k_2$  is the integral gain. Considering (3.39), the error dynamics can be obtained as:

$$\ddot{e} + k_1 \dot{e} + k_2 e \quad (3.40)$$

Thus, the desired stabilizing controller can be designed by appropriately choosing the roots of “ $s$ ” in  $s^2 + k_1 s + k_2$ . In addition, the overshoots can be minimized by considering the following conditions:  $k_1 \leq 4k_2$  [163, 164].

### 3.5.2 Adaptive fault compensation feedback controller

As can be seen in Equation (3.38), the problem of disturbances and fault cannot be tackled in feedback linearization controller, thus, the following modification is suggested to make the controller resilient to fault and disturbances.

$$u = g^{-1}(x(t)) \left( \dot{x}_d(t) - f(x(t)) + D(t) + F(t) - M(t) \right) \quad (3.41)$$

where  $F(t)$  is the fault in the actuator and  $M(t)$  is the FDI output designed for detection of fault in the actuators described in the previous chapter. Figure 3.4 shows the block diagram of the proposed active FTC system for actuator faults in nonlinear systems. The mathematical stability of the proposed controller is investigated in the following subsection.

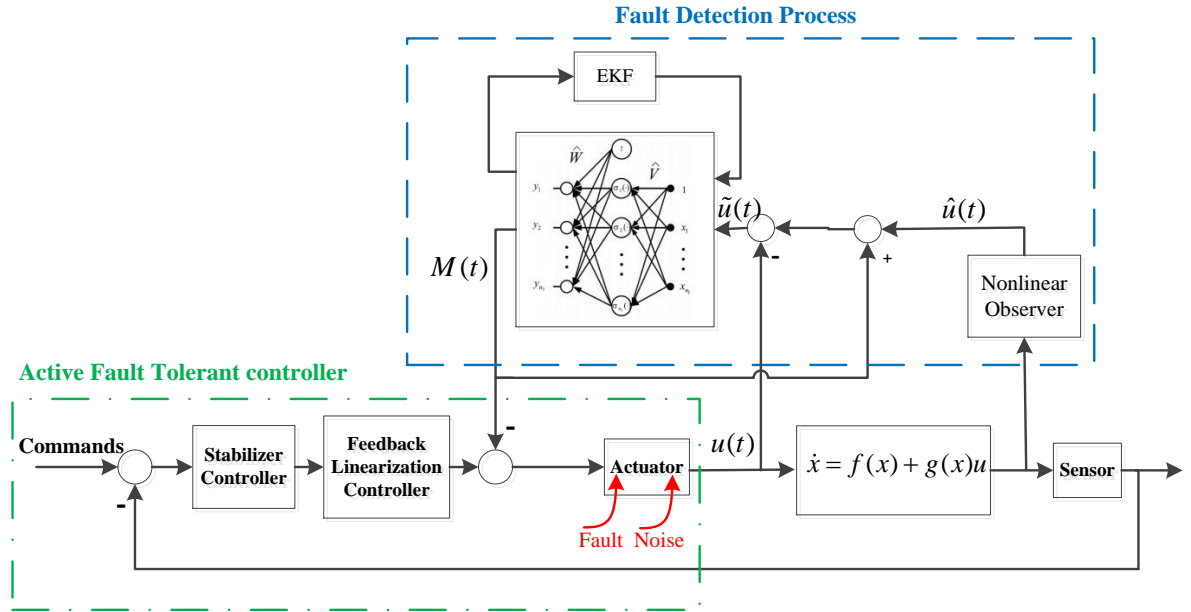


Figure 3.4: Block Diagram of the proposed Active FTC for actuator fault in nonlinear systems.

### 3.5.3 Active FTC Stability Analysis

To prove the stability of the designed active FTC system, we make the following assumptions.

**Assumption 1:** The state function  $f(x(t))$  can be differentiated at  $\hat{x}(t)$

$$Q(t) = \left. \frac{\partial f(x(t))}{\partial x(t)} \right|_{x(t)=\hat{x}(t)}$$

where  $Q(t)$  is an  $n \times n$  matrix.

The Taylor series expansion of  $f(x(t))$  at  $\hat{x}(t)$  can be presented as

$$f(x(t)) - f(\hat{x}(t)) = Q(t)\tilde{x}(t) + \Theta(\hat{x}(t), x(t)) \quad (3.42)$$

where  $\Theta(\hat{x}(t), x(t)) = o(\|\tilde{x}(t)\|^2)$  contains the higher order terms of the state estimation error. Here,  $\tilde{x}(t) = x(t) - \hat{x}(t)$ .

**Assumption 2:** The output function  $h(x(t))$  and the control input function  $g(x(t))$  satisfy the Lipschitz condition, i.e.,

$$\begin{aligned} \|h(x(t)) - h(\hat{x}(t))\| &\leq L_h \|\tilde{x}(t)\| \\ \|g(x(t)) - g(\hat{x}(t))\| &\leq L_g \|\tilde{x}(t)\| \end{aligned}$$

with the Lipschitz constant  $L_h$  and  $L_g$ , respectively. Here, we assume the detection system is accurate and the detection error is limited by  $L_g$  and  $L_h$ . The accuracy of the FDI system used in this work was investigated in the previous section we proved that detection error will be converged to zero.

**Assumption 3:** The control input vector of the system is bounded by  $L_u$  and the fault in the actuator,  $F(t)$ , is bounded by  $L_F$ , i.e.,

$$\begin{aligned} \|u(t)\| &\leq L_u \\ \|F(t)\| &\leq L_F \end{aligned}$$

Here, the actuation output and the occurred fault are considered to be bounded. This assumption can be always held by implementing a saturation filter with the amplitude of  $\pm 90^\circ$  to guarantee that the deflection of the actuators will not be over  $\pm 90^\circ$ .

**Assumption 4:**  $\Theta$  is bounded by a positive real number  $L_\Theta$  such that

$$\|\Theta(\hat{x}(t), x(t))\| \leq L_\Theta \|\tilde{x}(t)\|$$

This assumption is also related to the accuracy of the fault detection system that was proven in the previous section.

**Assumption 5:** The matrix  $P(t)$ , a symmetric matrix, that satisfies the following condition:

$$\lambda_1 I_n \leq P(t) \leq \lambda_2 I_n$$

where  $\lambda_1$  and  $\lambda_2$  are positive real numbers and  $P(t)$  can be found by solving the following Lyapunov equation:

$$Q^T(t)P(t) + P(t)Q(t) + \dot{P}(t) = -\Gamma \quad (3.43)$$

where  $\Gamma$  is a symmetric positive definite matrix.

Now, by subtracting the observer equation

$$\dot{\hat{x}} = f(\hat{x}(t)) + g(\hat{x}(t))u(t) + M(t)$$

from the nonlinear system equation

$$\dot{x} = f(x(t)) + g(x(t))u(t) + F(t)$$

and substituting (3.42), the effect of the fault detection error on the system  $\tilde{x}(t)$  can be written as

$$\begin{aligned} \dot{\tilde{x}}(t) &= \dot{x}(t) - \dot{\hat{x}}(t) \\ &= Q(t)\tilde{x}(t) + \Theta(\hat{x}(t), x(t)) + (g(x(t)) - g(\hat{x}(t)))u(t) \\ &\quad + F(t) - M(t) \end{aligned} \quad (3.44)$$

*Theorem:* With the Assumptions 1-5, the fault effect in Equation (3.44) is bounded on  $\tilde{x}(t)$  if the following condition is satisfied

$$\eta_{min}(\Gamma) > 2L_{\Theta}\lambda_2 + 2L_gL_u\lambda_2 + 2L_a\lambda_2 \quad (3.45)$$

where  $\|F(t) - M(t)\| \leq L_a$ .  $\lambda_2$  and  $L_a$  are both finite positive constant.

*Proof:* A Lyapunov function is selected as follows

$$V(\tilde{x}(t), t) = \tilde{x}(t)^T P(t) \tilde{x}(t) \quad (3.46)$$

Based on Assumption 5, we can conclude that  $V(\tilde{x}, t) \geq 0$  for the estimation error  $\tilde{x}(t)$ . Now for the stability consideration of the proposed FTC system we need to show that  $\dot{V}(\tilde{x}, t) < 0$ . The derivative of the  $V(\tilde{x}, t)$  with respect to time  $t$  can be expressed as

$$\dot{V}(\tilde{x}, t) = \dot{\tilde{x}}(t)^T P(t) \tilde{x}(t) + \tilde{x}(t)^T \dot{P}(t) \tilde{x}(t) + \tilde{x}(t)^T P(t) \dot{\tilde{x}}(t) \quad (3.47)$$

By substituting  $\tilde{\hat{x}}(t)$  from Equation (3.44) into  $\dot{V}(\tilde{x}(t), t)$  in (3.47), we have

$$\begin{aligned}
\dot{V}(\tilde{x}, t) &= \left( Q(t)\tilde{x}(t) + \Theta(x(t), \hat{x}(t)) + \right. \\
&\quad \left. (g(x) - g(\hat{x}))u(t) + F(t) - M(t) \right)^T P(t)\tilde{x}(t) \\
&\quad + \tilde{x}^T(t) \left( -Q^T(t)P(t) - P(t)Q(t) - \Gamma \right) \tilde{x}(t) \\
&\quad + \tilde{x}^T(t)P(t) \left( Q(t)\tilde{x}(t) + \Theta(x(t), \hat{x}(t)) \right. \\
&\quad \left. + (g(x(t)) - g(\hat{x}(t)))u(t) + F(t) - M(t) \right) \\
&= \tilde{x}^T(t)Q^T(t)P(t)\tilde{x}(t) + \Theta^T(x(t), \hat{x}(t))P(t)\tilde{x}(t) \\
&\quad + u^T(t) (g(x(t)) - g(\hat{x}(t)))^T P(t)\tilde{x}(t) + \\
&\quad \quad (F(t) - M(t))^T P(t)\tilde{x}(t) \\
&\quad - \tilde{x}^T(t)Q(t)P(t)\tilde{x}(t) - \tilde{x}^T(t)P(t)Q(t)\tilde{x}(t) \\
&\quad - \tilde{x}^T(t)\Gamma(t)\tilde{x}(t) + \tilde{x}^T(t)P(t)Q(t)\tilde{x}(t) \\
&\quad + \tilde{x}^T(t)P(t)\Theta(x(t), \hat{x}(t))\tilde{x}(t) \\
&\quad + \tilde{x}^T(t)P(t) (g(x(t)) - g(\hat{x}(t)))u(t) \\
&\quad + \tilde{x}^T(t)P(t) (F(t) - M(t)) \\
&= \Theta^T(x(t), \hat{x}(t))P(t)\tilde{x}(t) + \tilde{x}^T(t)P(t)\Theta(x(t), \hat{x}(t)) \\
&\quad + u^T(t) (g(x(t)) - g(\hat{x}(t)))^T P(t)\tilde{x}(t) \\
&\quad + \tilde{x}^T(t)P(t) (g(x(t)) - g(\hat{x}(t)))u(t) \\
&\quad + (F(t) - M(t))^T P(t)\tilde{x}(t) + \\
&\quad \tilde{x}^T(t)P(t) (F(t) - M(t)) - \tilde{x}^T(t)\Gamma\tilde{x}(t) \\
&= 2\Theta^T(x(t), \hat{x}(t))P(t)\tilde{x}(t) \\
&\quad + 2u^T(t) (g(x(t)) - g(\hat{x}(t)))^T P(t)\tilde{x}(t) \\
&\quad + 2(F(t) - M(t))^T P(t)\tilde{x}(t) - \tilde{x}^T\Gamma\tilde{x}(t)
\end{aligned} \tag{3.48}$$

Now, substituting the conditions in Assumptions 2-5, we have

$$\begin{aligned}
\dot{V}(\tilde{x}(t), t) &= 2\Theta^T(x(t), \hat{x}(t))P(t)\tilde{x}(t) \\
&+ 2u^T(t) (g(x(t)) - g(\hat{x}(t)))^T P(t)\tilde{x}(t) \\
&+ 2(F(t) - M(t))^T P(t)\tilde{x}(t) - \tilde{x}^T \Gamma \tilde{x}(t) \\
&\leq 2\|P(t)\|L_\Theta \|\tilde{x}(t)\| + 2L_g L_u \|P(t)\| \|\tilde{x}(t)\| \\
&\quad + 2\|P(t)\|L_a \|\tilde{x}(t)\| - \Gamma \tilde{x}(t) \\
&\leq (-\eta_{min}(\Gamma) + 2L_\Theta \lambda_2 + 2L_g L_u \lambda_2 + 2L_a \lambda_2) \|\tilde{x}(t)\|^2
\end{aligned} \tag{3.49}$$

Hence, to have a stable FTC, we must have

$$-\eta_{min}(\Gamma) + 2L_\Theta \lambda_2 + 2L_g L_u \lambda_2 + 2L_a \lambda_2 < 0$$

or

$$\eta_{min}(\Gamma) > 2L_\Theta \lambda_2 + 2L_g L_u \lambda_2 + 2L_a \lambda_2$$

which gives the sufficient condition of the stability. Thus, the condition in Equation (3.45) is sufficient to guarantee the convergence of the fault effect  $\tilde{x}(t)$  on the system to a small bounded value.

## 4.1 Introduction

Faults in aircraft actuators can cause serious issues in safety. Due to the autonomous nature of the unmanned aerial vehicles (UAVs), faults can lead to more serious problems in these systems. In this chapter, a new active fault tolerant control (FTC) system design for an UAV is presented. The proposed design uses a neural network adaptive structure (NNAS) for fault detection and isolation (FDI), then, the FDI signal combined with a nonlinear dynamic inversion (NDI) technique is used to compensate for the faults in the actuators. The proposed scheme detects and isolates faults in the actuators of the system in real-time without the need of controller reconfiguration in the presence of faults in the actuators. The simulation results of the designed FTC system when it is applied to WVU YF-22 UAV show that the proposed design can successfully detect and isolate the faults and compensate for their effect. The rest of this section reviews the fault effect on aircraft systems, FTC approaches used in flight control systems, and the main contributions of this chapter.

Faults and interruptions in flight control systems can cause serious safety problems for aircraft. Due to this fact, flight control systems need a highly reliable design. For UAVs, there is no opportunity to fix the faulty component after launching. In order to develop systems with satisfactory performance, controllers with the ability to tolerate potential faults should be considered. These reliable controllers are known as fault-tolerant control (FTC) systems. FTC systems have been developed to be able to control the system when malfunctions occur in system components. However, the conventional feedback control approaches are designed based on the

assumption that all the components work in an ideal condition which may not provide satisfactory results in faulty situations. Thus, FTCs have received much of attention in the recent decade [165–169]. Active FTC system has superiority over passive FTC due to their intelligent reaction faults based on the fault severity and the fault location.

Generally, active fault tolerant techniques can be designed for both linear and nonlinear systems. Linear models are popular in the literature due to their ease of use and simplicity [30, 138–140]. Ye et al. presented an adaptive trajectory tracking FTC system based on the online estimation of an eventual fault, which has been applied on a linear time-invariant (LTI) model of F-16 aircraft [138]. Alwi and Edward introduced an online sliding mode control (SMC) allocation scheme which was capable of tolerating faults in the actuators of the aircraft linear model [30]. In [139], Alwi and Edward modified their SMC design [30], by adding a back-stepping structure that in a faultless situation, the system switches to the backstepping controller to obtain a better control performance. Yu et al. introduced a hybrid FTC system which was able to reduce the rate of the fault effect on the system with minimal fault information which gives some extra time to fault detection and isolation (FDI) techniques to detect the fault more accurately [140].

Due to the complex and nonlinear behavior of the aircraft dynamics, linear control strategies are not a suitable candidate for an accurate and reliable control system. For this reason, nonlinear control strategies were used to design FTC systems [142–144]. Gao et al. presented an active FTC design based on adaptive sliding mode technique for a reusable launch vehicle (RLV) [142]. The active FTC system was designed for the actuators in the reentry phase of the RLV. The design was

based on reconfigurable control strategy that after detection of a fault, the system can switch between predesigned controllers. However, these switching controllers often suffer from the lag between the switches, which makes them unreliable for agile systems like jet UAVs. Park et al. analyzed the intentional attempts to disrupt the flight system through the satellite-based navigation system [144]. The proposed control system was designed through three mechanisms that allowed the aircraft to detect and isolate the attacks to the aircraft navigation system. A detection and defense technique using the Doppler/received signal strength and an FTC algorithm were used in their work. A Kalman filter was used to fuse high-frequency inertial sensor information with low-frequency GPS data. The results showed that their proposed mechanism robustly detects and corrects faults generated by injection of malicious data. However, the efficiency of this method for faults in the actuator is still questionable because it has not been applied yet.

The ability of Artificial Neural Network (ANN) in estimation and identification of nonlinear systems makes it a suitable candidate for FDI [8, 120, 158, 159, 170, 171]; but, none of these researches have investigated the application of FDI in designing active FTC systems. Application of ANN in active FTC design is limited to use as a fault compensator which analytically compensates the actuator/sensor error based on the observed error in the system [23, 25, 27, 28]. Chen et al. introduced a neural FTC design for faults in the actuators of a three degree-of-freedom (DoF) helicopter [23]. In their design, ANN observer was developed based on radial basis function to observe the error in the system and compensate it in a backstepping control structure. Similar approaches based on ANN observer have been applied to different applications [25, 27, 28].

In this chapter, we introduced a novel active FTC system design for an UAV. The proposed active FTC design consists of an ANN-based FDI system, a nonlinear dynamic inversion (NDI) based flight controller, and a new feedback structure which compensates the occurred fault based on the information received from the FDI system. The FDI system is designed based on the result of our previous work [159], in which we demonstrated that updating ANN weights with extended Kalman Filter (EKF) algorithm improves the accuracy and response time of ANN-based fault detection system. The proposed control design is implemented and evaluated on a six degree of freedom (DoF) model of an unmanned aircraft, WVU YF22. To the best of our knowledge, the problem of designing a united framework for FTC which uses FDI information has not been solved. Moreover, due to the complicated dynamic of a six degree of DoF model of the aircraft, there is no report on using six DoF model of aircraft in designing active FTC system. Thus, the main contributions of this work can be summarized as 1) a novel nonlinear active FTC design for aircraft actuators is developed , 2) the proposed design helps to detect and isolate abrupt faults without the need of control reconfiguration which is a challenge for other FTC designs, 3) the controller is designed based on the six-DoF nonlinear model. The rest of this chapter is organized as follows. Section 2 provides the nonlinear dynamic equation of the UAV, while Section 3 illustrates the FDI design. In Section 4 the proposed FTC design is presented and the simulation results are provided in Section 5. Finally, Section 6 discusses the results and the conclusion of this study.

## 4.2 UAV Nonlinear Dynamic

In this section, the nonlinear dynamic model of the aircraft is presented. Figure 4.1 shows the aircraft body coordination, attitude angles, and the actuators. Similar

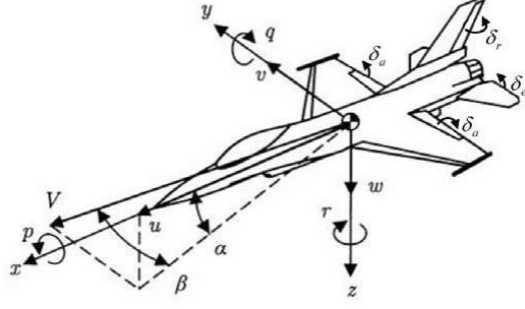


Figure 4.1: The aircraft coordinate system [2]

to other airplanes, the control inputs of the proposed system are deflections of the aileron ( $\delta_A$ ), elevator ( $\delta_E$ ), and rudder ( $\delta_R$ ).

The following equations illustrate the aircraft equations of motion [172]. Their aerodynamic coefficients can be found in [173]. The nonlinear six-DoF of motion for an aircraft over a flat earth are [174]:

$$\dot{p} = \frac{I_z I_{aero} + I_{xz} n_{aero}}{I_x I_z - I_{xz}^2} r + \frac{I_{xz}(I_x - I_y + I_z) p q}{I_x I_z - I_{xz}^2} + \frac{I[I_z(I_y - I_z) - I_{xz}^2] q r}{I_x I_z - I_{xz}^2} \quad (4.1)$$

$$\dot{q} = \frac{1}{I_y} [m_{aero} + p r (I_z - I_x) + I_{xz}(r^2 - p^2)] \quad (4.2)$$

$$\dot{r} = \left[ \frac{(I_x - I_y + I_z) I_{xz}}{I_x I_z - I_{xz}^2} r + \frac{I_x(I_x - I_y) + I_{xz}^2}{I_x I_z - I_{xz}^2} p \right] q + \frac{I_{xz} I_{aero} + I_{xz} n_{aero}}{I_x I_z - I_{xz}^2} \quad (4.3)$$

$$\dot{\beta} = p \sin \alpha - r \cos \alpha + \frac{1}{m v} [m g \sin \gamma \sin \mu] \quad (4.4)$$

$$+ \frac{1}{m v} [Y \cos \beta - T \sin \beta \cos \alpha]$$

$$\begin{aligned}\dot{\alpha} &= q - (p \cos \alpha + r \sin \alpha) \tan \beta \\ &+ \frac{1}{mv \cos \beta} [-L + mg \cos \gamma \cos \mu] \\ &+ \frac{1}{mv \cos \beta} [-T \sin \alpha]\end{aligned}\quad (4.5)$$

$$\begin{aligned}\dot{\mu} &= \frac{1}{\cos \beta} (p \cos \alpha + r \sin \alpha) - \frac{g}{v} \tan \beta \cos \mu \cos \gamma \\ &+ \frac{L + T \sin \alpha}{mv} [\tan \gamma \sin \mu + \tan \beta] \\ &+ \frac{Y}{mv} \tan \gamma \cos \mu \cos \beta\end{aligned}\quad (4.6)$$

$$\begin{aligned}\dot{\gamma} &= \frac{1}{mv} [L \cos \mu - mg \cos \gamma - Y \sin \mu \cos \beta] \\ &+ \frac{T}{mv} [\sin \mu \sin \beta \cos \alpha + \cos \mu \sin \alpha]\end{aligned}\quad (4.7)$$

$$\dot{v} = \frac{1}{m} [-D + Y \sin \beta - mg \sin \gamma + T \cos \beta \cos \alpha]\quad (4.8)$$

Equations (4.1)-(4.3) describe  $p$ ,  $q$ , and  $r$ , which are the roll, pitch, and yaw rates about the body-fixed frame, respectively.  $l_{aero}$ ,  $m_{aero}$ , and  $n_{aero}$  are aerodynamic rolling, pitching and yawing moments, respectively, and  $I_x$ ,  $I_y$ ,  $I_z$  are the moments of inertia about the  $x$ ,  $y$ , and  $z$  axis, respectively.  $I_{xz}$  is the inertia moment about the  $xz$  plane. Equations (4.4)-(4.6) describe  $\alpha$ ,  $\beta$ , and  $\mu$ , which are the angle of attack, sideslip angle, and the bank angle, respectively;  $T$  is the thrust, and  $L$  is the lift. Equations (4.7) and (4.8) describe the flight path angle  $\gamma$ , and the indicated air speed  $v$ .

### 4.3 FDI Design

Active FTC design needs an online FDI strategy to update the control system with the information related to the occurred fault. Faults in the system do not have any specific and predictable pattern. Therefore, detection of faults need an accurate

detection strategy. The proposed FDI technique is a Neural Network (NN)-based detection design in which its learning weights are updated online through the EKF algorithm. This FDI strategy is adopted due to its accurate and fast detection ability [159]. In the following, the proposed neural network adaptive structure (NNAS) is presented.

### 4.3.1 NNAS

The proposed NNAS used for FDI is developed in this subsection. Faults in a system may be nonlinear and unpredictable; hence, ANN can be a suitable candidate for their estimation. Unlike the direct ANN modeling procedures that use an ANN to simulate the system behavior [157, 158], the NNAS detects faults based on the output of the nonlinear observer

$$\begin{aligned}\dot{\hat{x}} &= f(\hat{x}(t)) + g(\hat{x}(t))u(t) + M(t) \\ \hat{y} &= h(\hat{x}(t))\end{aligned}\tag{4.9}$$

where  $\hat{x}(t)$  is the state vector of the nonlinear observer and  $M(t)$  is the neural network observer that is defined as [159]:

$$M_i(t) = W_i(t)\sigma(V_i(t)\delta_i(t))\tag{4.10}$$

where  $M_i(t)$  is the  $i$ th vector of  $M(t)$  for  $i = 1, \dots, n$ .  $W_i(t)$  and  $V_i(t) = [V_{i,1}(t), \dots, V_{i,m+n}(t)]$  are the weights associated with the  $i$ th output of the NNAS at time  $t$ . Here,  $\delta_i(t)$  can be defined as  $\delta_i(t) = [M_i(t - \tau), \dots, M_i(t - m\tau), e_i(t - \tau), \dots, e_i(t - n\tau)]^T$ . Here,  $\tau$  indicates the sampling period or the step size of the observer;  $e_i(t) = y_i(t) - \hat{y}_i(t)$ ,

and  $\sigma(\cdot)$  is a *tanh* activation function which is selected due to its gradient strength.

$$\sigma(x) = (1 - e^{-x})/(1 + e^{-x}) \quad (4.11)$$

In terms of the  $i$ th element  $M_i(t)$  of  $M(t)$  for  $i=1,\dots,n$ , the NN observer can be represented as

$$M_i(t) = W_i(t)\sigma(Z_i(t)) \quad (4.12)$$

where

$$Z_i(t) = \sum_{j=1}^m V_{i,j}(t)M_i(t - j\tau) + \sum_{j=1}^n V_{i,m+j}(t)e_i(t - j\tau) \quad (4.13)$$

The input of the observer  $M(t)$  is recursively updated with the previous  $m$  samples of the observer inputs for  $j = 1, 2, \dots, m$ , and also previous  $n$  samples of the system output error  $e_i(t - j\tau)$  for  $j = 1, 2, \dots, n$ . Here,  $m$  and  $n$  are chosen based on the needed accuracy and training time in the system. Large values of  $m$  and  $n$  guaranty the convergence of the training and the accuracy of the ANN; however, large values of them may increase the computation time and add unnecessary delays due to increasing the training duration [159]. Thus, to have a real-time and accurate fault detection,  $m$  and  $n$  should be chosen based on the needed accuracy and the system frequency response.

### 4.3.2 Neural network weight update law

In order to achieve real-time performance, the NN weights should be tuned effectively [160]. In this study an adaptive tuning algorithm based on EKF is introduced. The EKF helps to update the NN weighting parameters online, so that fast convergence rate of the NN learning will be guaranteed. Through the updating process, if we consider the  $i$ th element of NNAS, then the EKF updating parameters can be

described by [159]:

$$\theta_i(k) = [W_i(k), V_{i,1}(k), \dots, V_{i,m+n}(k)]^T \quad (4.14)$$

where  $k$  is the  $k$ th sampling instant, and  $t = k\tau$ . The parameters will be calculated in each sampling time with the following rules [159].

$$\begin{aligned} \theta_i(k) &= \theta_i(k-1) + \eta_i K_i(k) [y_i(k) - \hat{y}_i(k)] \\ K_i(k) &= P_i(k) H_i(k) [H_i(k)^T P_i(k) H_i(k) + R_i(k)]^{-1} \\ P_i(k+1) &= P_i(k) - K_i(k) H_i(k)^T P_i(k) \end{aligned} \quad (4.15)$$

where  $\eta_i$  is the learning coefficient,  $P_i(k)$  is the covariance matrix of the state estimation error,  $K_i(k)$  is the Kalman gain, and  $R_i(k)$  is the covariance matrix of the estimated noise, which is computed recursively by [161]:

$$R_i(k) = R_i(k-1) + [e_i^T(k) e_i(k) - R_i(k-1)] / k \quad (4.16)$$

Here  $H_i(k)$  is the derivative of  $e_i(k)$  with respect to  $\theta_i(k)$ . Based on the observer input in Equation (4.10),  $H_i(k)$  can be calculated as follow:

$$\begin{aligned} H_i(k) &= \frac{\partial e_i(k)}{\partial \theta_i} \Big|_{\theta_i = \theta_i(k-1)} \\ &= \begin{cases} \sigma(Z_i(k)), & \theta_i = W_i \\ W_i(k) M_i(k-j) \acute{\sigma}(Z_i(k)), & \theta_i = V_{i,j} \\ W_i(k) e_i(k-j) \acute{\sigma}(Z_i(k)), & \theta_i = V_{i,m+j} \end{cases} \end{aligned} \quad (4.17)$$

### 4.3.3 Actuator FDI design

Here, the design procedure of the proposed actuator FDI using NNAS will be explained. Aileron  $\delta_a$ , elevator  $\delta_e$ , and rudder  $\delta_r$  are the three main actuators which are used in control of the airplane attitude. Typical motion equations of the airplane

angular rate with actuator faults can be described as

$$\begin{aligned} \dot{x} &= f(x) + g(x)_{in}u + F(t) \\ x &= [p, q, r]^T, f(x) = [f_p, f_q, f_r]^T \\ g_{in}(x) &= \begin{bmatrix} L_{\delta_a} & 0 & L_{\delta_r} \\ 0 & M_{\delta_e} & 0 \\ N_{\delta_a} & 0 & N_{\delta_r} \end{bmatrix} \end{aligned} \quad (4.18)$$

where  $F(t)$  is the fault which occurs in the actuators;  $L_{\delta_a}$ ,  $L_{\delta_r}$ ,  $M_{\delta_e}$ ,  $N_{\delta_a}$ ,  $N_{\delta_r}$  are rolling, pitching and yawing moments about the control input deflections.  $f_p$ ,  $f_q$  and  $f_r$  can be derived from Equations (4.1-4.3) as

$$\begin{aligned} f_p &= I_z l_{aero} + I_{xz} n_{aero} + I_{xz}(I_x - I_y + I_z)pq \\ &\quad + \frac{(I_z(I_y - I_z) - I_{xz}^2)qr}{I_z I_z - I_{xz}^2} \\ f_q &= m_{aero} + pr(I_z - I_x) + \frac{I_{xz}(r^2 - p^2)}{I_y} \\ f_r &= I_{xz} l_{aero} + I_x n_{aero} + (I_x(I_x - I_y) + I_{xz}^2)pq \\ &\quad - \frac{I_{xz}(I_x - I_y + I_z)qr}{I_x I_{xz} - I_{xz}^2} \end{aligned} \quad (4.19)$$

Considering Equations (4.18) and (4.19), the FDI design for airplane actuators can be presented by

$$\begin{aligned} \hat{u} &= g(x)_{in}^{-1}(\dot{x} - f(x)) \\ \tilde{u} &= u - (\hat{u} + M_i(t)) \end{aligned} \quad (4.20)$$

where  $\hat{u}$  in Equation (4.20) represents the nonlinear observer model of the actuator,  $\tilde{u}$  is the FDI error which is used as an NN input in  $\delta_i(t)$ , and  $M_i(t)$  which is updated at each sample time can be described with the following equation.

$$M_i(k+1) = W_i \sigma \left( \sum_{j=1}^m V_{i,j} M_i(k-j+1) + B_i(k) \right) \quad (4.21)$$

where  $B_i(k) = \sum_{j=1}^n V_{i,m+j} e_i(k-j+1)$ .

## 4.4 Active FTC design

In this Section, the proposed active FTC design is presented. The proposed controller consists of two parts: 1) the nonlinear dynamic inversion (NDI) control, and 2) the adaptive fault compensation feedback controller.

### 4.4.1 Nonlinear Dynamic Inversion Controller

Nonlinear dynamic inversion (NDI) is one of feedback linearization techniques that received a great deal of attention in flight control design [175–177]. This technique which commonly consists of two control loops eliminates the need for gain scheduling by inversion and cancellation of the inherent dynamics and replacement of a set of desired dynamics in each loop. In the proposed NDI design, two control loops have been considered. This two-loop design requires the assumption of time scale separation between the two loops, which means that the outer control loop should have considerably lower bandwidth than that of the inner control loop to prevent interaction between the loops [160, 175]. By separating state dynamics into two groups, the faster state dynamics will be controlled by the inner loop and the slower state dynamics will be controlled by the outer control loop.

#### 4.4.1.1 Inner loop design

In the inner loop, faster states will be controlled. In the airplane model, these states are the attitude rates  $p$ ,  $q$ ,  $r$ , which are getting controlled with actuators input  $\delta_a$ ,  $\delta_e$ , and  $\delta_r$ , and the desired values of the fast states come from the outer control loop.

The fast attitude rate dynamics can be extracted from (4.1)-(4.3) as follows

$$\begin{bmatrix} \dot{p} \\ \dot{q} \\ \dot{r} \end{bmatrix} = \begin{bmatrix} f_p(x) \\ f_q(x) \\ f_r(x) \end{bmatrix} + g_{in}(x) \begin{bmatrix} \delta_a \\ \delta_e \\ \delta_r \end{bmatrix} \quad (4.22)$$

where  $f_p$ ,  $f_q$ ,  $f_r$ , and  $g_{in}(x)$  are given in Equations (4.18) and (4.19). Then, the inner loop controller yields:

$$u = \begin{bmatrix} \delta_a \\ \delta_e \\ \delta_r \end{bmatrix} = g_{in}^{-1}(x) \left( \begin{bmatrix} \dot{p}_d \\ \dot{q}_d \\ \dot{r}_d \end{bmatrix} - \begin{bmatrix} f_p(x) \\ f_q(x) \\ f_r(x) \end{bmatrix} \right) \quad (4.23)$$

where  $\dot{p}_d$ ,  $\dot{q}_d$ ,  $\dot{r}_d$  are the desired angular rates which are defined as follows

$$\begin{bmatrix} \dot{p}_d \\ \dot{q}_d \\ \dot{r}_d \end{bmatrix} = \begin{bmatrix} \omega_p & 0 & 0 \\ 0 & \omega_q & 0 \\ 0 & 0 & \omega_r \end{bmatrix} \begin{bmatrix} p_c - p \\ q_c - q \\ r_c - r \end{bmatrix} \quad (4.24)$$

where  $p_c$ ,  $q_c$ ,  $r_c$  are the angular rates received from the outer loop controller, and  $\omega_p$ ,  $\omega_q$ ,  $\omega_r$  are the inner loop gains which are selected by the designer to obtain the desired performance. Choosing sufficiently large inner-loop gains will guarantee the stability of  $g_{in}(x)$  and its inverse matrix [162].

#### 4.4.1.2 Outer loop controller

The outer loop controller is designed to control the slow states  $\alpha$ ,  $\beta$ ,  $\mu$  where the inputs  $\alpha_c$ ,  $\beta_c$ ,  $\mu_c$  are the input commands from the guidance system and the outputs  $p_c$ ,  $q_c$ ,  $r_c$  are the reference commands for the inner-loop controller. The assumption of the time scale separation between the inner loop and the outer loop controllers ensures that the deflections of the control surfaces  $(\delta_a, \delta_e, \delta_r)$  have no interaction

with the outer-loop states. Then, based on Equations (4.4)-(4.6), the outer loop states yields

$$\begin{bmatrix} \dot{\beta}_d \\ \dot{\alpha}_d \\ \dot{\mu}_d \end{bmatrix} = \begin{bmatrix} f_\beta \\ f_\alpha \\ f_\mu \end{bmatrix} + g_{out}(x) \begin{bmatrix} p \\ q \\ r \end{bmatrix} \quad (4.25)$$

while the desired slow states are defined as follows

$$\begin{bmatrix} \dot{\beta}_d \\ \dot{\alpha}_d \\ \dot{\mu}_d \end{bmatrix} = \begin{bmatrix} \omega_\beta & 0 & 0 \\ 0 & \omega_\alpha & 0 \\ 0 & 0 & \omega_\mu \end{bmatrix} \begin{bmatrix} \beta_c - \beta \\ \alpha_c - \alpha \\ \mu_c - \mu \end{bmatrix} \quad (4.26)$$

where  $\omega_\beta, \omega_\alpha, \omega_\mu$  are the outer-loop gains that are selected by the designer to achieve the desired performance, and  $\beta_c, \alpha_c, \mu_c$  are the commands that are generated by the guidance system. The outer-loop controller is derived using (4.25) as follows

$$\begin{bmatrix} p_c \\ q_c \\ r_c \end{bmatrix} = g_{out}^{-1} \left( \begin{bmatrix} \dot{\beta}_d \\ \dot{\alpha}_d \\ \dot{\mu}_d \end{bmatrix} - \begin{bmatrix} f_\beta \\ f_\alpha \\ f_\mu \end{bmatrix} \right) \quad (4.27)$$

Stability of the matrix  $g_{out}$  and its inverse can be also guaranteed by choosing large enough outer-loop gains [162].

#### 4.4.2 Adaptive Fault Compensation Feedback Controller

In this subsection, the FTC design is finalized. This controller consists of a two-loop DI controller, an adaptive NN FDI structure, and a feedback signal to compensate for the occurred fault in real time. The structure of the FTC design is as follows

$$\begin{bmatrix} \dot{p} \\ \dot{q} \\ \dot{r} \end{bmatrix} = \begin{bmatrix} f_p(x) \\ f_q(x) \\ f_r(x) \end{bmatrix} + g_{in}(x) \begin{bmatrix} \delta_a \\ \delta_e \\ \delta_r \end{bmatrix} + F(t) - M(t) \quad (4.28)$$

where the  $F(t)$  is the fault in the actuator, and  $M(t)$  is the NNAS detection signal to compensate for the occurred fault in the system. Using Equation (4.28), the FTC is derived as follows:

$$\begin{bmatrix} \delta_a \\ \delta_e \\ \delta_r \end{bmatrix} = g_{in}^{-1}(x) \left( \begin{bmatrix} \dot{p}_d \\ \dot{q}_d \\ \dot{r}_d \end{bmatrix} - \begin{bmatrix} f_p(x) \\ f_q(x) \\ f_r(x) \end{bmatrix} + F(t) - M(t) \right) \quad (4.29)$$

Figure 4.2 shows the proposed united framework of FTC and FDI. In this figure, the FDI part is separated by dashed lines, the FTC is separated by dashed-dot lines.

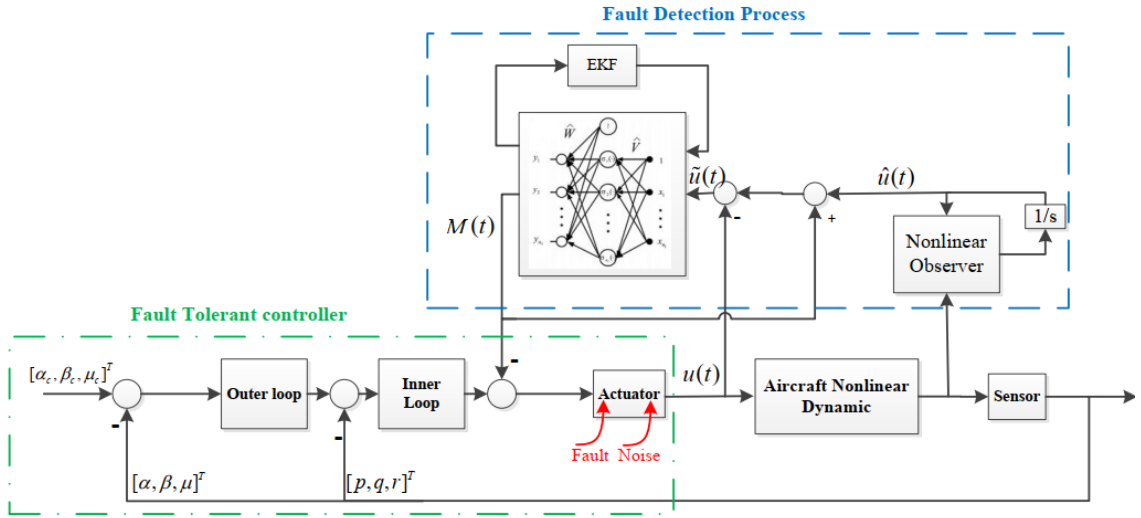


Figure 4.2: The proposed united framework for fault detection and compensation (active FTC) diagram for an aircraft.

## 4.5 Numerical Simulations

This section shows that fault in the actuators of an aircraft would degrade the control performance of the aircraft and illustrates that the proposed design is able to detect and isolate the fault and compensate for the effects of faults on the system performance. The numerical simulations are performed using MATLAB SIMULINK

software and the proposed FTC is applied to a nonlinear model of WVU YF-22 aircraft [173]. To show the advantages of the proposed method, the results are compared with one of the recent ANN-based adaptive FTC design [178], and nonlinear dynamic inversion (NDI) control technique described in the literature [179]. In the simulation results, in Figs. (4.4-4.9), the ANN-based adaptive FTC in [178] and the proposed method are abbreviated as adaptive FTC and active FTC, respectively. In the following subsections, a triangular-shaped fault is inserted to the aileron, elevator, and rudder of the aircraft, respectively. This kind of faults in the actuators can occur for various reasons, such as a fall in a supply voltage or the actuator current (because they normally need a separated power supply), interruptions in communication between the actuator and control, noise effect on the actuator (environmental noise like a magnetic field), floating actuator faults, denial of service for a period of time due to processor speed and network bandwidth, etc. [5, 6]. These kinds of faults can be compensated with a supervisory system by inserting an artificial control signal on the faulty actuator. This artificial signal should be injected in a way to remove the effect of fault on the actuator. In the simulation, actuators are modeled using a batch least squares (BLS) technique [173]:

$$G_{actuator}(s) = \frac{1}{1 + 0.0424s} e^{-0.02s} \quad (4.30)$$

where the actuator deflections are bounded through a saturation filter between  $\pm 90^\circ$  [180]. This saturation filters any false data larger than the defined boundary in the communication links and the rest will be compensated through the proposed resilient controller. Finally, the control performance of the proposed design (active FTC) is compared with the NDI controller [179], and the adaptive FTC system [23].

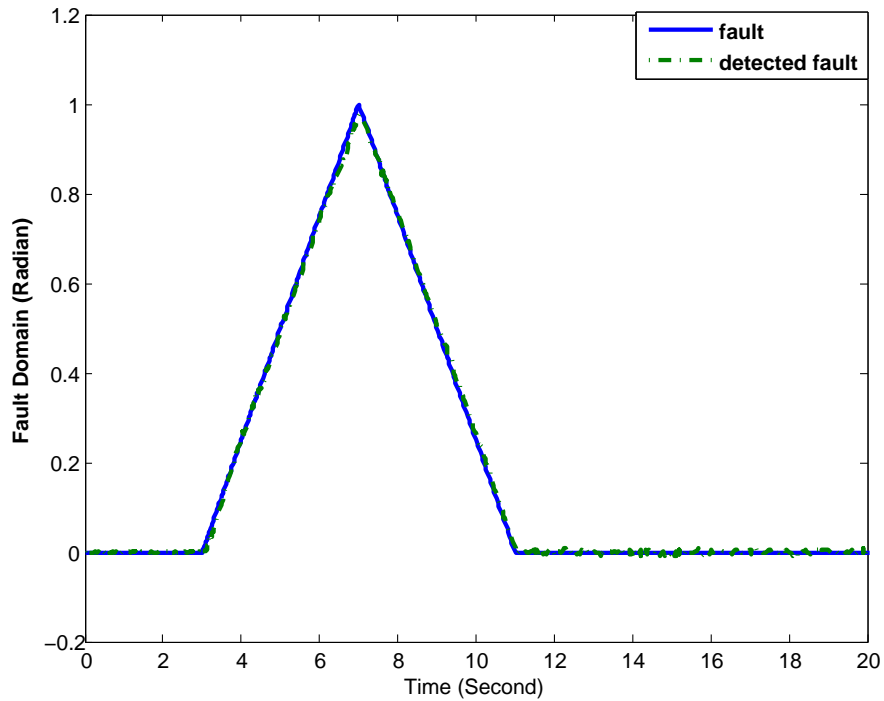


Figure 4.3: Fault detection using NNAS.

#### 4.5.1 Fault in the Aileron

A triangular fault is applied to the aileron. Figure 4.3 shows the injected (solid line) and detected (dashed line) fault in the aileron actuator. As it can be seen in the Figure, the proposed NNAS has successfully detected the fault in the actuator. Figure 4.4 shows that the proposed FTC design can compensate for the fault effects based on the detected fault and the aircraft is able to track the given commands from the pilot/autopilot, while, the NDI and adaptive FTC controller performance degraded in the presence of this fault. Figure 4.5 shows the deflections of the aircraft actuators in the presence of the fault in the aileron for the proposed active FTC, the adaptive FTC, and the NDI controller. By comparing the aileron deflections of these three controllers, it can be clearly seen that the fault has a direct effect on

Table 4.1: RMSE in the presence of a fault in aileron.

Control Approach	$\beta$	$\alpha$	$\mu$
Active FTC	0.0061	0.1036	0.0208
Adaptive FTC [178]	0.0956	17.58	2.0746
NDI [179]	14.615	14.700	491.0362

the aileron for an amplitude of 55 degrees with the NDI control technique, while it is successfully compensated using the proposed technique. The adaptive FTC damped the fault in the aileron but had some harsh effects on the other actuators. This harsh effect is due to the fact that the suggested ANN works based on the error in the actuation system and tries to damp the error without considering the system performance. From these figures, it can be also seen that fault in aileron has no significant effect on the other actuators in the proposed active FTC, while this has a significant impact on the other actuators using other techniques. This impact is due to the fact that NDI and adaptive FTC controller try to make the system stable using other actuators; however, according to Figure 4.4, the NDI and adaptive FTC were not successful in tracking the desired attitude commands. In order to compare the tracking error of the proposed controller with the adaptive FTC and the NDI controller numerically, the root mean square error (RMSE) is calculated using the following formula

$$RMSE = \sqrt{\frac{\sum_{i=1}^N (Command - Tracking)^2}{N}} \quad (4.31)$$

The results are shown in Table.4.1. The numerical analysis results in Table. 4.1 clearly show that the proposed method has significant advantages in compensating for the effect of the fault in the aircraft attitude tracking system.

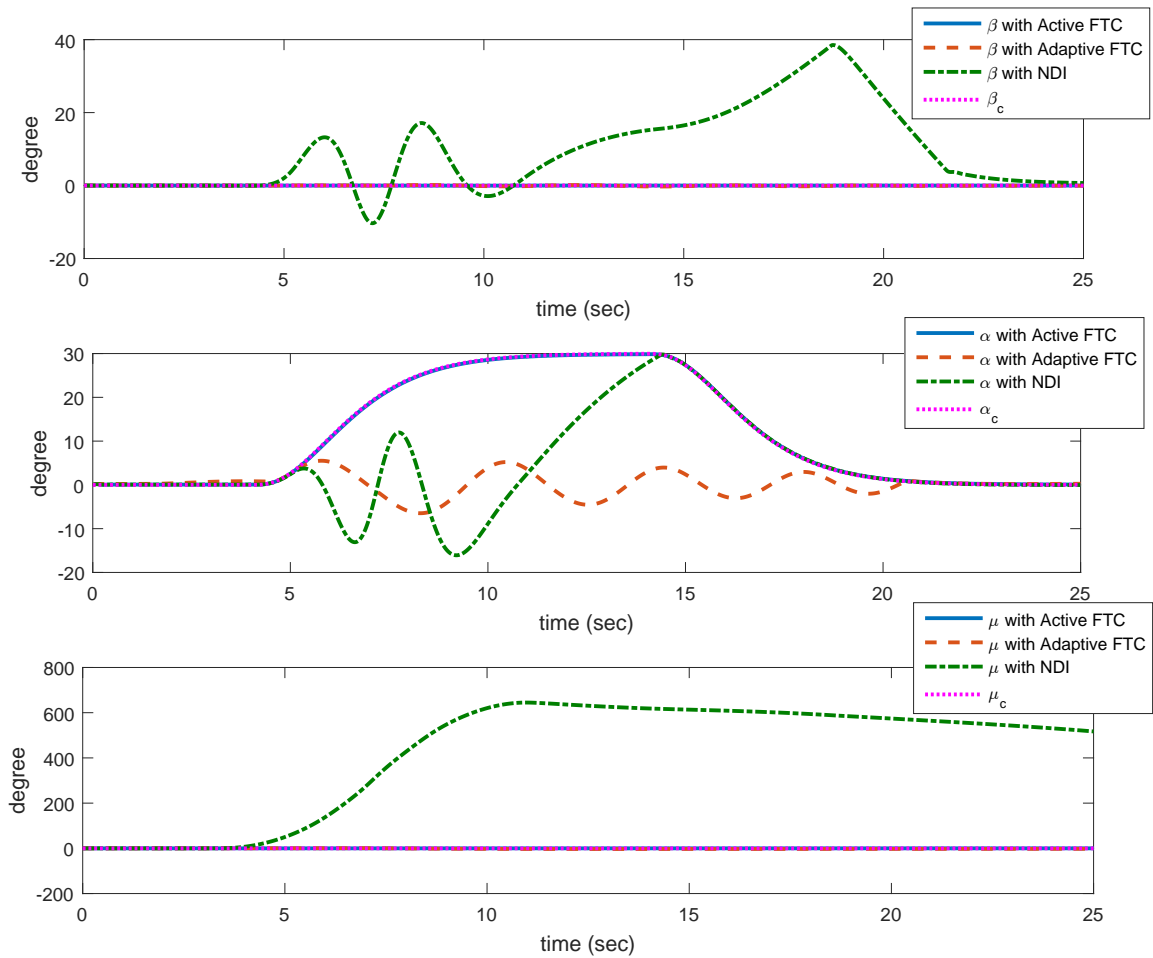


Figure 4.4: Attitude tracking control of the aircraft in presence of fault in the aileron actuator.

### 4.5.2 Fault in the Elevator

In the second scenario, the triangular fault was also applied to the elevator, and the NNAS was able to detect the applied fault accurately. Figure 4.6 shows that the proposed active FTC controller successfully tracks the given commands in the presence of the fault in the elevator. It should also be mentioned that the angle of attack ( $\alpha$ ) control has a direct relationship to the elevator actuator. Figure

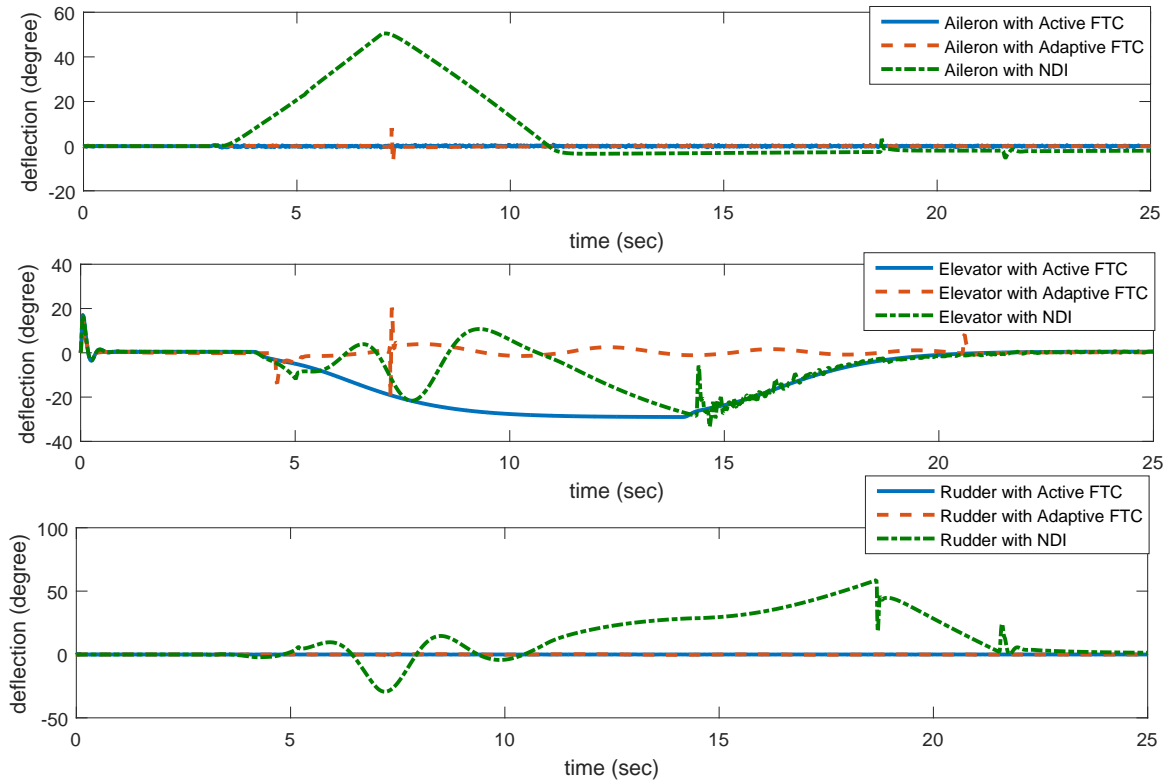


Figure 4.5: Actuator deflections in the presence of a fault in the aileron actuator.

4.7 shows the actuators of the aircraft in the presence of faults in the elevator for the proposed active FTC, adaptive FTC, and NDI controller, respectively. It can be clearly seen that the fault has not disturbed the elevator actuation for the system designed with the proposed active FTC, while fault interrupted the elevator actuation in the NDI and the adaptive FTC. Moreover, it can be seen that FTC did not deteriorate the healthy actuators, while the NDI controller and adaptive FTC had a disruptive impact on the healthy actuators to keep the aircraft stable. Like the previous subsection, to demonstrate the advantages of the proposed active FTC numerically, the RMSE of tracking in the presence of a fault in the elevator is shown in Table 4.2.

Table 4.2: RMSE in the presence of a fault in the elevator.

Control Approach	$\beta$	$\alpha$	$\mu$
Active FTC	0.00004	0.0922	0.000346
Adaptive FTC [178]	0.0026	17.23	0.0282
NDI [179]	0.000343	2.4885	0.00036

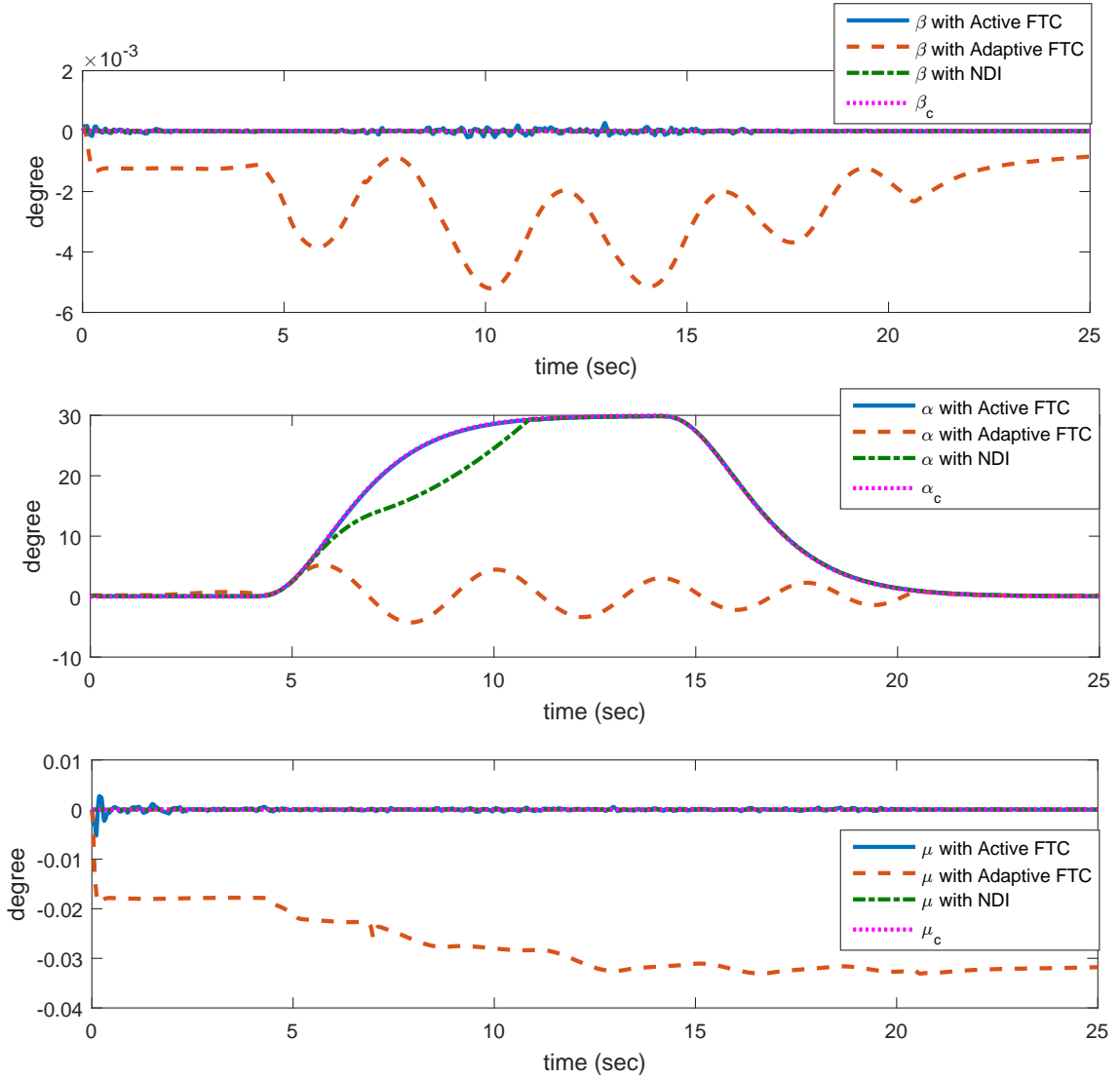


Figure 4.6: Attitude tracking control of the aircraft in presence of fault in the elevator actuator.

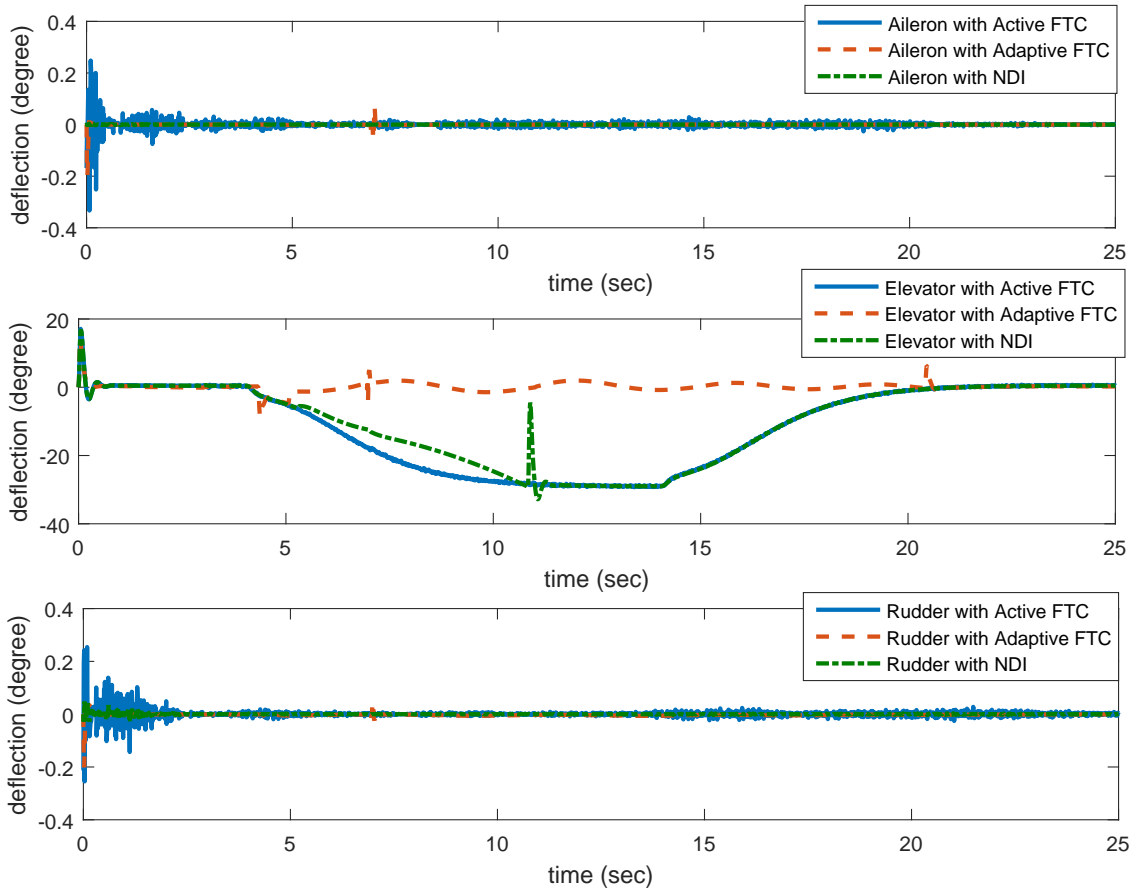


Figure 4.7: Actuator deflections in presence of fault in the elevator.

### 4.5.3 Fault in the Rudder

The third scenario investigates fault occurrence in the rudder and its effect on aircraft performance. Figure 4.8 shows that the proposed FTC design is not only able to tolerate the fault in the rudder but also can keep the control performance in a desired condition. The results show that the NDI control technique and adaptive FTC performances are degraded in the presence of fault in the rudder. Figure 4.9 shows the actuator deflections of the aircraft in the presence of fault in the rudder. Due to the fact that the rudder has direct relation with the side slip angle control and the

Table 4.3: RMSE in presence of fault in rudder.

Control Approach	$\beta$	$\alpha$	$\mu$
Active FTC	0.0201	0.1036	0.0033
Adaptive FTC [178]	0.0998	17.5117	0.1430
NDI [179]	5.9077	0.1090	11.35

desired side slip angle is zero, the rudder should try to keep its position in presence of the inserted fault. As it can be seen in Figure 4.9, the proposed active FTC was able to keep the rudder position in presence of large amount of fault (with the amplitude of one radian), while the NDI and the adaptive FTC were not able to control the fault in the actuator. In addition, it can be seen that the applied fault does not have any significant impact on the other actuators using the proposed active FTC, while the NDI and adaptive FTC influenced the operation of other actuators to keep the aircraft stable but they were not successful in tracking the reference attitudes. To demonstrate the advantages of proposed active FTC numerically, the RMSE of the tracking commanded attitudes from the pilot in presence of fault in the rudder are calculated and presented in Table.4.3.

## 4.6 Conclusion

This chapter introduced a novel active FTC design for UAV systems. The proposed design consists of an ANN-based FDI system, a nonlinear dynamic inversion (NDI) based flight controller, and a new feedback structure which compensated the occurred fault based on the information received from the FDI system. Active FTC design helped to detect and reduce the effect of faults in the actuators in the real-time and eliminated the needs for reconfiguring the controller structure. A six-DoF model of WVU YF-22 aircraft was used to evaluate the proposed FTC design through numerical simulation. The simulation result showed that the proposed

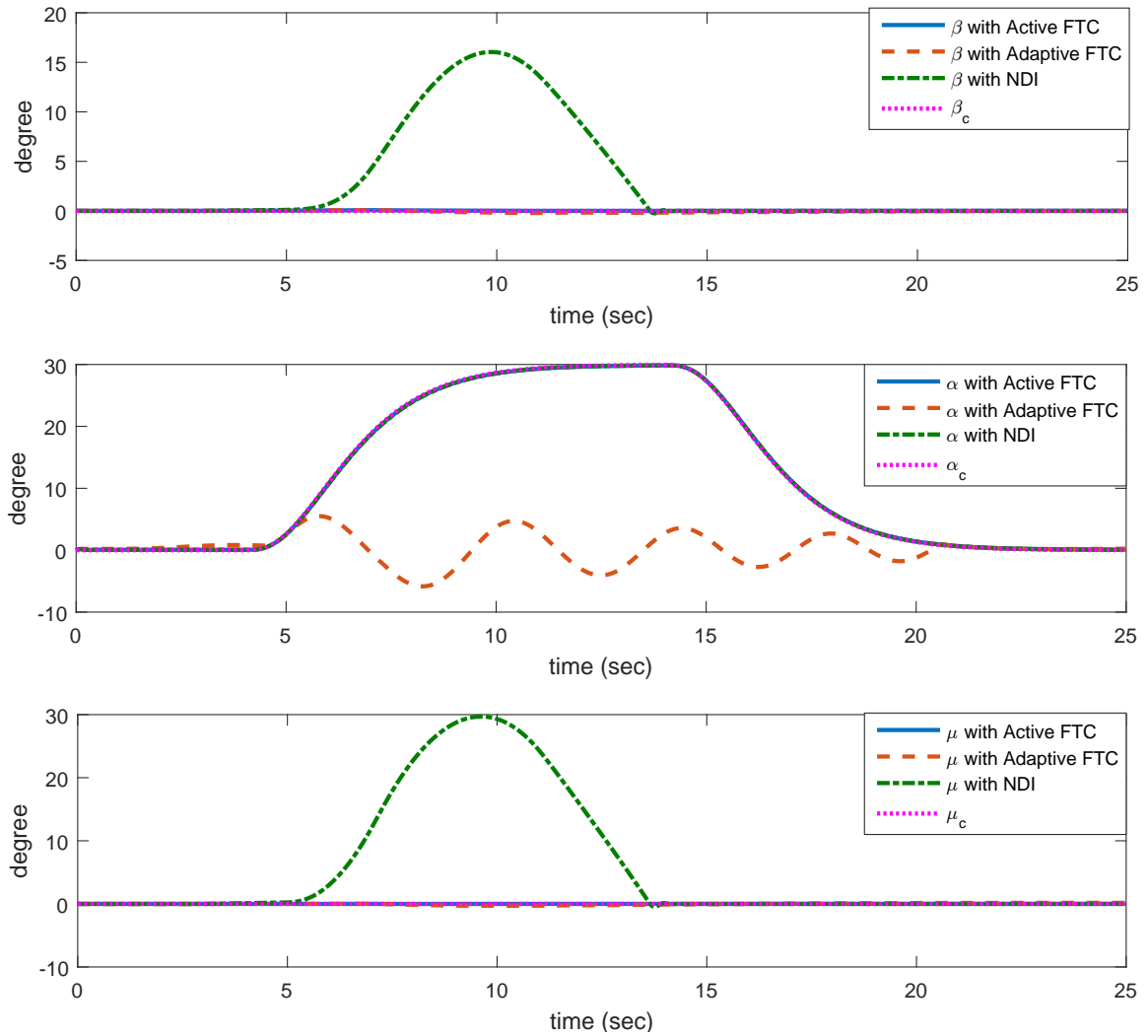


Figure 4.8: Attitude tracking control of the aircraft in the presence of fault in the rudder actuator.

strategy has significant tolerance against faults in the actuator and helps to keep the control performance without any interruption in presence of faults in the actuator. In this strategy, NNAS came to action when a fault happened in the actuators and did not limit the controller performance; moreover, the accurate fault detection in this design helped to avoid any significant interruption in presence of actuator faults in the control performance.

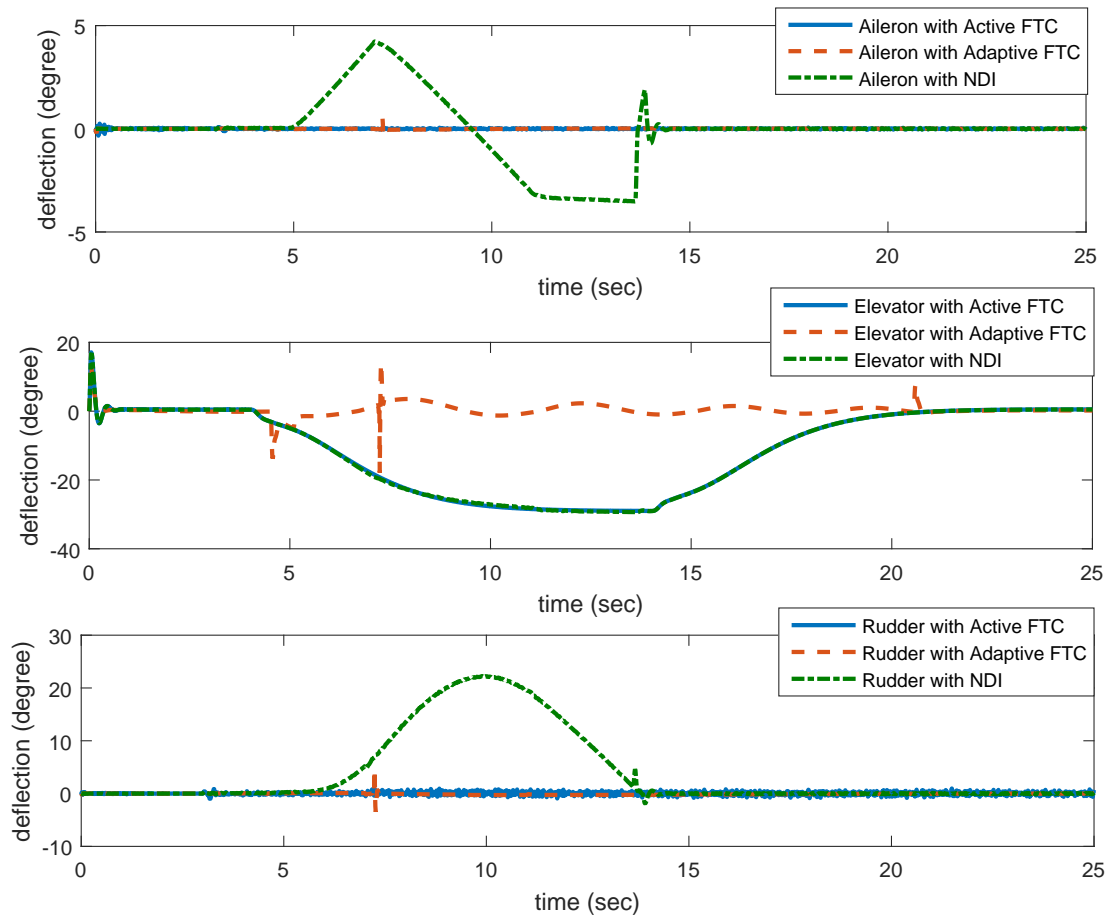


Figure 4.9: Actuator deflections in presence of fault in the rudder.

## CHAPTER 5

# A NEURAL NETWORK-BASED ACTIVE FAULT-TOLERANT DESIGN FOR PRESSURE CONTROL IN PROTON EXCHANGE MEMBRANE FUEL CELLS

### 5.1 Introduction

This chapter introduces a novel controller design for pressure control in proton exchange membrane (PEM) fuel cells. The proposed controller is able to control the system under fault/failure of the actuators. The introduced design uses an artificial neural network (ANN) for online fault detection and isolation (FDI) in the pressure valves of the PEM fuel cell (PEMFC). A nonlinear controller based on feedback linearization (FBL) technique is designed to compensate for the fault effects in real time. The simulation results clearly show that the proposed active fault-tolerant control (FTC) design can accurately detect, estimate and track the PEMFC actuators faults and failure, and compensate for their negative impacts while following the desired control performances. The rest of this chapter investigates the importance of having a reliable controller in PEMFC system, the recent achievements in the field of FTC design for PEMFC systems, and the main contributions of this chapter.

Achieving a clean, reliable, and sustainable energy source is one of the urgent needs, that has received a great deal of attention among the researchers in the past several years. Among various approaches in energy production, proton exchange membrane (PEM) fuel cell is a suitable candidate for both stationary and portable applications. In the PEM fuel cells (PEMFCs) electricity and water are produced through a chemical reaction between Oxygen and Hydrogen; therefore, it is con-

sidered as a green and clean energy source. In this process, pressure control is not only important in obtaining a reliable electricity production but also plays an important role in the PEMFC stack life [181–183]. An accurate control of air pressure in PEMFC helps to prevent damages to the membranes that would increase the life-cycle of the PEMFC. Various control approaches have been applied to control the PEMFC varied from linear [184] to nonlinear [185, 186] strategies. However, most of the control strategies assume that all of the components in the system work perfectly. For this reason, they might not provide a satisfactory result in the presence of faults and failures in the system components. Therefore, resiliency and robustness of control system against faults and failures have received a great attention among the control designers in the recent decades [183, 187–190].

Fault tolerant control (FTC) design deals with the control of the system in the presence of faults in the system. These kinds of controllers are mainly divided into two categories [191]: passive FTC [188, 192–194], and active FTC [23, 25, 27, 28, 187, 195–197]. Passive control strategies do not consider the size of fault or where it occurred. In other words, their performance does not rely on fault detection. Instead, they use a fixed compensator or switching among a bank of predefined controllers to reduce the effect of the potential faults in the system. For example, Bianchi et al. introduced a passive FTC named unfalsified control (UC) for PEMFC [188]. Their proposed UC consisted of a bank of controllers, and the falsified controller will be replaced by another remaining controller (unfalsified) from the bank of the controller. However, there is no guarantee that the controllers in the bank can achieve the desired performance in the presence of faults. Passive FTCs have been widely used due to their simplicity and low computation load [188, 192–194]; however, they have three major drawbacks: (1) most of the passive FTCs use hardware redundancy to tackle the fault problem which increases the cost and weight of the product; (2)

they are susceptible to large faults; (3) the passive FTC design is commonly based on some conservative restrictions that might limit the nominal performance of the system. Therefore, most of the recent studies focused on the active FTC systems.

Active FTCs perform based on the received fault detection (FD) data and use them to tackle the fault problem in the control system. Various FD and control techniques have been used widely for PEMFC. However, there is still a need for more research to have a united FD and FTC design.

Artificial neural networks (ANNs) are an ideal mathematical tool to estimate the system dynamics due to their nonlinear function estimation property and learning ability. ANNs have been widely used for fault detection [187, 198–200]. Kamal et al. introduced a radial basis function (RBF) neural network to obtain faults in the actuators and sensors of the PEMFC system [198]. Their RBF-based neural network FD design could detect faults up to 10% of the nominal value of the parameter. Wu et al. used a backpropagation NN to simulate the normal behavior of the PEMFC system and detect flooding by comparing the simulated data with the actual performance of the PEMFC; then, based on the occurred fault, a reconfiguration mechanism decides which backup controller to be used [187]. In their later work, they introduce an active FTC controller for a solid oxide fuel cell (SOFC) which switches among the predefined optimal PID controllers based on the detected fault [195]. Their proposed controller worked well under predefined faults. However, the performance of the controller under unknown faults was not investigated. A self-tuning PID controller with a neural-based fault detection was used to design an active FTC system for water management of a PEMFC system [199]. The designed FTC system was able to detect faults in the actuators. Despite the mentioned advantages of ANNs, their heavy computation load for estimation of complex systems may make them

inappropriate for real-time FD applications. Machine learning (ML) based algorithms have also been used for fault detection in the fuel cell system. In a recent work, an ML-based approach based on support vector machine (SVM) learning was introduced to diagnose a fault in an SOFC system [201]. Despite the acceptable accuracy of ML-based approaches, the need for substantial training data and huge computation load are two drawbacks that hindered the broad application of them in fuel cell systems.

The model-based observer is another tool that can be applied for detection of faults in the systems [202–204]. Rosich et al. introduced a nonlinear model-based observer design for sensor fault detection in PEMFC system [202]. The model-based observers are very dependent on the model accuracy, and a small deviation from the model or uncertainties would lead to false fault alarm. Lira et al. used a linear parameter varying (LPV) model of PEMFC to design a model-based FD system [203]. They obtained the LPV model from linearizing the nonlinear model around a set of operating points. A fault diagnosis strategy was introduced based on modified super-twisting (ST) sliding mode control technique for PEMFCs system by Liu et al. [204]. Their proposed FD system consisted of two linear and two nonlinear terms to estimate states and detect fault signals. A fault scenario, i.e., sudden air-leak in air supply manifold was considered, and their proposed FD system could detect faults with sufficient accuracy. Davoodi et al. introduced a linear matrix inequality approach to detect faults and control them in a linear time-invariant (LTI) model [205]. As it mentioned before, the model-based observers are sensitive to the model accuracy where LPV and LTI models are not sufficiently accurate to be applied for detection of faults in a highly nonlinear plant like PEMFC air-feed model.

To tackle the problem of inaccuracy in the model-based observer and the computational load in ANN, a combination of these two methods was suggested to estimate the unmodeled and uncertain dynamics of the system and reduce the computation load by using the model-based observer data [?, 129, 159]. Talebi et al. introduced an integrated recurrent ANN nonlinear observer to design an FD system for sensor and actuator faults in a satellite [129]. Abbaspour et al. introduced an extended Kalman filter (EKF) approach to improve the accuracy and speed response of the ANN observer in fault detection and isolation in nonlinear systems. However, the works in [129, 159] did not propose any solution for fault compensation. ANN has been widely used for fault compensation [23, 25, 27, 28, 197]; however, neither of these works did locate and isolate the fault in the system, and they used the ANN observer to compensate the actuation error in the system analytically. This kind of fault compensation does not identify the fault location and cannot be used for further supervision procedures, e.g., control reconfiguration or actuator replacement. Moreover, in case of failure in the actuator, they cannot keep the system performance in the desired condition, which motivates the present research work.

In this chapter, a unified framework for the detection of faults/failures and compensation of its effect in PEMFC system is proposed. The proposed FD system gives us the fault/failure data and location which is used to design an active FTC for nonlinear model of PEMFC system. The proposed active FTC design consists of a feedback linearization (FBL) controller, an ANN-based FD feedback structure that can reduce the fault effect in the actuators by compensating for the detected fault in the actuator system, and a fault analyzer algorithm which is developed to use the redundant actuator in case of actuator failure. To the best of my knowledge, the problem of designing an active FTC controller for nonlinear systems which can detect the fault and failure, and compensate for it in real-time has not been solved

for PEMFC system. The proposed active FTC design is implemented and evaluated on a nonlinear model of the PEMFC system. The simulation results show that the proposed active FTC system has successfully detected the fault/failure in the actuator and reduced its effect on the system in real time. The main contributions in this chapter can be summarized as 1) a novel active FTC design for nonlinear systems to compensate faults and failures without the need of control reconfiguration is designed for the first time, 2) the FD system and the active FTC controller are designed based on the nonlinear model of the PEMFC which increases the accuracy of the proposed design. 3) the proposed design can detect and compensate for simultaneous faults and failures in real-time.

The rest of this chapter is organized as follows: Section 2 describes the nonlinear dynamic model of PEMFC. In Section 3, the proposed FD system is presented. In Section 4, the design procedures of the proposed active FTC design for PEMFC system is illustrated. The simulation results of our proposed active FTC design are provided in Section 5. Finally, the concluding remarks are brought in Section 6.

## 5.2 PEMFC MODEL

This section presents the dynamic model of the PEMFC [181], which will be used for designing the active FTC system. The anode equations are described as:

$$\begin{aligned} \dot{P}_{H_2} = \frac{RT}{V_a} & \left( u_{H_2} k_a Y_{H_2} \lambda_{H_2} - C_1 I_{fc} \right. \\ & \left. - (u_{H_2} k_a \lambda_{H_2} - C_1 I_{fc}) F_{H_2} \right) \end{aligned} \quad (5.1)$$

$$\begin{aligned} \dot{P}_{H_2 O_a} = \frac{RT}{V_a} & \left( u_{H_2} k_a \lambda_{H_2} \frac{\phi_a P_{vs}}{P_{H_2} + P_{H_2 O_a} - \phi_a P_{vs}} \right. \\ & \left. - (u_{H_2} k_a \lambda_{H_2} - C_2 I_{fc}) F_{H_2 O_a} - C_2 I_{fc} \right) \end{aligned} \quad (5.2)$$

and the equations of the cathode side are

$$\begin{aligned} \dot{P}_{O_2} = & \frac{RT}{V_c} \left( u_{O_2} k_c Y_{O_2} \lambda_{O_2} - \frac{C_1}{2} I_{fc} \right. \\ & \left. - (u_{O_2} k_c Y_{N_2} \lambda_{O_2} - \frac{C_1}{2} I_{fc}) F_{O_2} \right) \end{aligned} \quad (5.3)$$

$$\dot{P}_{N_2} = \frac{RT}{V_c} \left( u_{O_2} k_c Y_{N_2} \lambda_{O_2} - u_{O_2} k_c \lambda_{O_2} F_{N_2} \right) \quad (5.4)$$

$$\begin{aligned} \dot{P}_{H_2O_c} = & \frac{RT}{V_c} \left( u_{O_2} k_c \lambda_{O_2} \frac{\phi_c P_{vs}}{P_{O_2} + P_{N_2} + P_{H_2O_c} - \phi_c P_{vs}} + C_1 I_{fc} \right. \\ & \left. - (u_{O_2} k_c \lambda_{O_2} + C_1 I_{fc} + C_2 I_{fc}) F_{H_2O_c} + C_2 I_{fc} \right) \end{aligned} \quad (5.5)$$

where the anode and cathode variables are denoted by subscript of 'a' and 'c', respectively.  $u_{H_2}$  and  $u_{O_2}$  are the input control variables, which are the flow rates of Hydrogen and Oxygen gases, respectively;  $k_a$  and  $k_c$  are the conversion factors;  $Y_{O_2}$ ,  $Y_{H_2}$ , and  $Y_{N_2}$  are the initial mole fractions of Oxygen, Hydrogen and Nitrogen which are set as 0.21, 0.99, and 0.79, respectively;  $\lambda_{H_2}$  is the ratio of the Hydrogen supplied to the anode side,  $\phi_a$  and  $\phi_c$  are the humidity on the anode side and cathode side, respectively;  $I_{fc}$  is the current density of the fuel cell;  $P_{vs}$  is the pressure of the saturation;  $F_{O_2}$ ,  $F_{H_2}$ ,  $F_{N_2}$ ,  $F_{H_2O_a}$ ,  $F_{H_2O_c}$ ,  $C_1$  and  $C_2$  are some defined factors to simplify the representation of the dynamic model equations and they are

$$\begin{aligned} F_{O_2} &= \frac{P_{O_2}}{P_{O_2} + P_{N_2} + P_{H_2O_c}}, & F_{H_2} &= \frac{P_{H_2}}{P_{H_2} + P_{H_2O_a}} \\ F_{N_2} &= \frac{P_{N_2}}{P_{O_2} + P_{N_2} + P_{H_2O_c}}, & F_{H_2O_a} &= \frac{P_{H_2O_a}}{P_{H_2} + P_{H_2O_a}} \\ F_{H_2O_c} &= \frac{P_{H_2O_c}}{P_{O_2} + P_{N_2} + P_{H_2O_c}}, & C_1 &= \frac{NA_{fc}}{2F}, & C_2 &= 2.5368C_1 \end{aligned} \quad (5.6)$$

where  $F$  is the Faraday constant.

The following MIMO nonlinear system with disturbances is constructed to obtain an affine model to control the Oxygen and Hydrogen pressure in the PEMFC [206]:

$$\begin{aligned} \dot{x} &= f(x) + g_1(x)u_{H_2} + g_2(x)u_{O_2} + p(x)d \\ y &= [y_1, y_2]^T = [P_{H_2}, P_{O_2}]^T = [h_1(x), h_2(x)]^T \end{aligned} \quad (5.7)$$

where

$$x = \begin{bmatrix} P_{H_2} \\ P_{H_2O_a} \\ P_{O_2} \\ P_{N_2} \\ P_{H_2O_c} \end{bmatrix}, u = \begin{bmatrix} u_{H_2} \\ u_{O_2} \end{bmatrix}, y = \begin{bmatrix} P_{H_2} \\ P_{O_2} \end{bmatrix}, d = I_{fc}; \quad f(x) = 0;$$

$$g_1(x) = RT\lambda_{H_2} \begin{bmatrix} \frac{k_a Y_{H_2}}{V_a} - \frac{k_a}{V_a} F_{H_2} \\ \frac{k_a \phi_a P_{vs}}{V_a(P_{H_2} + P_{H_2O_a} - \phi_a P_{vs})} - \frac{k_a}{V_a} F_{H_2} \\ 0 \\ 0 \\ 0 \end{bmatrix}, \quad (5.8)$$

$$g_2(x) = RT\lambda_{air} \begin{bmatrix} 0 \\ 0 \\ \frac{k_c Y_{O_2}}{V_c} - \frac{k_c}{V_c} F_{O_2} \\ \frac{k_c Y_{N_2}}{V_c} - \frac{k_c}{V_c} F_{N_2} \\ \frac{k_c \phi_c P_{vs}}{V_c(P_{O_2} + P_{N_2} + P_{H_2O_c} - \phi_c P_{vs})} - \frac{k_c}{V_c} F_{H_2O_c} \end{bmatrix}$$

$$p(x) = RT \begin{bmatrix} \frac{C_1}{V_a}(-1 + F_{H_2}) \\ \frac{C_1}{V_a}(-1 + F_{H_2O_a}) \\ \frac{C_1}{2V_c}(-1 + \frac{P_{H_2O_a}}{P_{O_2} + P_{N_2} + P_{H_2O_c}}) \\ 0 \\ -\frac{C_1}{V_c}(1 + F_{H_2O_c}) + \frac{C_2}{V_c}(1 - F_{H_2O_c}) \end{bmatrix}$$

As it can be seen in Equation (5.7), the input-output behavior of the system is nonlinear and coupled. Considering Equation (5.7), the PEMFC dynamic model with faults in the actuator can be described as follows:

$$\dot{x} = f(x) + g_1(x)u_{H_2} + g_2(x)u_{O_2} + p(x)d + F(x, t) \quad (5.9)$$

where  $F(x, t)$  is the fault in the PEMFC actuators. Figure 5.1 shows the overall structure of a PEMFC with its air pressure control unit.

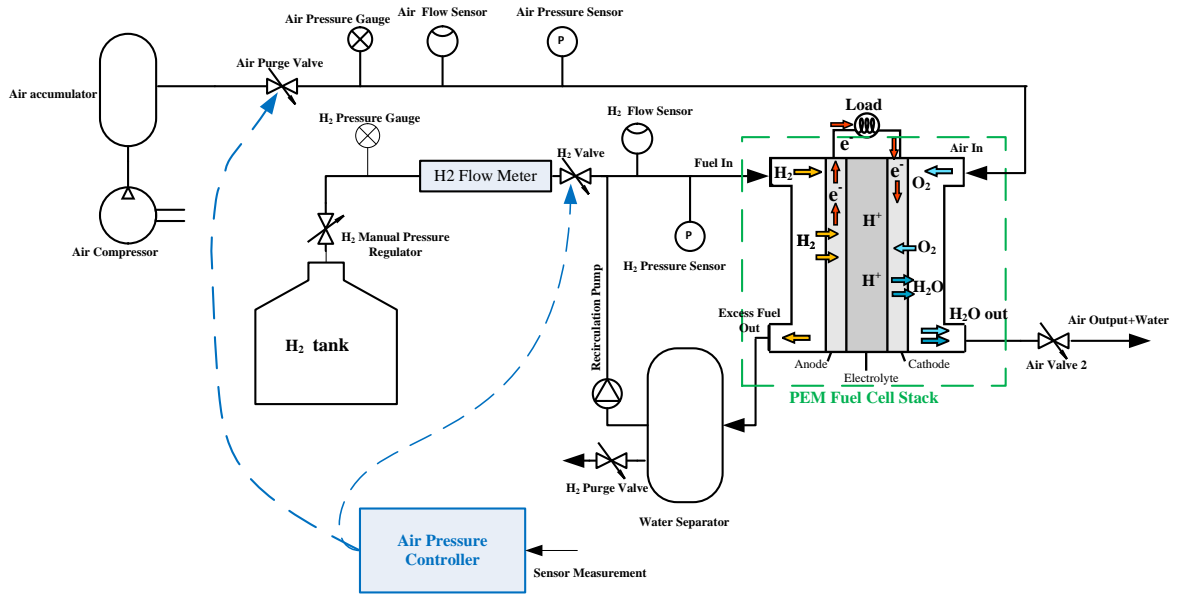


Figure 5.1: The diagram of the operation and air pressure control of the PEMFC.

### 5.3 FD Design

A new design for actuator fault detection (FD) in PEMFC is introduced in this section. The proposed FD system is designed based on a nonlinear observer and a neural network adaptive structure (NNAS). The proposed NNAS is described as

follows

$$M_i(t) = W_i(t)\sigma(V_i(t)\delta_i(t)) \quad (5.10)$$

where  $M(t)$  is the output of neural network observer and the subscript  $i$  denotes the  $i$ th vector of  $M(t)$  for  $i = 1, \dots, n$ .  $W_i(t)$  and  $V_i(t) = [V_{i,1}(t), \dots, V_{i,m+n}(t)]$  are the weights associate with the  $i$ th output of the NNAS at time  $t$ . Here,  $\delta_i(t)$  can be defined as  $\delta_i(t) = [M_i(t - \tau), \dots, M_i(t - m\tau), e_i(t - \tau), \dots, e_i(t - n\tau)]^T$ . Here,  $\tau$  indicates the sampling period or the step size of the observer;  $e_i(t) = y_i(t) - \hat{y}_i(t)$ , and  $\sigma(\bullet)$  is the sigmoid activation function in the form of  $\sigma = (1 - e^{-x})/(1 + e^{-x})$ . In terms of the  $i$ th element  $M_i(t)$  of  $M(t)$  for  $i = 1, \dots, n$ , the ANN observer can be represented as

$$M_i(t) = W_i(t)\sigma(Z_i(t)) \quad (5.11)$$

where

$$Z_i(t) = \sum_{j=1}^m V_{i,j}(t)M_i(t - j\tau) + \sum_{j=1}^n V_{i,m+j}(t)e_i(t - j\tau) \quad (5.12)$$

The input of the observer  $M(t)$  is recursively updated with the previous  $m$  samples of the observer inputs for  $j = 1, 2, \dots, m$ , and also previous  $n$  samples of the system output error  $e_i(t - j\tau)$  for  $j = 1, 2, \dots, n$ . Here,  $m$  and  $n$  are chosen based on the needed speed response in the system. Large values of  $m$  and  $n$  guaranty the convergence of the training; however, they may increase the computation time and add unnecessary delays [159].

### 5.3.1 ANN Weight Update Law

It is well known that online tuning of ANN weights helps to improve the response speed of the ANN detection [159]. In this paper, an EKF is used for online updating

of the ANN gains. The EKF updating parameter can be described by [159]:

$$\theta_i(k) = [W_i(k), V_{i,1}(k), \dots, V_{i,m+n}(k)]^T \quad (5.13)$$

where  $k$  is the  $k$ th sampling instant, and  $t = k\tau$ . The Kalman gain and the updating rules can be defined as follows [159]

$$\begin{aligned} \theta_i(k) &= \theta_i(k-1) + \eta K_i(k)[y_i(k) - \hat{y}_i(k)] \\ K_i(k) &= P_i(k)H_i(k)[H_i(k)^T P_i(k)H_i(k) + R_i(k)]^{-1} \\ P_i(k+1) &= P_i(k) - K_i(k)H_i(k)^T P_i(k) \end{aligned} \quad (5.14)$$

where  $\eta$  is the learning coefficient,  $P_i(k)$  is the covariance matrix of the state estimation error,  $K_i(k)$  is the Kalman gain, and  $R_i(k)$  is the covariance matrix of the estimated noise which is computed recursively by [159]:

$$R_i(k) = R_i(k-1) + [e_i^T(k)e_i(k) - R_i(k-1)]/k \quad (5.15)$$

And  $H_i(k)$  is the derivative of  $e_i(k)$  with respect to  $\theta_i$ . Based on the observer input in (5.13),  $H_i(k)$  can be calculated as follow:

$$\begin{aligned} H_i(k) &= \frac{\partial e_i(k)}{\partial \theta_i} \Big|_{\theta_i = \theta_i(k-1)} \\ &= \begin{cases} \sigma(Z_i(k)), & \theta_i = W_i \\ W_i(k)M_i(k-j)\sigma(Z_i(k)), & \theta_i = V_{i,j} \\ W_i(k)e_i(k-j)\sigma(Z_i(k)), & \theta_i = V_{i,m+j} \end{cases} \end{aligned} \quad (5.16)$$

Since  $M_i(t)$  is updated at each sample time, its updating process can be described with the following equation:

$$M_i(k+1) = W_i \sigma \left( \sum_{j=1}^m V_{i,j} M_i(k-j+1) + B_i(k) \right) \quad (5.17)$$

where  $B_i(k) = \sum_{j=1}^n V_{i,m+j} e_i(k-j+1)$ . The prove of the stability of EKF updating can be found in our previous work [159].

### 5.3.2 Actuator FD design for PEMFC

In this subsection, the nonlinear observer design for the actuators of the PEMFC system will be illustrated, then, application of of this observer for the proposed actuator FD in a PEMFC system will be explained. In this study, faults in the pressure valve of the actuators of the PEMFC are considered. There are two main actuators in the air pressure control of the PEMFC:  $u_{H_2}$  and  $u_{O_2}$  are electronic valves for regulating Hydrogen and Oxygen gas pressure in the PEMFC.

Considering Equation (5.7) and  $f(x) = 0$  in (5.8), the control law  $u$  can be extracted as follows

$$u = G^{-1}(x)(v - p(x)d) \quad (5.18)$$

where  $v = [\dot{y}_1, \dot{y}_2]^T$ ,  $G(x)$  is the decoupling matrix. The matrix  $G(x)$  is exponentially stable for large enough gain in the controller design [162]. The control variable  $u$  showed up after the first derivative of  $y_1 = P_{H_2}$  and  $y_2 = P_{O_2}$ , so the relative degree

vector  $[r_1 \ r_2]$  is  $[1 \ 1]$ , and  $G(x)$  can be defined as

$$\begin{aligned}
 G(x) &= \begin{bmatrix} L_{g_1} h_1(x) & L_{g_2} h_1(x) \\ L_{g_1} h_2(x) & L_{g_2} h_2(x) \end{bmatrix} \\
 &= \begin{bmatrix} \frac{RT\lambda_{H_2}}{V_a}(k_a Y_{H_2} - k_a F_{H_2}) & 0 \\ 0 & \frac{RT\lambda_{O_2}}{V_c}(k_c)Y_{O_2} - k_c Y_{N_2} F_{O_2} \end{bmatrix} \\
 u &= \begin{bmatrix} u_{H_2} \\ u_{O_2} \end{bmatrix}, y = \begin{bmatrix} y_1 \\ y_2 \end{bmatrix}, d = I_{fc},
 \end{aligned} \tag{5.19}$$

$$p(x) = RT \begin{bmatrix} \frac{C_1}{V_a}(-1 + F_{H_2}) \\ \frac{C_1}{2V_c}(-1 + \frac{P_{H_2}O_a}{P_{O_2} + P_{N_2} + P_{H_2}O_c}) \end{bmatrix}$$

where  $L_{g_1}$  and  $L_{g_2}$  are the Lie derivative of  $g_1$  and  $g_2$ , respectively. Considering (5.18), the FD system for PEMFC can be designed as follows

$$\begin{aligned}
 \hat{u} &= G^{-1}(x)(v - p(x)d) \\
 \tilde{u} &= u - (\hat{u} + M(t))
 \end{aligned} \tag{5.20}$$

where  $\hat{u}$  is the output of the nonlinear observer of the actuator that can be obtained by substituting  $p(x)$  and  $G(x)$  in (5.19) into (5.20),  $M(t)$  is the NNAS output, and  $\tilde{u}$  is the FD error which is the input to the ANN.

## 5.4 Active FTC Design

In this section, the proposed active FTC system design is illustrated. The active nonlinear FTC controller which is designed based on FBL technique, received data

from the FD system, and a fault analyzer block is illustrated in the following subsections.

### 5.4.1 FBL Controller

FBL controller is one of the most common and efficient nonlinear control strategies used in the field of PEMFC control [181]. This control technique uses feedback signal to cancel the inherent nonlinear dynamic in the system and eliminates the common needs of gain scheduling in comparison with the linear control strategies. Considering (5.9-5.19), the nonlinear control law for Hydrogen and Oxygen pressure control in PEMFC can be derived as

$$u = G^{-1}(x) \left( \begin{bmatrix} \dot{P}_{H_2D} \\ \dot{P}_{O_2D} \end{bmatrix} - p(x)d \right) \quad (5.21)$$

where  $\dot{P}_{H_2D}$  and  $\dot{P}_{O_2D}$  are the derivatives of the desired value of Hydrogen and Oxygen pressure that can be obtained using a linear stabilizer controller, i.e., a proportional-integral (PI) controller [181].

### 5.4.2 FTC Design

The FTC design introduced in this paper consists of a nonlinear FBL controller and the online NNAS fault detection system. Here, we illustrate how to link the nonlinear controllers and the NNAS fault detection system.

Considering the nonlinear FBL control law in (5.21), the actuator fault in (5.9), and the detected fault in (5.11), the nonlinear FTC law to compensate for the occurred fault in the real time can be written as

$$u = G^{-1}(x) \left( \begin{bmatrix} \dot{P}_{H_2D} \\ \dot{P}_{O_2D} \end{bmatrix} - p(x)d - M(t) \right) \quad (5.22)$$

where  $M(t)$  is the output of the NNAS which is the detected fault using online FD system.

### 5.4.3 Fault Analyzer

In order to guarantee the system performance from severe faults/failure that cannot be tackled by analytical redundancy, we introduced a fault analyzer (FA) block to our controller to put a redundant actuators in the control loop. In the FA block, 0.2 second time is given to the analytical redundancy to fix the problem and if it cannot fix the fault/failure problem, the redundant actuator will be in the control loop to fix it. Algorithm 1 is designed for fault analyzing. In the algorithm, an actuator failure is considered as a situation that the fault is not fixed after 0.2 second analytical fault compensation and there still 0.1 per unit (pu) fault in the system. Figure 5.2 shows the block diagram of the proposed FTC system and the stability of the proposed design is investigated in the following subsection.

```

while  $\|M(t) - u(t)\| \geq 0.1pu$  do
    |  $t_f = t_f + 0.01$ ;
    | if  $t_f \geq 0.2$  then
    | | Switch on redundant actuator;
    | else
    | | Do not involve the redundant actuator;
    | end
end

```

**Algorithm 1:** Fault Analyzer Algorithm.

## 5.5 Numerical Simulation

Numerical simulations have been performed to examine the performance of the proposed control strategy in the presence of fault and failure in the PEMFC actuators.

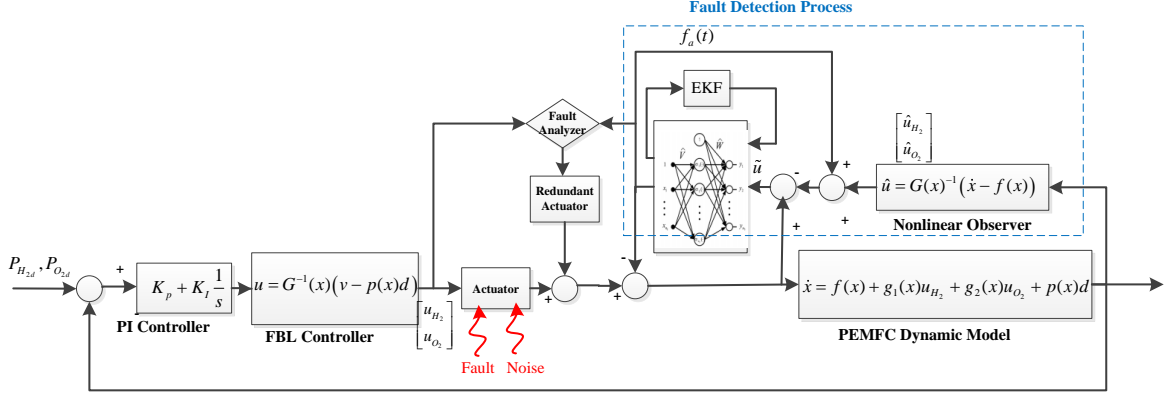


Figure 5.2: Block diagram of the proposed active FTC controller for PEMFC.

For simplicity, we will not consider the fuel processor, air compressor model, and water management. The PEMFC model parameters used in this paper are based on fuel cell system Ballard MK5-E-based PGS105B and can be found in [181]. To validate the behavior of the dynamic model, the simulation results of the model behavior were compared with the results in [207]. The PEMFC stack used in our simulation has totally 35 series connected cells, and the area of each cell is  $232 \text{ cm}^2$ . The purpose of the designed controller is to regulate the Hydrogen and Oxygen pressure to 3 atmosphere in the PEMFC stack. The temperature of the stack at the air outlet is kept between  $72^\circ\text{C}$  and  $75^\circ\text{C}$  to maximize the output power. The simulations are done with MATLAB SIMULINK on a core i7 desktop computer. In the proposed active FTC system, the initial values of the NNAS parameters are selected as follows:  $P_0 = 15 \times \text{eye}(3)$ ,  $\theta_0 = [2, 2, 2]^T$ ,  $R_0 = 2 \times 10^{-5}$ ,  $K = 1$ , and  $y_0 = 0.1$ . These values are selected based on the system performance and the designer objectives. The load profile connected to the PEMFC is shown in Fig. 5.3. Two scenarios have been considered in the simulations: 1) Fault in the actuator, 2) Simultaneous actuator faults and failure.

### 5.5.1 Fault in the actuator

In this scenario, a step fault which is shown in Fig.5.4 is inserted into the PEMFC actuators, i.e., Hydrogen and Oxygen pressure valves. To show the advantages of the proposed method, its performance is compared with that of the simple FBL controller [181] and the result is illustrated in the following.

Figure 5.4 shows that the designed FD system can successfully detect the fault in the PEMFC actuators. As it can be seen, there are some small overshoots at the beginning of the fault detection process that are eliminated by training of the ANN after a portion of a second. This kind of fault can occur for various reasons, e.g., severe vibrations, metal flakes, actuator inaccuracy, improper connection of electrical wires to the actuators, etc. [159]. This detection of a fault in the PEMFC actuators helps the controller to reduce the fault effect on the system performance which can be seen in Figs. 5.5 and 5.6. Figure 5.5 shows the performance of the pressure valves of the PEMFC stands along fault effects, which compares the proposed FTC with the FBL controller in damping the fault effect. This figure shows that the proposed strategy successfully reduces the fault effect in the Hydrogen and Oxygen pressure valves, while the FBL controller is unable to damp the inserted fault in the actuators. Figure 5.6 shows the fault effect on the performance of the controller in controlling the air pressure. In this figure, it can be seen that in the proposed active FTC, the fault cannot deteriorate the control performance and the pressure of the PEMFC can track the desired value (3 atm). The comparison of the performance between FTC and FBL controller in Fig. 5.6 demonstrates that the FBL controller is not effective in reduction of the fault effect in the system and its performance will be degraded severely in the presence of a fault in the actuators. The fault tolerance ability of the system is demonstrated in Figs. 5.5-5.8 and this ability helps to

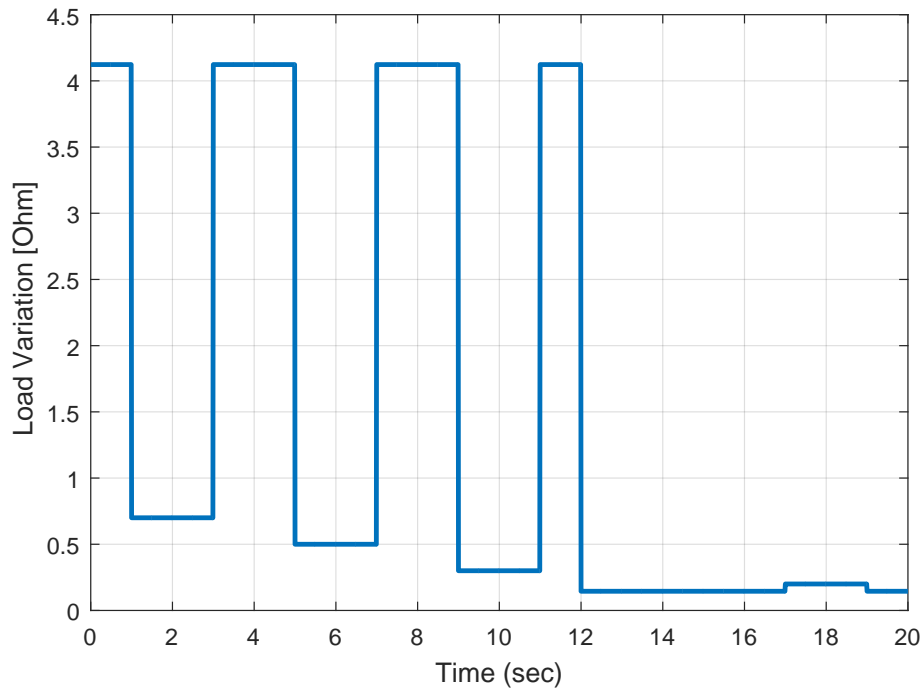


Figure 5.3: The load profile of connected to the PEMFC.

have stable and reliable energy production. Moreover, accurate pressure control in PEMFC prevents membrane damages and subsequently increases the lifetime of the PEMFC system [181].

### 5.5.2 Simultaneous Actuator Faults and Failure

In the second scenario, we examined the proposed control system performance against a simultaneous fault and failure on Hydrogen pressure valves. This kind of faults and failure can happen when the system has actuator malfunction, and at the same time, some faults or false data is injected into the control structure. The goal of this scenario is to test the system performance against one of the worst incidents that can happen to a PEMFC system. The step fault in Fig. 5.4 is repeated in this scenario, and a short circuit failure in the Hydrogen pressure valve occurs

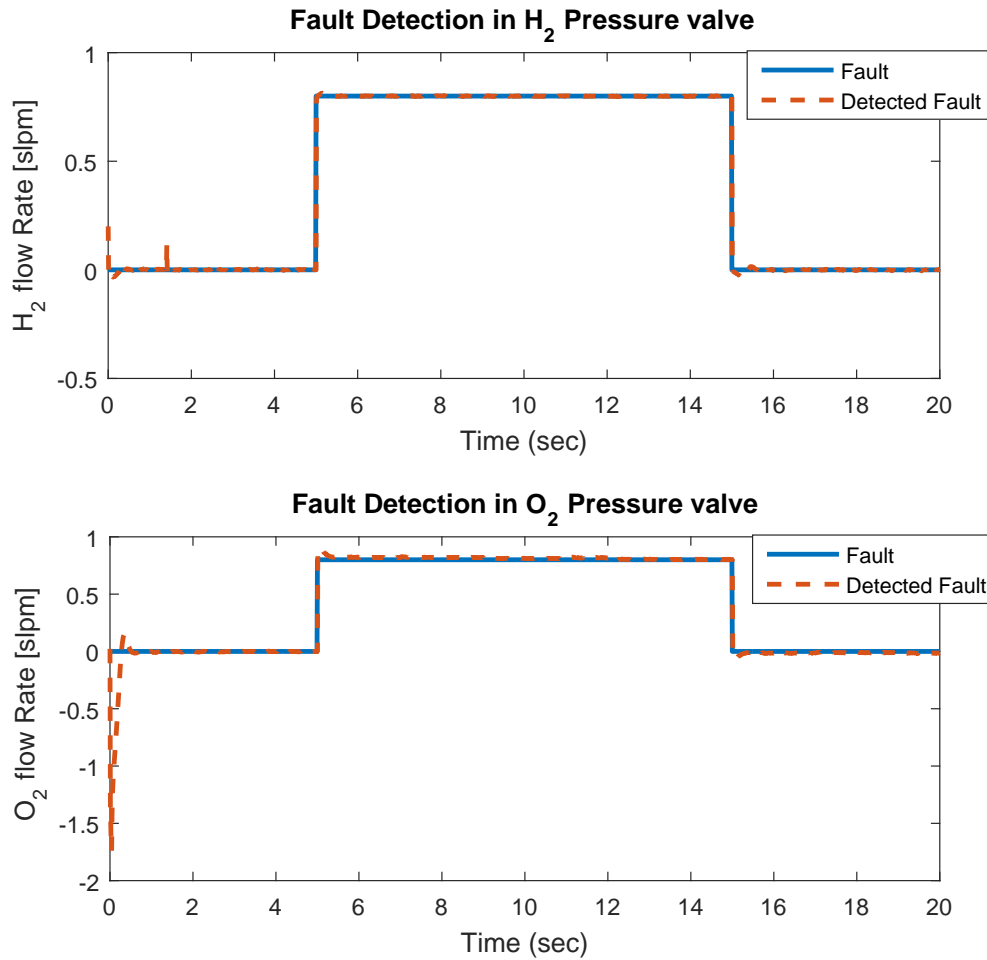


Figure 5.4: Fault detection in actuators of PEMFC.

between the second 8 to the end of the simulation. Figs. 5.7 and 5.8 compare the performance of the proposed controller with the FBL controller. As it can be seen in Fig. 5.7, the pressure valve in FBL controller is directly affected by the fault and at the second 6 by the short circuit failure while the FTC system switches to the redundant actuator and the false data in the feedback system are compensated through FD system. Fig. 5.8 shows that FTC can keep the desired pressure in the presence of faults and failure while the FBL lost its stability.

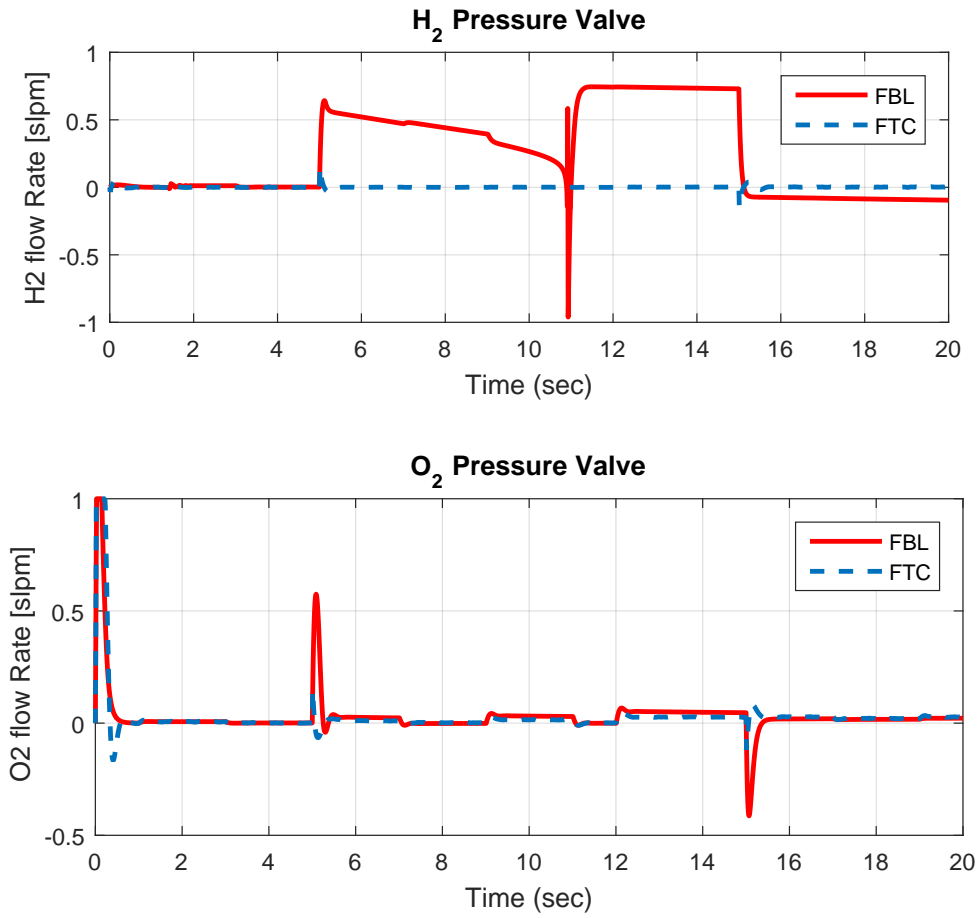


Figure 5.5: Fault effect on the actuators.

## 5.6 Conclusion

In this chapter, a novel active FTC design is introduced to control the gas pressures in the PEMFC in the presence of faults in the actuators. The simulation results showed that the proposed control design is able to detect and reduce the effect of faults in the actuator in real time. This tolerance against faults helps to maintain the PEMFC gas pressure at the desired values, keeping the PEMFC in a desirable condition and subsequently lengthen its lifetime. In order to demonstrate the advantages of our proposed active FTC system, the results were compared with the FBL

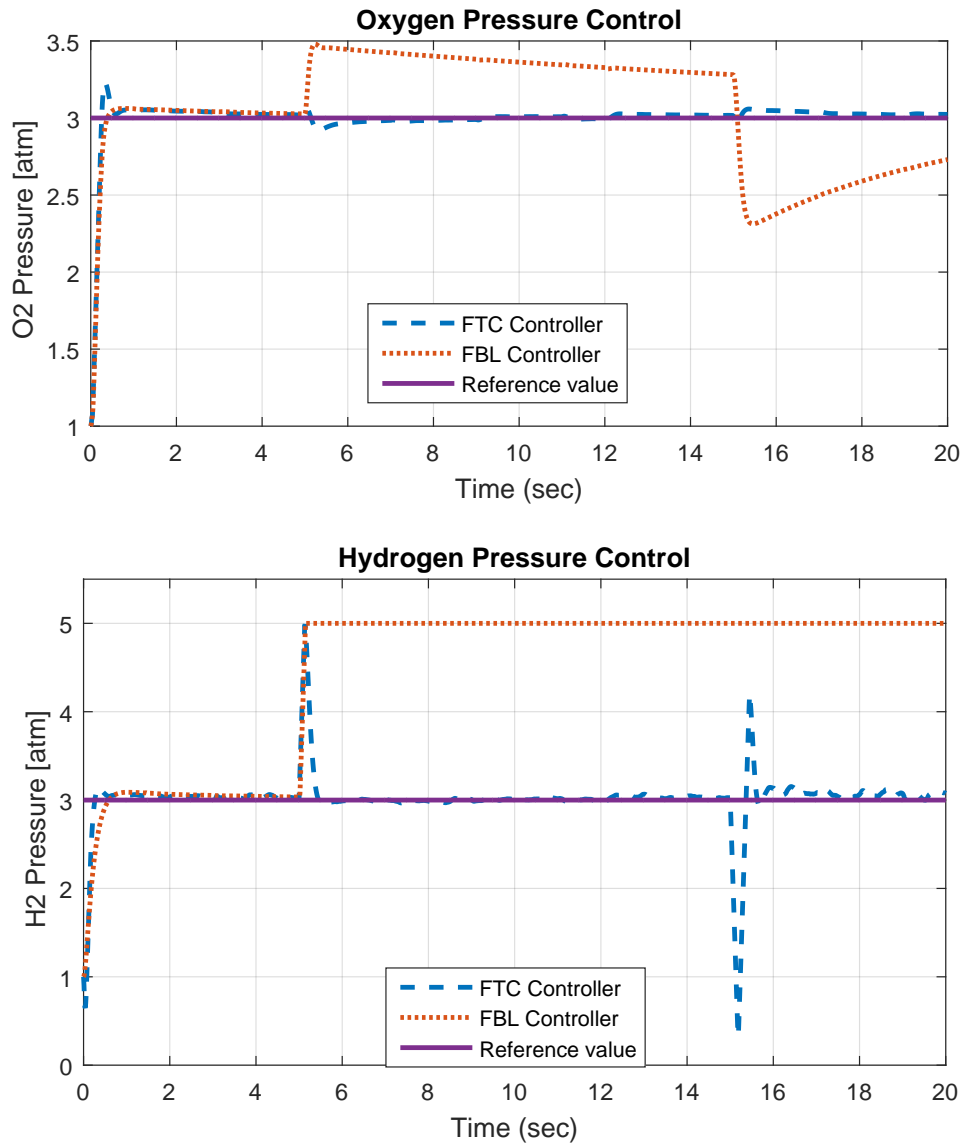


Figure 5.6: Pressure control in the presence of a fault in the actuators.

control system. The outcome of the simulation showed the significant advantage of the proposed design in the presence of faults in the actuators.

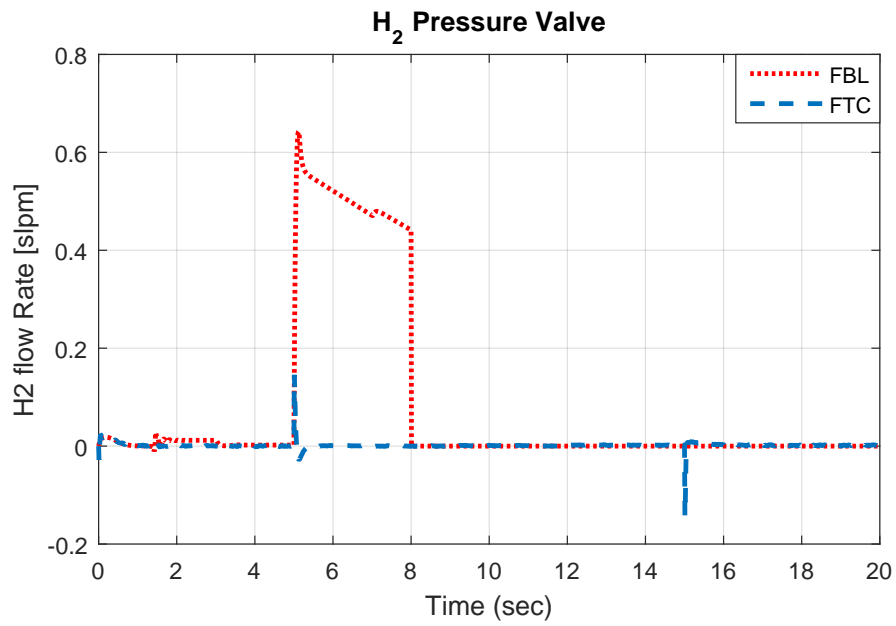


Figure 5.7: Fault effect on the actuators.

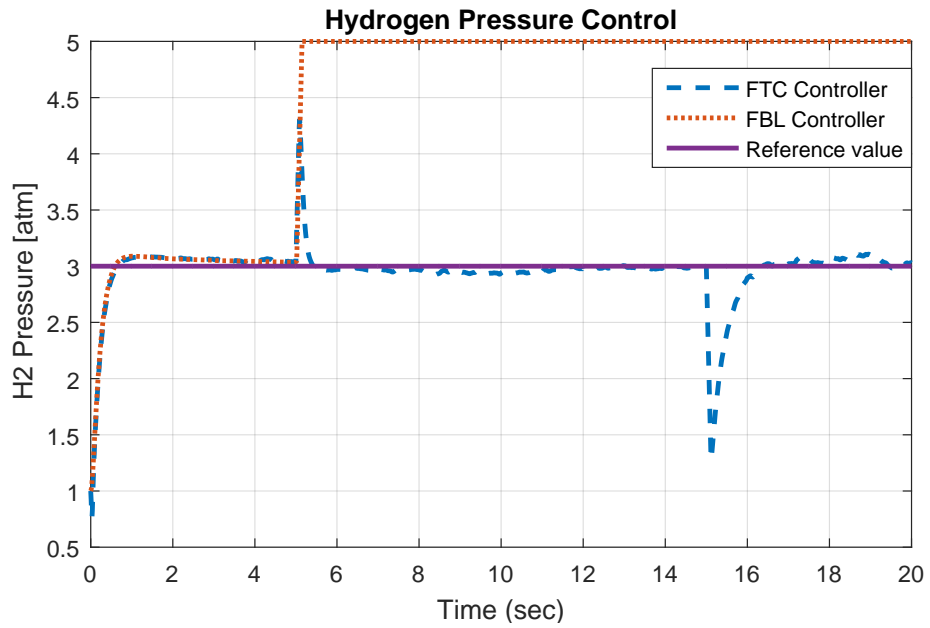


Figure 5.8: Pressure control in the presence of a fault in the actuators.

CHAPTER 6

**RESILIENT CONTROL DESIGN FOR LOAD FREQUENCY  
CONTROL OF POWER GRID SYSTEM UNDER FALSE DATA  
INJECTION ATTACKS**

## **6.1 Introduction**

The power grid is identified as one of the critical infrastructures for our nation. Smart power grids are being enhanced by adding communication infrastructure to improve their reliability, sustainability, and efficiency. Despite all of these great advantages, these open communication architecture and connectivity renders the power systems' vulnerability to a range of cyber attacks. This chapter proposes a novel active resilient control system for distributed power systems (DPSs) under false data injection (FDI) attacks. The proposed system is able to jointly detect and mitigate FDI attacks on nonlinear power systems. The design works based on a new anomaly detection (AD) technique which consists of a Luenberger observer and an artificial neural network (ANN). Since FDI attacks can happen rapidly, the observer structure is enhanced by Extended Kalman filter (EKF) to improve the ANN ability for the online detection and estimation. The resilient controller is designed based on the attack estimation, which can eliminate the need for control reconfiguration. The resiliency of the proposed design against FDI attacks is tested on a Load Frequency Control (LFC) system. The simulation results clearly show that the proposed active resilient control system can successfully detect anomalies and compensate for their negative effects. In the rest of this section, a brief introduction of the AD approaches in power systems, the importance of FDI attack detection, and our main contributions are discussed.

Anomalies can cause destructive effects on the control system performance by disturbing the integrity of sensor data. These anomalies can occur due to malicious cyber-attacks, faults, and failures in the system components. FDI attack, a type of cyber-attack that aims the integrity of data, is emerging as a serious threat to smart grid systems, which can degrade the system performance or endanger its stability [5,8,135,190]. Faults and failures in the system components are also threatening the system performance and stability, and can occur at any moment due to various reasons such as metal flakes, severe vibrations, short circuits, overloads, malicious attempts, etc [159,208].

Even small FDI attacks can cause a major problem in the power system and can disturb the lives of consumers, government corporations and businesses if they are not timely diagnosed and tackled [209]. Thus, an accurate anomaly detection (AD) and a resilient control strategy are needed to detect and keep the system reliable. An adversary can inject FDI attacks to power grid network. Attacking one node can affect the other nodes by redistributing the load to them, which can cause cascade overload and consequently failure in the interconnected network [210]. A major cyber-attack can be as devastating as the North-eastern blackout which occurred in August 2003. This Incident was one example of the cascade failure in the power grids and clearly shows that our power grids are vulnerable. Therefore, there is a need for the resilient and intelligent controller to prevent such incidents [210].

The role of load frequency control (LFC), in a smart grid, is to keep the desired frequency and power interchanges at the desired level [211]. Resiliency in an LFC system improves the reliability of the power grid system. The very first step in designing an LFC system resilient to anomalies in data integrity is to develop an accurate AD system. The detection algorithm should be able to provide information on size, location and time of the intrusion in real-time [52].

In FDI attacks, false data are injected maliciously to the original data to damage the system operation or breaking the communication between the system components [212]. In [213], the effects of an FDI attack on a smart grid system was investigated. A hardware platform was introduced in [214], to examine the impact of FDI attacks on microgrid performance index, i.e., the total load lost, the frequency nadir, and the time needed to reach frequency stability.

In this work, sensor spoofing is considered as the main scenario of the FDI attack. Sensor spoofing can be defined as injecting false data to the sensors of the system in a way that are not detectable by the bad data detection algorithms [215]. Thus, a second defending mechanism is needed to keep the system secure.

Phasor measurement units (PMUs) in smart grids is one of the potential gates that the attacker can inject malicious data into the system through sensor spoofing. In PMUs, the global positioning system (GPS) is used for sub-station clock synchronization. Thus, by mimicking the GPS signal, the attacker can alter the GPS time estimation in the PMU [215,216]. These induced errors in time estimation will lead to wrong phase angle measurement in the PMU. The role of PMU in the LFC system is the acquisition of time-synchronized measurements of its state variables. PMUs are able to process the synchronized measurements of the states of the LFC system at a rate up to 120 samples/second which makes them superior to conventional sensors of the supervisory control and data acquisition (SCADA) systems [217].

An accurate AD mechanism is necessary to report/monitor faults, failures, and FDI attacks in real time. Numerous studies have been done for the detection of anomalies and FDI attacks in power systems using different techniques. In

general, they can be classified into two approaches: 1) model based approaches [9, 10, 52, 218, 219], and 2) learning based approaches [220–226].

In model-based approaches, an observer based on the model dynamics is used to estimate system dynamics, e.g., sliding mode observer (SMO) [9], Kalman filter [52, 218], weighted least square (WLS) observer [10], and principal component analysis (PCA) [219, 227]. An SMO-based detection approach was introduced by Ao et al. to detect FDI attacks in power system [9]. In their design, two sliding mode observer were used, one for attacks on the state estimation, and the other one for attacks on the sensor measurements. An FDI detection framework based on the Kalman filter and  $\chi^2$  observer was introduced by Mandhar et al. [52]. In their design, Kalman filter estimates the grid states and  $\chi^2$  trigger the alarm in case of an intrusion. Deng et al. introduced a WLS-based FDI attack-detection framework where the WLS observers were used to construct the residuals, and the residuals were compared with the predefined threshold to judge whether any attacks occurred or not [10]. In [219] and [227], PCA was used to ensure the integrity of the data in state estimation of the power grid by filtering of faulty measurements. Despite the advantages of model-based approaches in real-time anomaly detection and low computation, their pure dependency on a mathematical model of the system makes them vulnerable to model uncertainties and disturbances.

Learning-based approaches include methods that use artificial intelligence for observing system states, e.g., artificial neural networks (ANN) [220–222], machine learning approaches [223–226]. The property of nonlinear function estimation and the learning ability of the ANNs make them ideal mathematical tools for dynamic system estimation. However, their heavy computation load for state estimation of

complex systems may make them inappropriate for real-time AD applications. Machine learning approaches also suffer from the same problem; moreover, they need substantial training data for different FDI attack scenarios.

Most of the researches mentioned above have focused on the detection and estimation of FDI attacks in power systems. However, none of them can detect and compensate FDI attacks automatically in the real time. Furthermore, most of the model-based estimation techniques for FDI attack detections relies on an accurate model of power systems and ignore the system uncertainties, nonlinearities, and noises. In this work, to tackle the problem of inaccuracy in the model-based observer and the computational load in ANN, we proposed a novel design based on their combination to estimate the unmodeled and uncertain dynamics of the system. Furthermore, the proposed technique reduces the computation load by using the model-based observer data. A Luenberger observer is designed based on the system dynamics and combined with a three layer feed-forward ANN to make it robust against model uncertainties. The ANN learning weights are updated by an extended Kalman filter (EKF) to improve its learning ability and reduce response time. Then, a resilient control system is devised to compensate for the occurred FDI attacks by using the information obtained by the detection algorithm. The stability of the proposed control design is mathematically proven using Lyapunov theory, and its advantages against FDI attacks are demonstrated through numerical simulations. The contributions of this chapter are: 1) designing a novel resilient control strategy to jointly detect and mitigate FDI attacks in real time for nonlinear power systems, 2) introducing a united framework for detection and control of LFC systems, 3) eliminating the need for control reconfiguration in presence of anomalies in the LFC system. 4) proving the stability of the proposed controller for the power

system under attacks.

The rest of this chapter is organized as follows: Section 6.2 illustrates the dynamic model of LFC system. Section 6.3 presents the design procedure of the proposed AD system while Section 6.4 illustrates the design strategy for the proposed resilient control system. Section 6.5 presents the simulation results of the proposed resilient system and investigates the results for different scenarios. Finally, Section 6.6 discusses the results and the conclusions of this chapter

## 6.2 LFC Model

The mathematical model of an interconnected multi-area power system is briefly described in this section. Each power area transmits sensor measurements to a centralized load frequency controller (LFC) to generate the appropriate control signals. The detail description of the model can be found in [5].

$$\begin{cases} \dot{X}(t) = AX(t) + BU(t) + D\Delta P_l + d(t) \\ Y(t) = CX(t) \end{cases} \quad (6.1)$$

where  $X(t) \triangleq [X_1(t)^T X_2(t)^T \cdots X_N(t)^T]^T \in \mathbb{R}^{m+N}$  and  $U(t) \in \mathbb{R}^{n+N}$  are the state and input vectors, respectively. The  $d(t)$  is a bounded disturbance. The  $\Delta P_l$  is the load deviation.  $N$  is the number of interconnected power areas and  $C$  is an identity matrix with appropriate dimensions. The states of the  $i^{th}$  power area are defined as  $X_i = [x_{i,1}(t)^T, x_{i,2}(t)^T, x_{i,3}(t)^T, x_{i,4}(t)^T, x_{i,5}(t)^T]^T$  where  $x_{i,1}$ ,  $x_{i,2}$ ,  $x_{i,3}$ ,  $x_{i,4}$  and  $x_{i,5}$  are frequency deviation  $\Delta f^i$ , generator power deviation  $\Delta P_g^i$ , turbine valve position  $\Delta P_{tu}^i$ , power flow of the tie-line  $\Delta P_{pf}^i$  and control error  $e^i$ , respectively. The power area control error is

$$e^i(t) = \int_0^t \beta^i \Delta f^i dt \quad (6.2)$$

where  $\beta^i$  is the frequency bias factor.

The  $A$ ,  $B$ ,  $C$  and  $D$  are constant matrices and can be defined as

$$A = \begin{bmatrix} A_{1,1} & A_{1,2} & \cdots & A_{1,N} \\ A_{2,1} & A_{2,2} & \cdots & A_{2,N} \\ \vdots & \vdots & \vdots & \vdots \\ A_{N,1} & A_{N,2} & \cdots & A_{N,N} \end{bmatrix} \quad (6.3)$$

$$B = \text{diag}\left\{ \begin{bmatrix} B_1^T & B_2^T & \cdots & B_N^T \end{bmatrix}^T \right\} \quad (6.4)$$

$$D = \text{diag}\left\{ \begin{bmatrix} D_1^T & D_2^T & \cdots & D_N^T \end{bmatrix}^T \right\} \quad (6.5)$$

where the matrix  $B_i$  and  $D_i$ ,  $A_{i,i}$  and  $A_{i,j}$  for  $i, j = 1, 2, \dots, N$  can be determined as follows

$$B_i = \begin{bmatrix} 0 & 0 & \frac{1}{T_{g,i}} & 0 & 0 \end{bmatrix}^T \quad (6.6)$$

$$D_i = \begin{bmatrix} -\frac{1}{J_i} & 0 & 0 & 0 & 0 \end{bmatrix}^T \quad (6.7)$$

$$A_{i,i} = \begin{bmatrix} \frac{-\mu_i}{J_i} & \frac{1}{J_i} & 0 & \frac{-1}{J_i} & 0 \\ 0 & \frac{-1}{T_{tu,i}} & \frac{1}{T_{tu,i}} & 0 & 0 \\ \frac{-1}{\omega_i T_{g,i}} & 0 & \frac{-1}{T_{g,i}} & 0 & 0 \\ \sum_{i=j=1}^2 2\pi T_{i,j} & 0 & 0 & 0 & 0 \\ \beta_i & 0 & 0 & 0 & 1 \end{bmatrix} \quad (6.8)$$

$$A_{i,j} = \begin{bmatrix} 0 & 0 & 0 & 0 & 0 \\ 0 & 0 & 0 & 0 & 0 \\ 0 & 0 & 0 & 0 & 0 \\ -2\pi T_{i,j} & 0 & 0 & 0 & 0 \\ 0 & 0 & 0 & 0 & 0 \end{bmatrix} \quad (6.9)$$

where  $T_{i,j}$  is the stiffness constant between the  $i^{th}$  and  $j^{th}$  power areas.  $J_i$ ,  $\omega_i$ ,  $\mu_i$ ,  $T_{g,i}$ , and  $T_{tu,i}$  are the  $i^{th}$  power area's moment of inertia of generator, the speed-droop coefficient, damping coefficient, the governor time constant, and turbine time constant.

## 6.3 Anomaly Detection

In this section, the proposed AD along with the resilient control structure are illustrated. The proposed AD system is able to detect anomalies in real time and consists of an ANN observer and a Luenberger observer that are explained in details in the following subsections.

### 6.3.1 ANN observer

Due to the fact that FDI attacks have no fixed pattern, and can be extremely nonlinear and unpredictable, an ANN is a suitable candidate for estimation of their behavior. The proposed anomaly observer, which consists of a Luenberger observer and an ANN, can be described by

$$\begin{aligned}\dot{\hat{X}} &= A\hat{X}(t) + Bu(t) + L(y - \hat{y}) \\ \hat{y} &= C\hat{X}(t) + O_s(t)\end{aligned}\tag{6.10}$$

where  $\hat{X}$  is the state vector of the Luenberger observer,  $L$  is the Luenberger gain, and  $O_s(t)$  is the ANN observer that defines as [159]:

$$O_{s_i}(t) = W_i(t)\sigma(V_i(t)\delta_i(t))\tag{6.11}$$

where  $O_{s_i}(t)$  is the  $i$ th vector of  $O_s(t)$  for  $i = 1, \dots, n$ .  $W_i(t)$  and  $V_i(t) = [V_{i,1}(t), \dots, V_{i,a+b}(t)]$

are the weights associate with the  $i$ th output of the ANN at time  $t$ . Here,  $\delta_i(t)$  can be defined as  $\delta_i(t) = [O_{s_i}(t - \tau), \dots, O_{s_i}(t - a\tau), e_i(t - \tau), \dots, e_i(t - b\tau)]^T$ . where  $\tau$  indicates the sampling period or the step size of the observer;  $e_i(t) = y_i(t) - \hat{y}_i(t)$ , and  $\sigma(\cdot)$  is a *tanh* activation function:

$$\sigma(x) = (1 - e^{-x}) / (1 + e^{-x}) \quad (6.12)$$

In terms of the  $i$ th element  $O_{s_i}(t)$  of  $O_s(t)$  for  $i = 1, \dots, b$ , the NN observer can be represented as

$$O_{s_i}(t) = W_i(t)\sigma(Z_i(t)) \quad (6.13)$$

where

$$Z_i(t) = \sum_{j=1}^a V_{i,j}(t)O_{s_i}(t - j\tau) + \sum_{j=1}^b V_{i,a+j}(t)e_i(t - j\tau) \quad (6.14)$$

The input of the observer  $O_s(t)$  is recursively updated with the previous  $a$  samples of the observer inputs for  $j = 1, 2, \dots, a$ , and also previous  $b$  samples of the system output error  $e_i(t - j\tau)$  for  $j = 1, 2, \dots, b$ . Here,  $a$  and  $b$  are chosen based on the needed accuracy and training time in the system. Large values of  $a$  and  $b$  guaranty the convergence of the training and the accuracy of the ANN; however, large values of them may increase the computation time and add unnecessary delays by increasing the training duration [159]. Furthermore, this is not helpful in case on non-periodic FDI attacks. Thus, to have a real-time and accurate anomaly detection,  $a$  and  $b$  should be chosen based on the needed accuracy and the system frequency response.

### 6.3.2 ANN update law

An active resilient LFC system needs a real-time anomaly detection performance, to this aim, ANN weights should be updated in a fast rate [160, 171]. In this study, we introduced an adaptive tuning algorithm based on EKF. The proposed algorithm

helps online updating of the ANN learning weights based on the EKF algorithm and guarantees the fast convergence rate of the ANN learning weights. The EKF updating parameter for the  $i$ th element of ANN can be described by [159]:

$$\theta_i(k) = [W_i(k), V_{i,1}(k), \dots, V_{i,a+b}(k)]^T \quad (6.15)$$

where  $k$  is the  $k$ th sampling instant, and  $t = k\tau$ . Using the EKF algorithm, the ANN parameters will be updated in each sampling time as follows [159]

$$\begin{aligned} \theta_i(k) &= \theta_i(k-1) + \eta_i K_i(k) [y_i(k) - \hat{y}_i(k)] \\ K_i(k) &= P_i(k) H_i(k) [H_i(k)^T P_i(k) H_i(k) + R_i(k)]^{-1} \\ P_i(k+1) &= P_i(k) - K_i(k) H_i(k)^T P_i(k) \end{aligned} \quad (6.16)$$

where  $\eta_i$  is the learning coefficient,  $P_i(k)$  is the covariance matrix of the state estimation error,  $K_i(k)$  is the Kalman gain, and  $R_i(k)$  is the covariance matrix of the estimated noise, which is computed recursively by [161]:

$$R_i(k) = R_i(k-1) + [e_i^T(k) e_i(k) - R_i(k-1)] / k \quad (6.17)$$

Here,  $H_i(k)$  is the derivative of  $e_i(k)$  with respect to  $\theta_i(k)$ . Based on the observer input in Equation (6.11),  $H_i(k)$  can be calculated as follow

$$\begin{aligned} H_i(k) &= \frac{\partial e_i(k)}{\partial \theta_i} \Big|_{\theta_i = \theta_i(k-1)} \\ &= \begin{cases} \sigma(Z_i(k)), & \theta_i = W_i \\ W_i(k) O_{s_i}(k-j) \acute{\sigma}(Z_i(k)), & \theta_i = V_{i,j} \\ W_i(k) e_i(k-j) \acute{\sigma}(Z_i(k)), & \theta_i = V_{i,a+j} \end{cases} \end{aligned} \quad (6.18)$$

### 6.3.3 Luenberger Observer

A Luenberger observer is designed to estimate the  $\hat{X}$ , and it sends the observed data to the ANN unit to reduce the computational load on the ANN. The ANN will use

the difference between Luenberger observer and system output as an input to detect the anomalies in the system. The rate of error for the proposed AD is defined as  $\tilde{\dot{X}}(t) = \dot{X}(t) - \hat{\dot{X}}(t)$ , and can be calculated by subtracting (6.10) from (6.1)

$$\tilde{\dot{X}}(t) = A\tilde{X}(t) + D\Delta P_l + d(t) - LC\tilde{X}(t) - LO_s(t) \quad (6.19)$$

Here, we neglected the nonlinear term  $D\Delta P_l$  to simplify the Luenberger design because it will be identified with the ANN observer ( $O_s(t)$ ), which yields

$$\tilde{\dot{X}}(t) = (A - LC)\tilde{X}(t), \quad \tilde{X}(0) = X_0 \quad (6.20)$$

$L$  is the Luenberger gain and should be defined in a way that the eigenvalues of the  $A - LC$  are all negative real values, then, the estimation error will converge to zero as  $t \rightarrow \infty$ .  $L$  can be calculated using pole placement method [228].

## 6.4 Controller Design

The proposed resilient control system consists of a linear quadratic regulator (LQR) controller and a feedback controller based on the received information from the AD system. The details of the control design and the stability analysis are illustrated in the following subsections.

### 6.4.1 Resilient Controller

In LQR control theory, we minimize a predefined cost function

$$J = \int_0^{\infty} [X(t)^T Q X(t) + u(t) R u(t)] dt \quad (6.21)$$

where  $R > 0$ , and  $Q \geq 0$  are symmetric, positive (semi-) definite matrices. The optimal control law using LQR approach is described by

$$u = -K(X(t)) \quad (6.22)$$

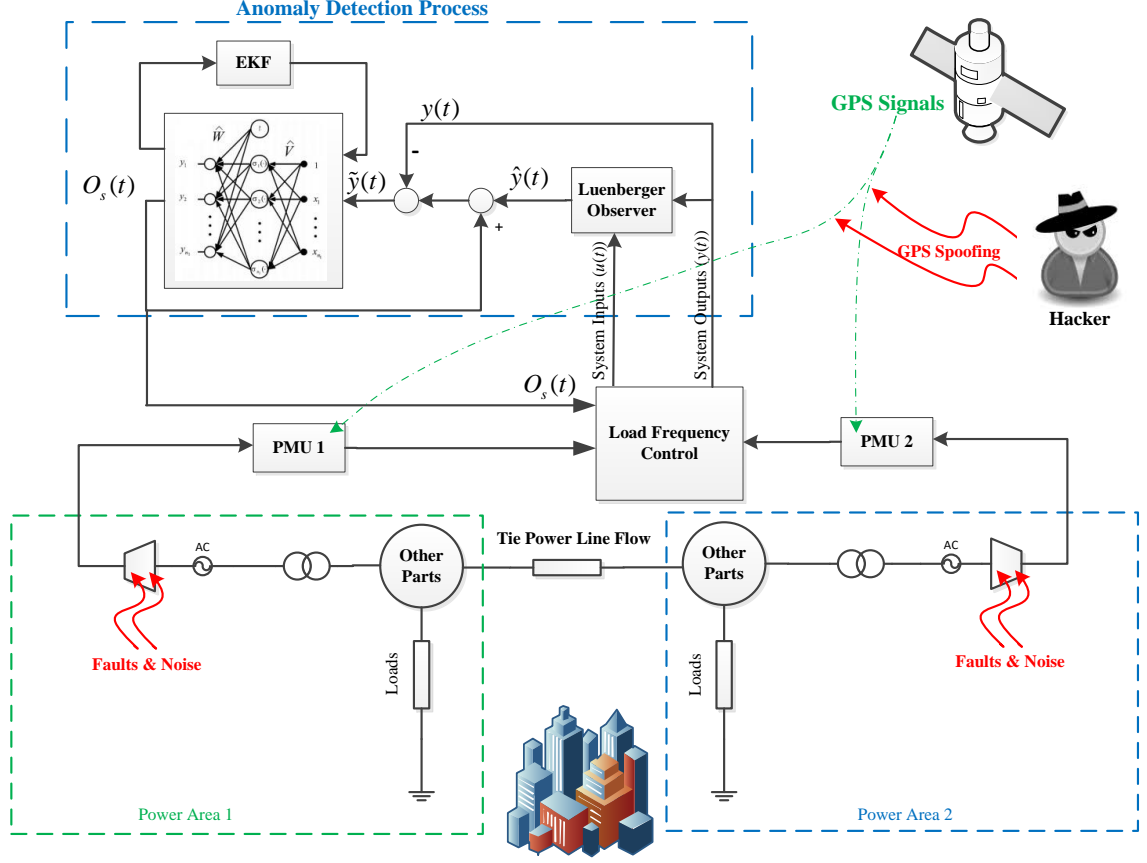


Figure 6.1: Overall diagram of the proposed control system.

where  $K = R^{-1}B^T P$  is the LQR control gain and  $P = P^T > 0$  is the solution of the following Riccati equation

$$PA + A^T + Q - PBR^{-1}B^T P = 0 \quad (6.23)$$

The resilient control law is defined as follows

$$u = -K(X - O_s(t)) \quad (6.24)$$

where  $K$  is the control gain that is obtained from the LQR technique, and  $O_s(t)$  is the AD signal. In case of an FDI attack in the system states, the AD system will detect it in real-time and will subtract it from the states of the system. The overall

diagram of the proposed resilient controller is depicted in Fig.6.1. The stability of the proposed control system is investigated in the following section.

## 6.5 Stability Analysis of the Controller

Here, we investigated the stability of the proposed resilient control system. Consider a general nonlinear system as follows

$$\begin{aligned}\dot{x}(t) &= f(x(t)) + g(x(t))u(t) \\ y(t) &= x(t) + A(t)\end{aligned}\tag{6.25}$$

where  $x(t)$  is the state vector,  $f(x(t))$  and  $g(x(t))$  are functions which separate the state parameters from the control function  $u(t)$ , and  $A(t)$  is the anomaly occurred in the system sensors. The following assumptions are considered in the stability proof of the controller designed for system described in Eq.(6.1).

**Assumption 1:** The state function  $f(x(t))$  can be differentiated at  $\hat{x}(t)$

$$\beta(t) = \left. \frac{\partial f(x(t))}{\partial x(t)} \right|_{x(t)=\hat{x}(t)}$$

where  $\beta(t)$  is an  $n \times n$  matrix.

Then, the Taylor series expansion of  $f(x)$  at  $\hat{x}$  can be presented as

$$f(x(t)) - f(\hat{x}(t)) = \beta(t)\tilde{x}(t) + \Theta(t)\tag{6.26}$$

where  $\Theta(t) = o(\|\tilde{x}(t)\|^2)$  contains the high order terms of the state estimation error. Here,  $\tilde{x}(t) = x(t) - \hat{x}(t)$ .

**Assumption 2:** The control input function  $g(x(t))$  satisfy the Lipschitz condition with the Lipschitz constant  $L_g$ , i.e.,

$$\|g(x(t)) - g(\hat{x}(t))\| \leq L_g \|\tilde{x}(t)\|$$

**Assumption 3:** The control input vector of the system is bounded by  $L_u$  and the anomaly in the actuator,  $A(t)$ , is bounded by  $L_F$ , i.e.,

$$\begin{aligned}\|u(t)\| &\leq L_u \\ \|A(t)\| &\leq L_F\end{aligned}$$

**Assumption 4:**  $\Theta$  is bounded by a positive real number  $L_\Theta$  such that

$$\|\Theta(\hat{x}(t), x(t))\| \leq L_\Theta \|\tilde{x}(t)\|$$

**Assumption 5:** The matrix  $P(t)$ , a symmetric matrix, that satisfies the following condition:

$$\lambda_{min} I_n \leq P(t) \leq \lambda_{max} I_n$$

where  $\lambda_{min}$  and  $\lambda_{max}$  are positive real numbers and  $P(t)$  can be found by solving the following Lyapunov equation:

$$\beta^T(t)P(t) + P(t)\beta(t) + \dot{P}(t) = -\Gamma \quad (6.27)$$

where  $\Gamma$  is a symmetric positive definite matrix.

Consider the observer equation as

$$\begin{aligned}\dot{\hat{x}} &= f(\hat{x}(t)) + g(\hat{x}(t))u(t) + L(y - \hat{y}) \\ \hat{y} &= \hat{x}(t) + O_s(t)\end{aligned} \quad (6.28)$$

where  $L$  is the Luenberger observer gain, and  $O_s(t)$  is the ANN signal. Now, by subtracting Eq.(6.28) from the Eq.(6.25), and substituting (6.26), the effect of the anomaly detection error on the system  $\tilde{x}(t)$  can be written as

$$\begin{aligned}\dot{\tilde{x}}(t) &= \dot{x}(t) - \dot{\hat{x}}(t) \\ &= \beta(t)\tilde{x}(t) + \Theta(t) + (g(x(t)) - g(\hat{x}(t)))u(t) \\ &\quad + L(-\tilde{x}(t) + O_s(t) - A(t))\end{aligned} \quad (6.29)$$

*Theorem:* With Assumptions 1-5, the FDI-attack effect in Equation (6.29) is bounded on  $\tilde{x}(t)$  if the following condition is satisfied

$$\eta_{min}(\Gamma) > 2L_{\Theta}\lambda_{max} + 2L_gL_u\lambda_{max} + 2LL_a\lambda_{max} \quad (6.30)$$

where  $\|O_s(t) - A(t)\| \leq L_a\|\tilde{x}(t)\|$ .  $\lambda_{max}$  and  $L_a$  are both finite positive constant.

*Proof:* A Lyapunov function is selected as follows

$$V(\tilde{x}(t), t) = \tilde{x}(t)^T P(t)\tilde{x}(t) \quad (6.31)$$

Based on Assumption 5, we can conclude that  $V(\tilde{x}, t) \geq 0$  for the estimation error  $\tilde{x}(t)$ . Now for the stability consideration of the proposed FTC system we need to show that  $\dot{V}(\tilde{x}, t) < 0$ . The derivative of the  $V(\tilde{x}, t)$  with respect to time  $t$  can be expressed as

$$\dot{V}(\tilde{x}, t) = \dot{\tilde{x}}(t)^T P(t)\tilde{x}(t) + \tilde{x}(t)^T \dot{P}(t)\tilde{x}(t) + \tilde{x}(t)^T P(t)\dot{\tilde{x}}(t) \quad (6.32)$$

By substituting  $\tilde{\hat{x}}(t)$  in Equation (6.29) into  $\dot{V}(\tilde{x}(t), t)$  in (6.32), we have

$$\begin{aligned}
\dot{V}(\tilde{x}, t) &= \left( \beta(t)\tilde{x}(t) + \Theta(t) + (g(x(t)) - g(\hat{x}(t)))u(t) \right. \\
&\quad \left. + L(-\tilde{x}(t) + O_s(t) - A(t)) \right)^T P(t)\tilde{x}(t) \\
&\quad + \tilde{x}^T(t) (-\beta^T(t)P(t) - P(t)\beta(t) - \Gamma) \tilde{x}(t) \\
&+ \tilde{x}^T(t)P(t) \left( \beta(t)\tilde{x}(t) + \Theta(t) + (g(x(t)) - g(\hat{x}(t)))u(t) \right. \\
&\quad \left. + L(-\tilde{x}(t) + O_s(t) - A(t)) \right) \\
&= \tilde{x}^T(t)\beta^T(t)P(t)\tilde{x}(t) + \Theta^T(t)P(t)\tilde{x}(t) \\
&\quad + u^T(t) (g(x(t)) - g(\hat{x}(t)))^T P(t)\tilde{x}(t) + \\
&\quad (O_s(t) - A(t))^T L^T P(t)\tilde{x}(t) - L\tilde{x}^T(t)P(t)\tilde{x}(t) \\
&- \tilde{x}^T(t)\beta^T(t)P(t)\tilde{x}(t) - \tilde{x}^T(t)P(t)\beta(t)\tilde{x}(t) - \tilde{x}^T(t)\Gamma\tilde{x}(t) \\
&\quad + \tilde{x}^T(t)P(t)\beta(t)\tilde{x}(t) + \tilde{x}^T(t)P(t)\Theta(t) \\
&\quad + \tilde{x}^T(t)P(t) (g(x(t)) - g(\hat{x}(t))) u(t) \\
&- \tilde{x}^T(t)P(t)L\tilde{x}(t) + \tilde{x}^T(t)P(t)L(O_s(t) - A(t)) \\
&= \Theta^T(t)P(t)\tilde{x}(t) + \tilde{x}^T(t)P(t)\Theta(t) \\
&\quad + u^T(t) (g(x(t)) - g(\hat{x}(t)))^T P(t)\tilde{x}(t) \\
&\quad + \tilde{x}^T(t)P(t) (g(x(t)) - g(\hat{x}(t))) u(t) \\
&\quad + (O_s(t) - A(t))^T L^T P(x)\tilde{x}(t) + \\
&\quad \tilde{x}^T(t)P(t)L(O_s(t) - A(t)) - \tilde{x}^T(t)\Gamma\tilde{x}(t) \\
&= 2\Theta^T(t)P(t)\tilde{x}(t) + 2u^T(t) (g(x(t)) - g(\hat{x}(t)))^T P(t)\tilde{x}(t) \\
&\quad + 2L(O_s(t) - A(t))^T P(t)\tilde{x}(t) - \tilde{x}^T\Gamma\tilde{x}(t)
\end{aligned} \tag{6.33}$$

Now, substituting the conditions in Assumptions 2-5, we have

$$\begin{aligned}
\dot{V}(\tilde{x}(t), t) &= 2\Theta^T(t)P(t)\tilde{x}(t) \\
&+ 2u^T(t)(g(x(t)) - g(\hat{x}(t)))^T P(t)\tilde{x}(t) \\
&+ 2L(O_s(t) - A(t))^T P(t)\tilde{x}(t) - \tilde{x}^T \Gamma \tilde{x}(t) \\
&\leq 2\|P(t)\|L_\Theta \|\tilde{x}(t)\|^2 + 2L_g L_u \|P(t)\| \|\tilde{x}(t)\|^2 \\
&\quad + 2\|P(t)\|L L_a \|\tilde{x}(t)\|^2 - \Gamma \|\tilde{x}(t)\|^2 \\
&\leq (-\eta_{min}(\Gamma) + 2L_\Theta \lambda_{max} + 2L_g L_u \lambda_{max} + 2L L_a \lambda_{max}) \|\tilde{x}(t)\|^2
\end{aligned} \tag{6.34}$$

Hence, to have a stable resilient controller, we must have

$$-\eta_{min}(\Gamma) + 2L_\Theta \lambda_{max} + 2L_g L_u \lambda_{max} + 2L L_a \lambda_{max} < 0$$

or

$$\eta_{min}(\Gamma) > 2L_\Theta \lambda_{max} + 2L_g L_u \lambda_{max} + 2L L_a \lambda_{max}$$

which gives the sufficient condition of the stability. Thus, the condition given in Equation (6.30) is sufficient to guarantee the convergence of the FDI-attack effect  $\tilde{x}(t)$  on the system to a small bounded value.

## 6.6 Numerical Simulation Result

The performance of the proposed resilient control system against FDI-attacks is investigated in this section. FDI attacks occur through malicious attempts and can target a specific part of the system which can collapse whole the system operation. In addition to the possibility of jamming communication links in the LFC system, an attacker can penetrate to the system by GPS spoofing the PMUs [215]. Here,

we assumed that the attacker spoofed the GPS by mimicking the GPS signal and altered the GPS time estimation in the PMUs of the LFC [215, 216]. However, the proposed method is a general method that can detect FDI attack from the other sources as well, i.e., intrusion through the communication links. The GPS spoofing will lead to wrong phase angle measurements which can deteriorate the efficiency of the LFC system and even destabilize the system.

It is evident that a large amount of false data is easily detectable and can be filtered using simple filter design, thus, in an intelligent attack, the amount of injected false data is selected in the range of nominal performance of the system states. The feedback signal of the controller under attack,  $\pi(\bullet)$ , can be expressed as

$$\pi(x_{i,l}(t)) = x_{i,l}(t) + \alpha_{i,l}(t) \quad (6.35)$$

where  $\alpha_{i,m}(t)$  is random variable which denotes the injected malicious signal (FDI) or faults to the  $l^{th}$  state of  $i^{th}$  power area. Three scenarios have been considered for  $\alpha$  to examine the proposed control system on a two power area LFC system: a single non-periodic FDI-attack, a single periodic FDI-attack, and simultaneous FDI-attacks on different nodes/states. The numerical simulations are conducted via MATLAB SIMULINK software.

### 6.6.1 Scenario I: Single non-periodic FDI attack

Here, we consider that the FDI attack occurs in the third state of the first power area as follows:

$$\alpha_{1,3}(t) = \begin{cases} 0 & t < 3 \\ 1 & t \geq 3 \end{cases} \quad (6.36)$$

The third state of the power area is selected because this is the feedback state and the hacker can inject the FDI attack and faults to this state. This fault starts at

$t = 3sec$  for the amount of 1 per unit (PU). The result in Fig.6.2 shows that our proposed AD system can detect and track the inserted false data in real time. It should be noted that the proposed detection technique is able to estimate faults and attacks larger than perturbation due to its unique design approach. The performance of the proposed resilient controller is compared with an LQR controller, and the results are shown in Figs.6.3 and 6.4. Fig.6.3 compares the LQR and the proposed resilient controller performance in converging the states deviation to zero in the presence of the attack in the first scenario. This figure clearly shows that the proposed controller compensated for the attack effect and successfully damped it without affecting other states. Fig. 6.4 compares the performance of the LQR and the proposed controller in controlling the third state in the first scenario. As it can be seen, the proposed controller has compensated the FDI-attack effect significantly. In order to analyze the proposed AD detection numerically, the root mean square error of AD system calculated using the following formula

$$RMSE = \sqrt{\frac{\sum_{i=1}^S (f_i - \hat{f}_i)^2}{S}} \quad (6.37)$$

where  $S$  is the number of samples in the simulation process,  $f_i$  is the injected false data, and  $\hat{f}_i$  is the estimated one. The results are shown in the Table. 6.1. The RMSE of the detection for the non-periodic FDI-attack is 0.0681, which shows the accuracy of the proposed detection technique. The comparison of RMSE results of FDI-attack compensation in Table. 6.1 also confirms that the proposed resilient controller can significantly compensate for the effects of FDI-attack.

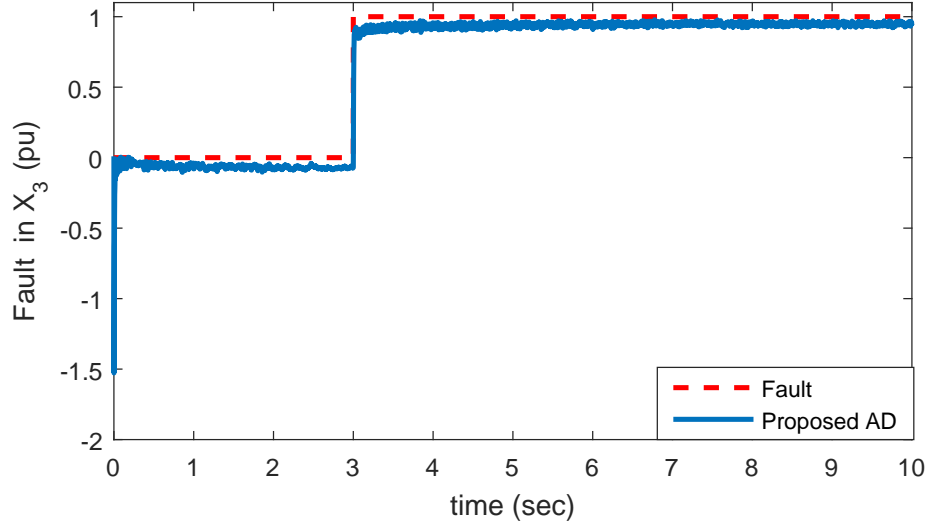


Figure 6.2: The performance of the proposed AD system in the detection of the scenario I.

### 6.6.2 Scenario II: Single periodic FDI attack

In this scenario, we consider that an adversary injected a sinusoidal signal to the third feedback state of the first power area that can be described as follows:

$$\alpha_{1,3}(t) = \begin{cases} 0 & t < 3 \\ 2\sin(2\pi t) & t \geq 3 \end{cases} \quad (6.38)$$

The simulation results for the second scenario are shown in Figs.6.5 and 6.6. Figure 6.5 demonstrates that the proposed AD system can detect the FDI attack accurately. The RMSE of detection error for this attack in Table. 6.1 denotes that the AD is able to estimate and detect FDI attacks. The comparison between the performance of the proposed resilient controller and LQR controller for the LFC system are given in Fig.6.6 which shows the advantages of the proposed system in compensating FDI attack effect.

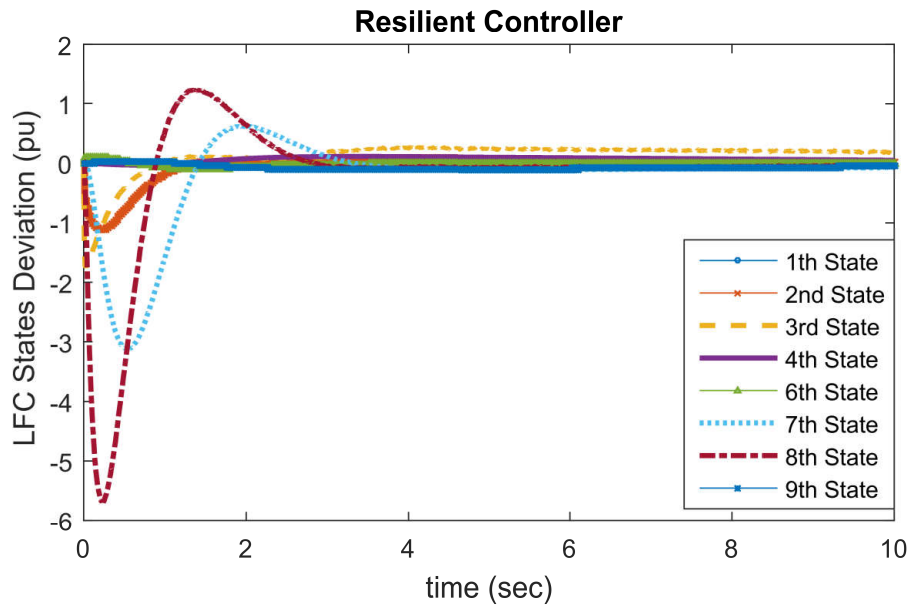
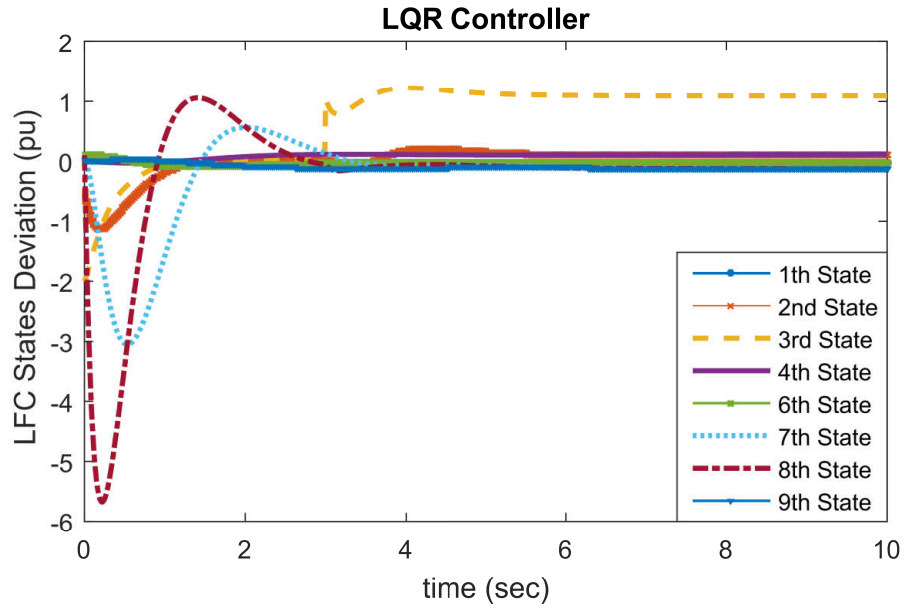


Figure 6.3: A comparison between the states of LFC system controlled with the proposed resilient controller and LQR controller in the presence of the attack in the first scenario.

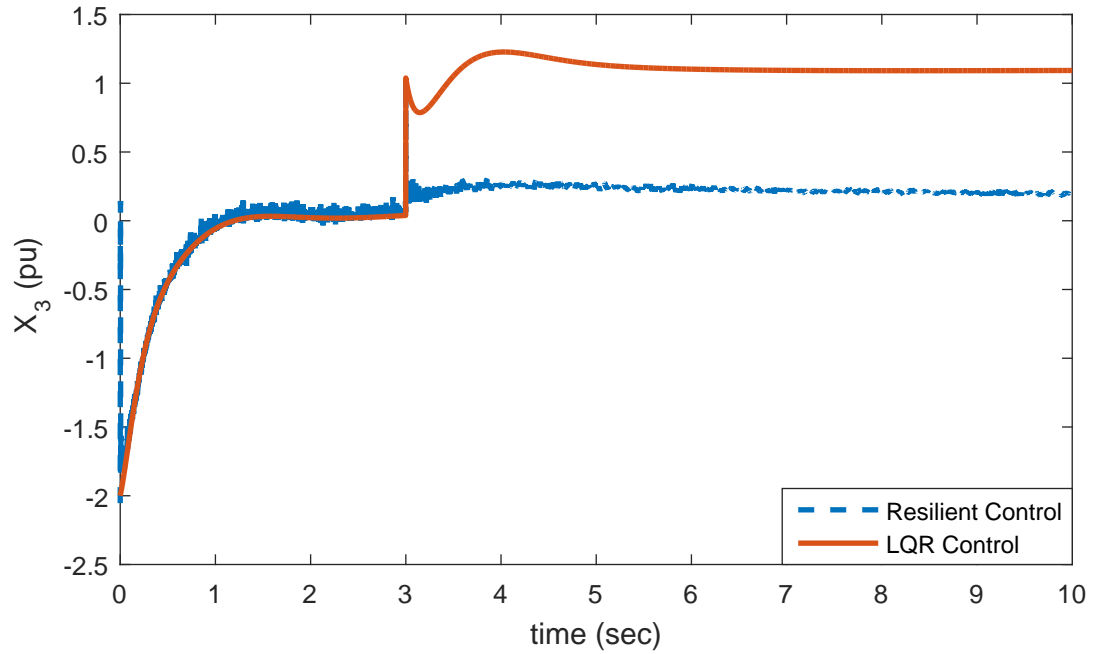


Figure 6.4: The performance comparison of the proposed resilient control system with LQR controller in presence of the attack in the first scenario.

### 6.6.3 Simultaneous FDI attacks

In this scenario, a square wave shape attack is considered on two main states of the LFC system (3rd and 8th states). These attacks occurs at the same time to examine the proposed AD and control design in presence of simultaneous FDI attacks which is the most difficult scenario for a detection system. Figs. 6.7 and 6.8 show the simulation results for this scenario. As it can be seen in Fig.6.7, the proposed AD system successfully detect the attack on both states. Table. 6.1 also confirms that the proposed AD with RMSE of 0.095 has sufficient accuracy. Fig.6.8 demonstrates that the proposed controller can significantly reduce the FDI-attack effect on both states.

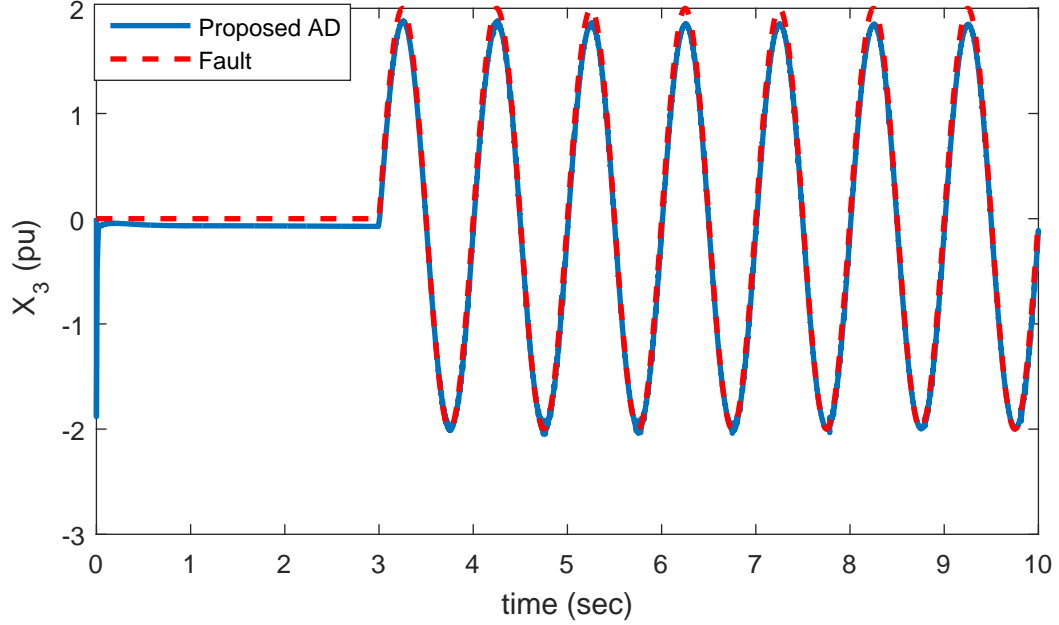


Figure 6.5: The performance of the proposed AD system in the detection of a single periodic FDI-attack in the second scenario.

Table 6.1: Analytical analysis of the proposed approach in detection and compensation of FDI-attack in the LFC system.

Anomaly	RMSE in AD	RMSE in Resilient Control	RMSE in LQR controller
Scenario I	0.0681	0.3144	0.9603
Scenario II	0.1219	0.2792	0.7076
Scenario III*	0.0952	0.3435	1.0489

\*For this case we calculated the average of accuracy in detection and compensation of two attacks.

### 6.6.4 Discussion

A novel resilient control design for the LFC system is developed which can automatically detect and eliminate FDI attack with sufficient accuracy. The proposed controller consists of a novel AD for online detection of FDI-attacks in the sensor system of an LFC system and a controller that can compensate for the detected anomaly in real-time. The simulation results and numerical comparison showed

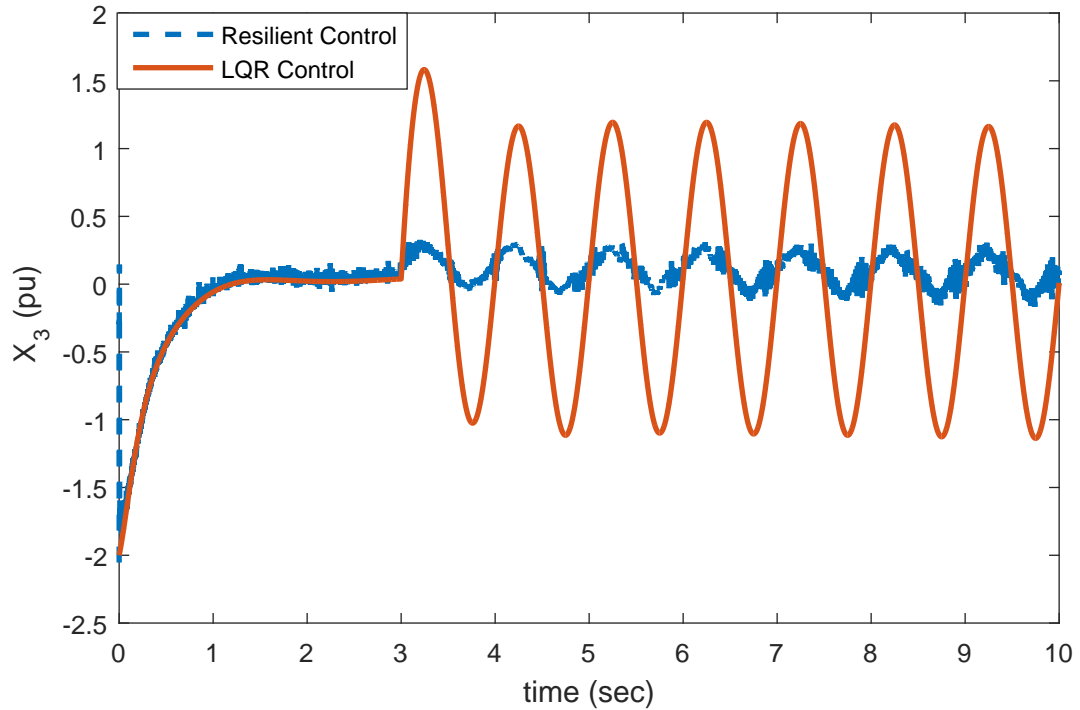


Figure 6.6: The performance comparison of the proposed resilient control system with LQR controller in presence of a single periodic FDI-attack in the second scenario.

that the proposed control approach could detect and compensate for different kinds of FDI attack. Unlike other research works, the proposed method is able to detect simultaneous faults and attack on different states of the system. This ability helps the system to defend against the total intrusion of an attacker. The other advantage of the proposed approach is the elimination of the need for control reconfiguration in the presence of attacks. Therefore, the complexity and cost of control design will be decreased.

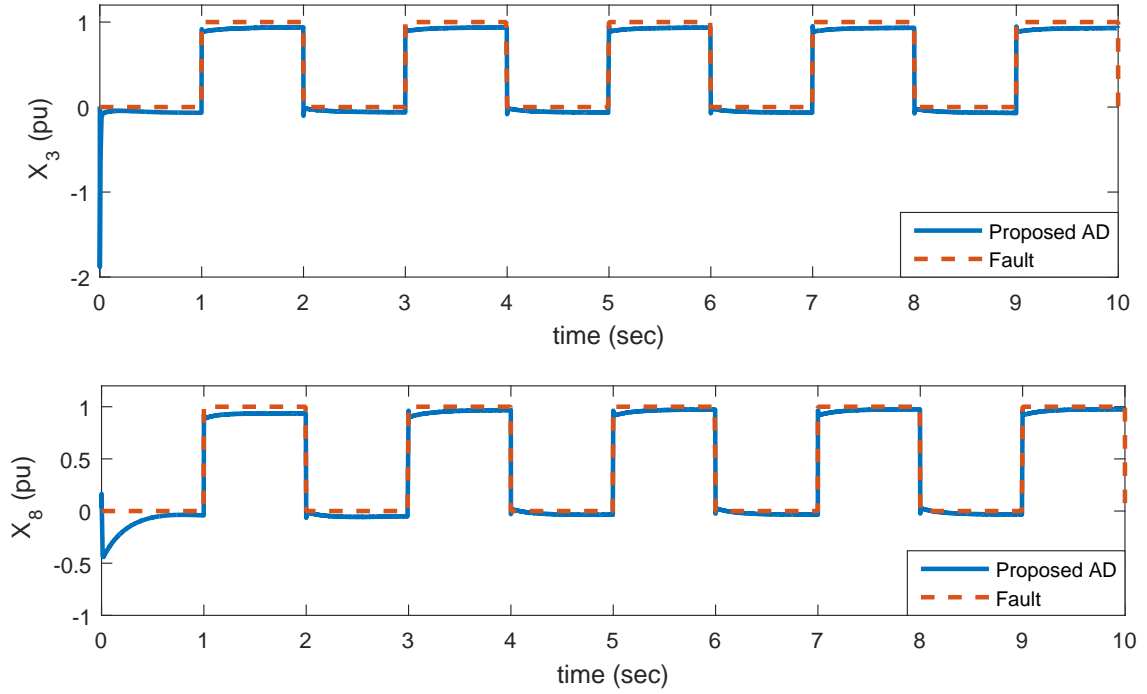


Figure 6.7: The performance of the proposed AD system in the detection of two simultaneous attack.

## 6.7 Conclusion

This chapter introduced a new resilient control architecture for LFC system in the presence of FDI attacks in communication feedback line which transmits the sensors data. The proposed control technique consists of an AD system which detects anomalies in the system using a Luenberger and an ANN observer, and a feedback system to compensate for the FDI-attack in the real time. The stability of the proposed control system against anomalies was mathematically proved using Lyapunov theory. The simulation results have shown that the proposed design is able to detect the anomalies with sufficient accuracy and compensate their effect on the LFC system. The proposed technique improved the resiliency and subsequently the reliability of the power grid systems.

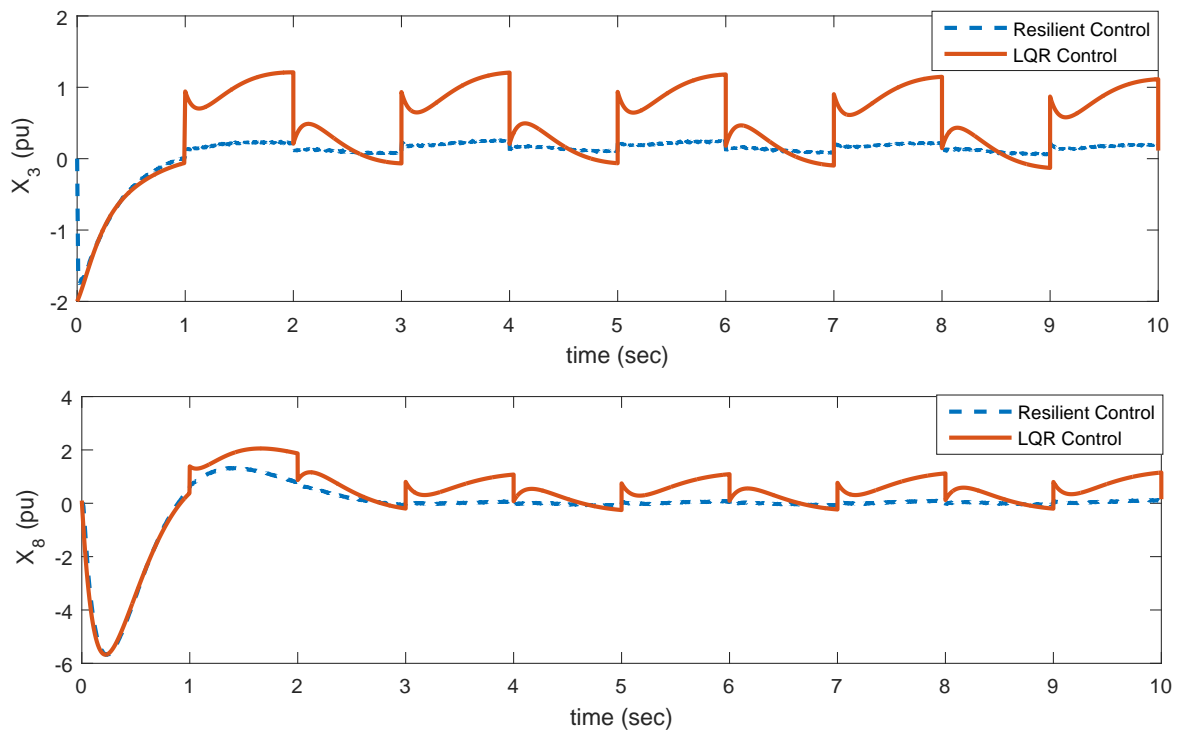


Figure 6.8: The performance comparison of the proposed resilient control system with LQR controller in presence of simultaneous FDI attacks on third and eighth states of the LFC system.

## CHAPTER 7

### CONCLUSION AND FUTURE WORKS

#### 7.1 Conclusion

In this dissertation, the problem of fault in the control system was investigated, and the state of the art methods in designing fault tolerant control (FTC) were reviewed and their pros and cons were discussed. Generally, FTC techniques can be classified into two major classes: active FTC and Passive FTC. Passive FTCs do not rely on fault information to control the system and are closely related to robust control systems while active FTC reacts to faults based on the size and the location of faults which results to more intelligent reaction to fault occurrence. Thus, this research work is based on the development of an efficient active FTC system. In order to improve the current active FTC techniques, a new fault detection and isolation (FDI) technique and a novel active FTC system for actuators and sensors in nonlinear systems were developed. The efficiency and stability analysis of the proposed FDI and the proposed active FTC technique were investigated and mathematically proven. Using the proposed technique, FDI systems and active FTC systems have been designed for several different platforms, and the efficiency of the proposed technique was demonstrated through numerical simulations.

The proposed FDI system incorporates the advantages of model-based observers and learning-based observers by combining these two methods. The proposed hybrid FDI method has higher accuracy than the model-based FDI strategies while deals with less computation load in comparison with learning-based FDI techniques. In the proposed design, a three-layer artificial neural network (ANN) was used for online learning, and a model-based observer based on the dynamic model of the system was designed and fed to the ANN to improve the accuracy and reduce the computation

burden. Then, to improve the ANN performance, the extended Kalman filter (EKF) was introduced to update ANN weights in realtime. The proposed application of EKF in ANN led to a faster learning rate of the ANN and reduced the computation time which makes the proposed design more efficient against abrupt faults.

The proposed active FTC design consists of the introduced FDI unit and new feedback structure to analytically compensate for the occurred fault in realtime. This novel structure helps to tackle the fault problem in the actuators and sensors of linear and nonlinear systems without the need of control reconfiguration. Particularly, when the weight and cost of the product have a major role in the design, this technique can be a very beneficiary by reducing the design time (eliminating reconfiguration scenarios) and product weight (eliminating redundancy).

The proposed active FTC were applied in designing flight control design of an unmanned aerial vehicle (UAV) in Chapter 4. This flight controller design will help to improve the reliability and safety of the flight system against unpredicted faults in the actuator and sensors. The efficiency of the proposed design was demonstrated against different fault scenarios, and the simulation result showed the advantages of the proposed design compared with the state of the art active FTC strategies.

A resilient control framework for proton exchange membrane fuel cell (PEMFC) system based on the proposed active FTC technique was introduced in Chapter 5. This controller was able to detect the faults in the actuators of the air valve of the PEMFC and compensate them in realtime. The proposed control design can accurately detect, estimate and track the PEMFC actuators faults and failures, and compensate for their negative impacts while following the desired control performances. This tolerance against faults and failures helps to maintain the PEMFC gas pressures at the desired values, keeping the PEMFC in a desirable condition, and subsequently, lengthen its lifetime by avoiding membrane damage.

Finally, in Chapter 6, a resilient controller for load frequency control (LFC) of a power grid system was designed based on the proposed active FTC technique. The proposed controller was able to detect faults and false data injection (FDI) attacks and compensate for their negative effects while achieving the desired control performances. The proposed control design could improve the resiliency and subsequently the reliability of the power grid systems. Furthermore, the stability of the proposed control system against anomalies was mathematically proved using Lyapunov theory.

## **7.2 Future Works**

In this study, the proposed active FTC technique has been applied for three different platforms, and the efficiency of the approach has been demonstrated theoretically and numerically. However, this research work has the potential be continued in three general aspects: 1) improving the FDI technique, 2) improving the FTC system, 3) application

### **7.2.1 Improving FDI Accuracy**

The proposed strategy for FDI was based on a combination of a model-based observer and the ANN. In this aspect, obtaining a more accurate model-based observer would help to improve the accuracy of the FDI system. To this aim, the combination of sliding mode observer (SMO) with ANN is suggested to leverage the robustness of SMO against false data alarm and sensitivity of the ANN against the incipient fault. Furthermore, we used EKF to update ANN weights while investigating new algorithms, e.g., UKF, in the future may improve the accuracy of the FDI.

## **7.2.2 Improving the FTC system**

In this research work, an active FTC technique for the nonlinear system was introduced. Active FTC system relies on the accuracy of the FDI information and delay in receiving this information or inaccuracy of this information would result in an undesirable transient response. In order to prevent this transient response, a combination of active FTC and passive FTC is suggested. The suggested hybrid FTC algorithm would benefit from the advantages of active FTC (reacting to fault intelligently) and passive FTC (desirable transient response).

## **7.2.3 Applications**

This research applied the proposed active technique to three different platforms to obtain efficient performance against faults and failures in sensors and actuators. However, there are other applications with the need for reliable controllers that would need attention. For example, the network control system is one of the complicated platforms that fault and failure in one of its components would have catastrophic results. Thus, designing an active FTC system for network control system can be considered as the future goal of this research.

## BIBLIOGRAPHY

- [1] D. L. Simon, S. Borguet, O. Léonard, and X. F. Zhang, “Aircraft engine gas path diagnostic methods: public benchmarking results,” in *ASME Turbo Expo 2013: Turbine Technical Conference and Exposition*, pp. V004T06A014–V004T06A014, American Society of Mechanical Engineers, 2013.
- [2] M. Sadeghi, A. Abaspour, and S. H. Sadati, “A novel integrated guidance and control system design in formation flight,” *Journal of Aerospace Technology and Management*, vol. 7, no. 4, pp. 432–442, 2015.
- [3] Z. Gao, C. Cecati, and S. X. Ding, “A survey of fault diagnosis and fault-tolerant techniquespart i: Fault diagnosis with model-based and signal-based approaches,” *IEEE Transactions on Industrial Electronics*, vol. 62, no. 6, pp. 3757–3767, 2015.
- [4] T. Moor, “A discussion of fault-tolerant supervisory control in terms of formal languages,” *Annual Reviews in Control*, vol. 41, pp. 159–169, 2016.
- [5] A. Sargolzaei, K. K. Yen, and M. N. Abdelghani, “Preventing time-delay switch attack on load frequency control in distributed power systems,” *IEEE Transactions on Smart Grid*, vol. 7, no. 2, pp. 1176–1185, 2016.
- [6] G. Ducard and H. P. Geering, “Efficient nonlinear actuator fault detection and isolation system for unmanned aerial vehicles,” *Journal of Guidance, Control, and Dynamics*, vol. 31, no. 1, pp. 225–237, 2008.
- [7] A. Abbaspour, K. K. Yen, P. Forouzannezhad, and A. Sargolzaei, “A neural adaptive approach for active fault-tolerant control design in uav,” *IEEE Transactions on Systems, Man and Cybernetics: Systems*, 2018.
- [8] A. Abbaspour, K. K. Yen, S. Noei, and A. Sargolzaei, “Detection of fault data injection attack on uav using adaptive neural network,” *Procedia computer science*, vol. 95, pp. 193–200, 2016.
- [9] W. Ao, Y. Song, and C. Wen, “Adaptive cyber-physical system attack detection and reconstruction with application to power systems,” *IET Control Theory & Applications*, vol. 10, no. 12, pp. 1458–1468, 2016.
- [10] R. Deng, G. Xiao, and R. Lu, “Defending against false data injection attacks on power system state estimation,” *IEEE Transactions on Industrial Informatics*, vol. 13, no. 1, pp. 198–207, 2017.

- [11] A. Sargolzaei, K. Yen, M. Abdelghani, A. Abbaspour, and S. Sargolzaei, “Generalized attack model for networked control systems, evaluation of control methods,” *Intelligent Control and Automation*, vol. 8, no. 03, p. 164, 2017.
- [12] J. R. Fisher, *Aircraft control using nonlinear dynamic inversion in conjunction with adaptive robust control*. PhD thesis, Texas A&M University, 2005.
- [13] H. Alwi, C. Edwards, and C. P. Tan, “Fault tolerant control and fault detection and isolation,” in *Fault Detection and Fault-Tolerant Control Using Sliding Modes*, pp. 7–27, Springer, 2011.
- [14] F. W. Burcham Jr, T. A. Maine, J. J. Burken, and J. Bull, “Using engine thrust for emergency flight control: Md-11 and b-747 results,” 1998.
- [15] F. W. Burcham Jr, C. G. Fullerton, and T. A. Maine, “Manual manipulation of engine throttles for emergency flight control,” 2004.
- [16] B. Safarinejadian and E. Kowsari, “Fault detection in non-linear systems based on gp-ekf and gp-ukf algorithms,” *Systems Science & Control Engineering: An Open Access Journal*, vol. 2, no. 1, pp. 610–620, 2014.
- [17] J. Jiang and X. Yu, “Fault-tolerant control systems: A comparative study between active and passive approaches,” *Annual Reviews in control*, vol. 36, no. 1, pp. 60–72, 2012.
- [18] X. Yu and J. Jiang, “A survey of fault-tolerant controllers based on safety-related issues,” *Annual Reviews in Control*, vol. 39, pp. 46–57, 2015.
- [19] X. Qi, J. Qi, D. Theilliol, Y. Zhang, J. Han, D. Song, and C. Hua, “A review on fault diagnosis and fault tolerant control methods for single-rotor aerial vehicles,” *Journal of Intelligent & Robotic Systems*, vol. 73, no. 1-4, pp. 535–555, 2014.
- [20] B. Tabbache, N. Rizoug, M. E. H. Benbouzid, and A. Kheloui, “A control reconfiguration strategy for post-sensor ftc in induction motor-based evs,” *IEEE transactions on vehicular technology*, vol. 62, no. 3, pp. 965–971, 2013.
- [21] G. Zhang, H. Zhang, X. Huang, J. Wang, H. Yu, and R. Graaf, “Active fault-tolerant control for electric vehicles with independently driven rear in-wheel motors against certain actuator faults,” *IEEE Transactions on Control Systems Technology*, vol. 24, no. 5, pp. 1557–1572, 2016.

- [22] A. Cristofaro and T. A. Johansen, “Fault tolerant control allocation using unknown input observers,” *Automatica*, vol. 50, no. 7, pp. 1891–1897, 2014.
- [23] M. Chen, P. Shi, and C.-C. Lim, “Adaptive neural fault-tolerant control of a 3-dof model helicopter system,” *IEEE Transactions on Systems, Man, and Cybernetics: Systems*, vol. 46, no. 2, pp. 260–270, 2016.
- [24] A. Abbaspour, A. Sargolzaei, and K. Yen, “Detection of false data injection attack on load frequency control in distributed power systems,” in *Power Symposium (NAPS), 2017 North American*, pp. 1–6, IEEE, 2017.
- [25] X.-J. Li and G.-H. Yang, “Neural-network-based adaptive decentralized fault-tolerant control for a class of interconnected nonlinear systems,” *IEEE transactions on neural networks and learning systems*, 2016.
- [26] A. Abbaspour, A. Sargolzaei, and K. K. Yen, “A neural network based resilient control design for distributed power systems under faults and attacks,” in *2018 IEEE International Conference on Environment and Electrical Engineering and 2018 IEEE Industrial and Commercial Power Systems Europe (EEEIC/I&CPS Europe)*, pp. 1–6, IEEE, 2018.
- [27] H. Gao, Y. Song, and C. Wen, “Backstepping design of adaptive neural fault-tolerant control for mimo nonlinear systems,” *IEEE transactions on neural networks and learning systems*, vol. 28, no. 11, pp. 2605–2613, 2017.
- [28] S. Yin, H. Yang, H. Gao, J. Qiu, and O. Kaynak, “An adaptive nn-based approach for fault-tolerant control of nonlinear time-varying delay systems with unmodeled dynamics,” *IEEE transactions on neural networks and learning systems*, vol. 28, no. 8, pp. 1902–1913, 2017.
- [29] A. Abbaspour, M. Sanchez, A. Sargolzaei, K. Yen, and N. Sornkhampan, “Adaptive neural network based fault detection design for unmanned quadrotor under faults and cyber attacks,” in *25th International Conference on Systems Engineering, Las Vegas, USA*, 2017.
- [30] H. Alwi, C. Edwards, O. Stroosma, and J. Mulder, “Fault tolerant sliding mode control design with piloted simulator evaluation,” *Journal of Guidance, Control, and Dynamics*, vol. 31, no. 5, pp. 1186–1201, 2008.
- [31] H. Qinglei, Y. Zhang, H. Xing, and X. Bing, “Adaptive integral-type sliding mode control for spacecraft attitude maneuvering under actuator stuck failures,” *Chinese Journal of Aeronautics*, vol. 24, no. 1, pp. 32–45, 2011.

- [32] R. Wang and J. Wang, "Passive actuator fault-tolerant control for a class of overactuated nonlinear systems and applications to electric vehicles," *IEEE Transactions on Vehicular Technology*, vol. 62, no. 3, pp. 972–985, 2013.
- [33] Z. Yang, M. Blanke, and M. Verhaegen, "Robust control mixer method for reconfigurable control design using model matching," *IET Control Theory & Applications*, vol. 1, no. 1, pp. 349–357, 2007.
- [34] H. Shen, J. H. Park, and Z.-G. Wu, "Finite-time reliable 2- / control for takagi–sugeno fuzzy systems with actuator faults," *IET Control Theory & Applications*, vol. 8, no. 9, pp. 688–696, 2014.
- [35] H. Shen, L. Su, and J. H. Park, "Reliable mixed  $h_\infty$ /passive control for t–s fuzzy delayed systems based on a semi-markov jump model approach," *Fuzzy Sets and Systems*, vol. 314, pp. 79–98, 2017.
- [36] M. Staroswiecki, H. Yang, and B. Jiang, "Progressive accommodation of parametric faults in linear quadratic control," *Automatica*, vol. 43, no. 12, pp. 2070–2076, 2007.
- [37] H.-N. Wu, "Reliable lq fuzzy control for continuous-time nonlinear systems with actuator faults," *IEEE Transactions on Systems, Man, and Cybernetics, Part B (Cybernetics)*, vol. 34, no. 4, pp. 1743–1752, 2004.
- [38] S. Zeghlache, K. Kara, and D. Saigaa, "Fault tolerant control based on interval type-2 fuzzy sliding mode controller for coaxial trirotor aircraft," *ISA transactions*, vol. 59, pp. 215–231, 2015.
- [39] M. Benosman and K.-Y. Lum, "Passive actuators' fault-tolerant control for affine nonlinear systems," *IEEE Transactions on Control Systems Technology*, vol. 18, no. 1, pp. 152–163, 2010.
- [40] Y. Luo, A. Serrani, S. Yurkovich, M. W. Oppenheimer, and D. B. Doman, "Model-predictive dynamic control allocation scheme for reentry vehicles," *Journal of Guidance, Control, and Dynamics*, vol. 30, no. 1, pp. 100–113, 2007.
- [41] T. A. Johansen and T. I. Fossen, "Control allocationa survey," *Automatica*, vol. 49, no. 5, pp. 1087–1103, 2013.

- [42] M.-D. Hua, G. Ducard, T. Hamel, R. Mahony, and K. Rudin, “Implementation of a nonlinear attitude estimator for aerial robotic vehicles,” *IEEE Transactions on Control Systems Technology*, vol. 22, no. 1, pp. 201–213, 2014.
- [43] A. Fekih, “Fault diagnosis and fault tolerant control design for aerospace systems: A bibliographical review,” in *American Control Conference (ACC), 2014*, pp. 1286–1291, IEEE, 2014.
- [44] J. Gertler, *Fault detection and diagnosis*. Springer, 2013.
- [45] A. Willsky and H. Jones, “A generalized likelihood ratio approach to the detection and estimation of jumps in linear systems,” *IEEE Transactions on Automatic control*, vol. 21, no. 1, pp. 108–112, 1976.
- [46] R. V. Beard, *Failure accomodation in linear systems through self-reorganization*. PhD thesis, Massachusetts Institute of Technology, 1971.
- [47] M. Blanke, M. Kinnaert, J. Lunze, M. Staroswiecki, and J. Schröder, *Diagnosis and fault-tolerant control*, vol. 2. Springer, 2006.
- [48] S. X. Ding, *Model-based fault diagnosis techniques: design schemes, algorithms, and tools*. Springer Science & Business Media, 2008.
- [49] V. Venkatasubramanian, R. Rengaswamy, S. N. Kavuri, and K. Yin, “A review of process fault detection and diagnosis: Part iii: Process history based methods,” *Computers & chemical engineering*, vol. 27, no. 3, pp. 327–346, 2003.
- [50] R. Isermann, “Model-based fault-detection and diagnosis—status and applications,” *Annual Reviews in control*, vol. 29, no. 1, pp. 71–85, 2005.
- [51] M. Zhong, T. Xue, and S. X. Ding, “A survey on model-based fault diagnosis for linear discrete time-varying systems,” *Neurocomputing*, vol. 306, pp. 51–60, 2018.
- [52] K. Manandhar, X. Cao, F. Hu, and Y. Liu, “Detection of faults and attacks including false data injection attack in smart grid using kalman filter,” *IEEE transactions on control of network systems*, vol. 1, no. 4, pp. 370–379, 2014.
- [53] B. Pourbabae, N. Meskin, and K. Khorasani, “Sensor fault detection, isolation, and identification using multiple-model-based hybrid kalman filter for gas

- turbine engines.,” *IEEE Trans. Contr. Sys. Techn.*, vol. 24, no. 4, pp. 1184–1200, 2016.
- [54] S. Zhao and B. Huang, “Iterative residual generator for fault detection with linear time-invariant state–space models,” *IEEE Transactions on Automatic Control*, vol. 62, no. 10, pp. 5422–5428, 2017.
- [55] P. Lu, E.-J. van Kampen, C. de Visser, and Q. Chu, “Nonlinear aircraft sensor fault reconstruction in the presence of disturbances validated by real flight data,” *Control Engineering Practice*, vol. 49, pp. 112–128, 2016.
- [56] Z. Liu and H. He, “Sensor fault detection and isolation for a lithium-ion battery pack in electric vehicles using adaptive extended kalman filter,” *Applied Energy*, vol. 185, pp. 2033–2044, 2017.
- [57] A. Rahimi, K. D. Kumar, and H. Alighanbari, “Enhanced adaptive unscented kalman filter for reaction wheels,” *IEEE Transactions on Aerospace and Electronic Systems*, vol. 51, no. 2, pp. 1568–1575, 2015.
- [58] M. Zhong, S. Liu, and H. Zhao, “Krein space-based  $h_\infty$  fault estimation for linear discrete time-varying systems,” *Acta Automatica Sinica*, vol. 34, no. 12, pp. 1529–1533, 2008.
- [59] S. Aouaouda, M. Chadli, P. Shi, and H. R. Karimi, “Discrete-time  $h/h_\infty$  sensor fault detection observer design for nonlinear systems with parameter uncertainty,” *International Journal of Robust and Nonlinear Control*, vol. 25, no. 3, pp. 339–361, 2015.
- [60] H. Dong, Z. Wang, X. Bu, and F. E. Alsaadi, “Distributed fault estimation with randomly occurring uncertainties over sensor networks,” *International Journal of General Systems*, vol. 45, no. 5, pp. 662–674, 2016.
- [61] X. Li, H. H. Liu, and B. Jiang, “Parametrization of optimal fault detection filters,” *Automatica*, vol. 56, pp. 70–77, 2015.
- [62] C. Zhang, H. Zhao, and T. Li, “Krein space-based  $h_\infty$  adaptive smoother design for a class of lipschitz nonlinear discrete-time systems,” *Applied Mathematics and Computation*, vol. 287, pp. 134–148, 2016.
- [63] K. Zhang, B. Jiang, X.-G. Yan, and Z. Mao, “Sliding mode observer based incipient sensor fault detection with application to high-speed railway traction device,” *ISA transactions*, vol. 63, pp. 49–59, 2016.

- [64] N. Djeghali, S. Djennoune, M. Bettayeb, M. Ghanes, and J.-P. Barbot, “Observation and sliding mode observer for nonlinear fractional-order system with unknown input,” *ISA transactions*, vol. 63, pp. 1–10, 2016.
- [65] I. Castillo, T. F. Edgar, and B. R. Fernández, “Robust model-based fault detection and isolation for nonlinear processes using sliding modes,” *International Journal of Robust and Nonlinear Control*, vol. 22, no. 1, pp. 89–104, 2012.
- [66] S. Bøgh, “Multiple hypothesis-testing approach to fdi for the industrial actuator benchmark,” *Control Engineering Practice*, vol. 3, no. 12, pp. 1763–1768, 1995.
- [67] I. Nikiforov, V. Varavva, and V. Kireichikov, “Application of statistical fault detection algorithms to navigation systems monitoring,” *Automatica*, vol. 29, no. 5, pp. 1275–1290, 1993.
- [68] S. Haykin, *Kalman filtering and neural networks*, vol. 47. John Wiley & Sons, 2004.
- [69] E. A. Wan and R. Van Der Merwe, “The unscented kalman filter for nonlinear estimation,” in *Adaptive Systems for Signal Processing, Communications, and Control Symposium 2000. AS-SPCC. The IEEE 2000*, pp. 153–158, Ieee, 2000.
- [70] H. R. Karimi, M. Zapateiro, and N. Luo, “A linear matrix inequality approach to robust fault detection filter design of linear systems with mixed time-varying delays and nonlinear perturbations,” *Journal of the Franklin Institute*, vol. 347, no. 6, pp. 957–973, 2010.
- [71] A. H. Hassanabadi, M. Shafiee, and V. Puig, “Uio design for singular delayed lpv systems with application to actuator fault detection and isolation,” *International Journal of Systems Science*, vol. 47, no. 1, pp. 107–121, 2016.
- [72] H. Behzad, A. Casavola, F. Tedesco, and M. A. Sadrnia, “A fault-tolerant sensor reconciliation scheme based on lpv unknown input observers,” in *Decision and Control (CDC), 2016 IEEE 55th Conference on*, pp. 2158–2163, IEEE, 2016.
- [73] S. Li, H. Wang, A. Aitouche, Y. Tian, and N. Christov, “Robust unknown input observer design for state estimation and fault detection using linear parameter varying model,” in *Journal of Physics: Conference Series*, vol. 783, p. 012001, IOP Publishing, 2017.

- [74] D. Du and B. Jiang, "Actuator fault estimation and accommodation for switched systems with time delay: Discrete-time case," *ISA transactions*, vol. 62, pp. 137–144, 2016.
- [75] H. Hur and H.-S. Ahn, "Unknown input  $h_\infty$  observer-based localization of a mobile robot with sensor failure," *IEEE/ASME Transactions on Mechatronics*, vol. 19, no. 6, pp. 1830–1838, 2014.
- [76] S. Ding, T. Jeinsch, P. Frank, and E. Ding, "A unified approach to the optimization of fault detection systems," *International journal of adaptive control and signal processing*, vol. 14, no. 7, pp. 725–745, 2000.
- [77] X. Li and K. Zhou, "A time domain approach to robust fault detection of linear time-varying systems," *Automatica*, vol. 45, no. 1, pp. 94–102, 2009.
- [78] B. Hassibi, A. H. Sayed, and T. Kailath, *Indefinite-Quadratic Estimation and Control: A Unified Approach to  $H_2$  and  $H$ -infinity Theories*, vol. 16. SIAM, 1999.
- [79] M. Zhong, D. Zhou, and S. X. Ding, "On designing  $h_{\infty}$  fault detection filter for linear discrete time-varying systems," *IEEE Transactions on Automatic Control*, vol. 55, no. 7, pp. 1689–1695, 2010.
- [80] D. Zhao, Y. Wang, Y. Li, and S. X. Ding, " $h_{\infty}$  fault estimation for 2-d linear discrete time-varying systems based on krein space method," *IEEE Transactions on Systems, Man, and Cybernetics: Systems*, 2017.
- [81] Y. Luo, Z. Wang, G. Wei, and F. E. Alsaadi, " $h_{\infty}$  fuzzy fault detection for uncertain 2-d systems under round-robin scheduling protocol," *IEEE Transactions on Systems, Man, and Cybernetics: Systems*, vol. 47, no. 8, pp. 2172–2184, 2017.
- [82] H. Dong, Z. Wang, S. X. Ding, and H. Gao, "On  $h$ -infinity estimation of randomly occurring faults for a class of nonlinear time-varying systems with fading channels," *IEEE Transactions on Automatic Control*, vol. 61, no. 2, pp. 479–484, 2016.
- [83] Y. Luo, Z. Wang, and G. Wei, "Fault detection for fuzzy systems with multiplicative noises under periodic communication protocols," *IEEE Transactions on Fuzzy Systems*, 2017.

- [84] Y. Zhou, Y. Soh, and J. Shen, “High-gain observer with higher order sliding mode for state and unknown disturbance estimations,” *International Journal of Robust and Nonlinear Control*, vol. 24, no. 15, pp. 2136–2151, 2014.
- [85] B. Walcott and S. Zak, “State observation of nonlinear uncertain dynamical systems,” *IEEE Transactions on automatic control*, vol. 32, no. 2, pp. 166–170, 1987.
- [86] C. Edwards, S. K. Spurgeon, and R. J. Patton, “Sliding mode observers for fault detection and isolation,” *Automatica*, vol. 36, no. 4, pp. 541–553, 2000.
- [87] A. J. Koshkouei and A. S. Zinober, “Sliding mode state observation for nonlinear systems,” *International Journal of Control*, vol. 77, no. 2, pp. 118–127, 2004.
- [88] S. Drakunov and V. Utkin, “Sliding mode observers. tutorial,” in *Decision and Control, 1995., Proceedings of the 34th IEEE Conference on*, vol. 4, pp. 3376–3378, IEEE, 1995.
- [89] J.-P. Barbot, T. Boukhobza, and M. Djemai, “Sliding mode observer for triangular input form,” in *Decision and Control, 1996., Proceedings of the 35th IEEE Conference on*, vol. 2, pp. 1489–1490, IEEE, 1996.
- [90] K. C. Veluvolu and Y. C. Soh, “High-gain observers with sliding mode for state and unknown input estimations,” *IEEE Transactions on Industrial Electronics*, vol. 56, no. 9, pp. 3386–3393, 2009.
- [91] A. F. de Loza, J. Cieslak, D. Henry, J. Dávila, and A. Zolghadri, “Sensor fault diagnosis using a non-homogeneous high-order sliding mode observer with application to a transport aircraft,” *IET Control Theory & Applications*, vol. 9, no. 4, pp. 598–607, 2015.
- [92] S. Laghrouche, J. Liu, F. S. Ahmed, M. Harmouche, and M. Wack, “Adaptive second-order sliding mode observer-based fault reconstruction for pem fuel cell air-feed system,” *IEEE Transactions on Control Systems Technology*, vol. 23, no. 3, pp. 1098–1109, 2015.
- [93] R. Galván-Guerra, L. Fridman, and J. Dávila, “High-order sliding-mode observer for linear time-varying systems with unknown inputs,” *International Journal of Robust and Nonlinear Control*, vol. 27, no. 14, pp. 2338–2356, 2017.

- [94] H. Ríos, E. Punta, and L. Fridman, “Fault detection and isolation for nonlinear non-affine uncertain systems via sliding-mode techniques,” *International Journal of Control*, vol. 90, no. 2, pp. 218–230, 2017.
- [95] X. Wang, C. P. Tan, and D. Zhou, “A novel sliding mode observer for state and fault estimation in systems not satisfying matching and minimum phase conditions,” *Automatica*, vol. 79, pp. 290–295, 2017.
- [96] W. Chen and F. N. Chowdhury, “A synthesized design of sliding-mode and luengerberger observers for early detection of incipient faults,” *International Journal of Adaptive Control and Signal Processing*, vol. 24, no. 12, pp. 1021–1035, 2010.
- [97] J. Zhang, A. K. Swain, and S. K. Nguang, “Detection and isolation of incipient sensor faults for a class of uncertain non-linear systems,” *IET Control Theory & Applications*, vol. 6, no. 12, pp. 1870–1880, 2012.
- [98] C. Cecati, “A survey of fault diagnosis and fault-tolerant techniques part ii: Fault diagnosis with knowledge-based and hybrid/active approaches,” *IEEE Transactions on Industrial Electronics*, 2015.
- [99] X. Wang, U. Kruger, G. W. Irwin, G. McCullough, and N. McDowell, “Non-linear pca with the local approach for diesel engine fault detection and diagnosis,” *IEEE Transactions on Control Systems Technology*, vol. 16, no. 1, pp. 122–129, 2008.
- [100] B. Jiang, J. Xiang, and Y. Wang, “Rolling bearing fault diagnosis approach using probabilistic principal component analysis denoising and cyclic bispectrum,” *Journal of Vibration and Control*, vol. 22, no. 10, pp. 2420–2433, 2016.
- [101] H. Chen, B. Jiang, N. Lu, and Z. Mao, “Deep pca based real-time incipient fault detection and diagnosis methodology for electrical drive in high-speed trains,” *IEEE Transactions on Vehicular Technology*, 2018.
- [102] T. Wang, H. Xu, J. Han, E. Elbouchikhi, and M. E. H. Benbouzid, “Cascaded h-bridge multilevel inverter system fault diagnosis using a pca and multiclass relevance vector machine approach,” *IEEE Transactions on Power Electronics*, vol. 30, no. 12, pp. 7006–7018, 2015.
- [103] G. Li, B. Liu, S. J. Qin, and D. Zhou, “Quality relevant data-driven modeling and monitoring of multivariate dynamic processes: The dynamic t-pls

- approach,” *IEEE transactions on neural networks*, vol. 22, no. 12, pp. 2262–2271, 2011.
- [104] S. X. Ding, S. Yin, K. Peng, H. Hao, B. Shen, *et al.*, “A novel scheme for key performance indicator prediction and diagnosis with application to an industrial hot strip mill,” *IEEE Trans. Industrial Informatics*, vol. 9, no. 4, pp. 2239–2247, 2013.
- [105] R. Vitale, O. E. de Noord, and A. Ferrer, “A kernel-based approach for fault diagnosis in batch processes,” *Journal of Chemometrics*, vol. 28, no. 8, pp. S697–S707, 2014.
- [106] S. Yin, X. Zhu, and O. Kaynak, “Improved pls focused on key-performance-indicator-related fault diagnosis,” *IEEE Transactions on Industrial Electronics*, vol. 62, no. 3, pp. 1651–1658, 2015.
- [107] J. Jiao, H. Yu, and G. Wang, “A quality-related fault detection approach based on dynamic least squares for process monitoring,” *IEEE Trans. Industrial Electronics*, vol. 63, no. 4, pp. 2625–2632, 2016.
- [108] Y. Zhang, N. Yang, and S. Li, “Fault isolation of nonlinear processes based on fault directions and features,” *IEEE Transactions on Control Systems Technology*, vol. 22, no. 4, pp. 1567–1572, 2014.
- [109] Y. Guo, J. Na, B. Li, and R.-F. Fung, “Envelope extraction based dimension reduction for independent component analysis in fault diagnosis of rolling element bearing,” *Journal of Sound and Vibration*, vol. 333, no. 13, pp. 2983–2994, 2014.
- [110] T. Yang, H. Pen, Z. Wang, and C. S. Chang, “Feature knowledge based fault detection of induction motors through the analysis of stator current data,” *IEEE Transactions on Instrumentation and Measurement*, vol. 65, no. 3, pp. 549–558, 2016.
- [111] Y. Xu, S.-Q. Shen, Y.-L. He, and Q.-X. Zhu, “A novel hybrid method integrating ica-pca with relevant vector machine for multivariate process monitoring,” *IEEE Transactions on Control Systems Technology*, no. 99, pp. 1–8, 2018.
- [112] A. Widodo and B.-S. Yang, “Support vector machine in machine condition monitoring and fault diagnosis,” *Mechanical systems and signal processing*, vol. 21, no. 6, pp. 2560–2574, 2007.

- [113] S. Yin, X. Gao, H. R. Karimi, and X. Zhu, “Study on support vector machine-based fault detection in tennessee eastman process,” in *Abstract and Applied Analysis*, vol. 2014, Hindawi, 2014.
- [114] M. Namdari, H. Jazayeri-Rad, and S.-J. Hashemi, “Process fault diagnosis using support vector machines with a genetic algorithm based parameter tuning,” *Journal of Automation and Control*, vol. 2, no. 1, pp. 1–7, 2014.
- [115] Z. Yi and A. H. Etemadi, “Line-to-line fault detection for photovoltaic arrays based on multiresolution signal decomposition and two-stage support vector machine,” *IEEE Transactions on Industrial Electronics*, vol. 64, no. 11, pp. 8546–8556, 2017.
- [116] S. Zidi, T. Moulahi, and B. Alaya, “Fault detection in wireless sensor networks through svm classifier,” *IEEE Sensors Journal*, vol. 18, no. 1, pp. 340–347, 2018.
- [117] X. Tang, X. Xie, B. Fan, and Y. Sun, “A fault-tolerant flow measuring method based on pso-svm with transit-time multipath ultrasonic gas flowmeters,” *IEEE Transactions on Instrumentation and Measurement*, 2018.
- [118] J. Zhou, Y. Yang, S. X. Ding, Y. Zi, and M. Wei, “A fault detection and health monitoring scheme for ship propulsion systems using svm technique,” *IEEE Access*, 2018.
- [119] Y. Shatnawi and M. Al-Khassaweneh, “Fault diagnosis in internal combustion engines using extension neural network,” *IEEE Transactions on Industrial Electronics*, vol. 61, no. 3, pp. 1434–1443, 2014.
- [120] T. de Bruin, K. Verbert, and R. Babuška, “Railway track circuit fault diagnosis using recurrent neural networks,” *IEEE transactions on neural networks and learning systems*, vol. 28, no. 3, pp. 523–533, 2017.
- [121] M. Bach-Andersen, B. Rømer-Odgaard, and O. Winther, “Deep learning for automated drivetrain fault detection,” *Wind Energy*, vol. 21, no. 1, pp. 29–41, 2018.
- [122] J. James, Y. Hou, A. Y. Lam, and V. O. Li, “Intelligent fault detection scheme for microgrids with wavelet-based deep neural networks,” *IEEE Transactions on Smart Grid*, 2017.

- [123] B. K. Panigrahi, P. K. Ray, P. K. Rout, A. Mohanty, and K. Pal, "Detection and classification of faults in a microgrid using wavelet neural network," *Journal of Information and Optimization Sciences*, vol. 39, no. 1, pp. 327–335, 2018.
- [124] F. Zidani, D. Diallo, M. E. H. Benbouzid, and R. Naït-Saïd, "A fuzzy-based approach for the diagnosis of fault modes in a voltage-fed pwm inverter induction motor drive," *IEEE Transactions on industrial electronics*, vol. 55, no. 2, pp. 586–593, 2008.
- [125] L. Li, S. X. Ding, J. Qiu, Y. Yang, and D. Xu, "Fuzzy observer-based fault detection design approach for nonlinear processes," *IEEE Transactions on Systems, Man, and Cybernetics: Systems*, vol. 47, no. 8, pp. 1941–1952, 2017.
- [126] L. Li, S. X. Ding, J. Qiu, and Y. Yang, "Real-time fault detection approach for nonlinear systems and its asynchronous t–s fuzzy observer-based implementation," *IEEE transactions on cybernetics*, vol. 47, no. 2, pp. 283–294, 2017.
- [127] L. Li, M. Chadli, S. X. Ding, J. Qiu, and Y. Yang, "Diagnostic observer design for t–s fuzzy systems: Application to real-time-weighted fault-detection approach," *IEEE Transactions on Fuzzy Systems*, vol. 26, no. 2, pp. 805–816, 2018.
- [128] Y. Luo, Z. Wang, and G. Wei, "Fault detection for fuzzy systems with multiplicative noises under periodic communication protocols," *IEEE Transactions on Fuzzy Systems*, vol. 26, no. 4, pp. 2384–2395, 2018.
- [129] H. A. Talebi, K. Khorasani, and S. Tafazoli, "A recurrent neural-network-based sensor and actuator fault detection and isolation for nonlinear systems with application to the satellite's attitude control subsystem," *IEEE Transactions on Neural Networks*, vol. 20, no. 1, pp. 45–60, 2009.
- [130] N. Sheibat-Othman, N. Laouti, J.-P. Valour, and S. Othman, "Support vector machines combined to observers for fault diagnosis in chemical reactors," *The Canadian Journal of Chemical Engineering*, vol. 92, no. 4, pp. 685–695, 2014.
- [131] R. Muradore and P. Fiorini, "A pls-based statistical approach for fault detection and isolation of robotic manipulators," *IEEE Transactions on Industrial Electronics*, vol. 59, no. 8, pp. 3167–3175, 2012.

- [132] M. M. Rashid and J. Yu, "Hidden markov model based adaptive independent component analysis approach for complex chemical process monitoring and fault detection," *Industrial & Engineering Chemistry Research*, vol. 51, no. 15, pp. 5506–5514, 2012.
- [133] A. Fekih, "Fault tolerant control design for complex systems: Current advances and open research problems," in *Industrial Technology (ICIT), 2015 IEEE International Conference on*, pp. 1007–1012, IEEE, 2015.
- [134] Y. Zhang and J. Jiang, "Bibliographical review on reconfigurable fault-tolerant control systems," *Annual reviews in control*, vol. 32, no. 2, pp. 229–252, 2008.
- [135] M. Ghanavati, A. Chakravarthy, and P. P. Menon, "Analysis of automotive cyber-attacks on highways using partial differential equation models," *IEEE Transactions on Control of Network Systems*, 2017.
- [136] S. Yin, B. Xiao, S. X. Ding, and D. Zhou, "A review on recent development of spacecraft attitude fault tolerant control system," *IEEE Transactions on Industrial Electronics*, vol. 63, no. 5, pp. 3311–3320, 2016.
- [137] Z. Wang, L. Liu, H. Zhang, and G. Xiao, "Fault-tolerant controller design for a class of nonlinear mimo discrete-time systems via online reinforcement learning algorithm," *IEEE Transactions on Systems, Man, and Cybernetics: Systems*, vol. 46, no. 5, pp. 611–622, 2016.
- [138] D. Ye and G.-H. Yang, "Adaptive fault-tolerant tracking control against actuator faults with application to flight control," *IEEE Transactions on control systems technology*, vol. 14, no. 6, pp. 1088–1096, 2006.
- [139] H. Alwi and C. Edwards, "Fault tolerant longitudinal aircraft control using non-linear integral sliding mode," *IET Control Theory & Applications*, vol. 8, no. 17, pp. 1803–1814, 2014.
- [140] X. Yu and J. Jiang, "Hybrid fault-tolerant flight control system design against partial actuator failures," *IEEE Transactions on Control Systems Technology*, vol. 20, no. 4, pp. 871–886, 2012.
- [141] P. Lu, L. Van Eykeren, E.-J. van Kampen, C. de Visser, and Q. Chu, "Double-model adaptive fault detection and diagnosis applied to real flight data," *Control Engineering Practice*, vol. 36, pp. 39–57, 2015.

- [142] Z. Gao, B. Jiang, P. Shi, M. Qian, and J. Lin, “Active fault tolerant control design for reusable launch vehicle using adaptive sliding mode technique,” *Journal of the Franklin Institute*, vol. 349, no. 4, pp. 1543–1560, 2012.
- [143] F. Bateman, H. Noura, and M. Ouladsine, “Fault diagnosis and fault-tolerant control strategy for the aerosonde uav,” *IEEE Transactions on Aerospace and Electronic Systems*, vol. 47, no. 3, pp. 2119–2137, 2011.
- [144] P. Park, H. Khadilkar, H. Balakrishnan, and C. J. Tomlin, “High confidence networked control for next generation air transportation systems,” *IEEE Transactions on Automatic Control*, vol. 59, no. 12, pp. 3357–3372, 2014.
- [145] P. Colaneri, “Dwell time analysis of deterministic and stochastic switched systems,” in *Control Conference (ECC), 2009 European*, pp. 15–31, IEEE, 2009.
- [146] L. I. Allerhand and U. Shaked, “Robust switching-based fault tolerant control,” *IEEE Transactions on Automatic Control*, vol. 60, no. 8, pp. 2272–2276, 2015.
- [147] H. Yang, B. Jiang, and M. Staroswiecki, “Supervisory fault tolerant control for a class of uncertain nonlinear systems,” *Automatica*, vol. 45, no. 10, pp. 2319–2324, 2009.
- [148] X. Zhang, M. M. Polycarpou, and T. Parisini, “Adaptive fault diagnosis and fault-tolerant control of mimo nonlinear uncertain systems,” *International Journal of Control*, vol. 83, no. 5, pp. 1054–1080, 2010.
- [149] S. Perk, Q. Shao, F. Teymour, and A. Cinar, “An adaptive fault-tolerant control framework with agent-based systems,” *International Journal of Robust and Nonlinear Control*, vol. 22, no. 1, pp. 43–67, 2012.
- [150] H. A. Izadi, B. W. Gordon, and Y. Zhang, “Hierarchical decentralized receding horizon control of multiple vehicles with communication failures,” *IEEE Transactions on Aerospace and Electronic Systems*, vol. 49, no. 2, pp. 744–759, 2013.
- [151] R. Gandhi and P. Mhaskar, “A safe-parking framework for plant-wide fault-tolerant control,” *Chemical Engineering Science*, vol. 64, no. 13, pp. 3060–3071, 2009.

- [152] M. Du, J. Nease, and P. Mhaskar, “An integrated fault diagnosis and safe-parking framework for fault-tolerant control of nonlinear systems,” *International Journal of Robust and Nonlinear Control*, vol. 22, no. 1, pp. 105–122, 2012.
- [153] A. Paoli, M. Sartini, and S. Lafortune, “Active fault tolerant control of discrete event systems using online diagnostics,” *Automatica*, vol. 47, no. 4, pp. 639–649, 2011.
- [154] J.-S. Wang and G.-H. Yang, “Data-driven output-feedback fault-tolerant compensation control for digital pid control systems with unknown dynamics,” *IEEE Transactions on Industrial Electronics*, vol. 63, no. 11, pp. 7029–7039, 2016.
- [155] M. Salimifard and H. A. Talebi, “Robust output feedback fault-tolerant control of non-linear multi-agent systems based on wavelet neural networks,” *IET Control Theory & Applications*, vol. 11, no. 17, pp. 3004–3015, 2017.
- [156] Q. Hu, G. Niu, and C. Wang, “Spacecraft attitude fault-tolerant control based on iterative learning observer and control allocation,” *Aerospace Science and Technology*, vol. 75, pp. 245–253, 2018.
- [157] H. C. Cho, J. Knowles, M. S. Fadali, and K. S. Lee, “Fault detection and isolation of induction motors using recurrent neural networks and dynamic bayesian modeling,” *IEEE Transactions on Control Systems Technology*, vol. 18, no. 2, pp. 430–437, 2010.
- [158] K. B. Lee, S. Cheon, and C. O. Kim, “A convolutional neural network for fault classification and diagnosis in semiconductor manufacturing processes,” *IEEE Transactions on Semiconductor Manufacturing*, vol. 30, no. 2, pp. 135–142, 2017.
- [159] A. Abbaspour, P. Aboutalebi, K. K. Yen, and A. Sargolzaei, “Neural adaptive observer-based sensor and actuator fault detection in nonlinear systems: Application in uav,” *ISA transactions*, vol. 67, pp. 317–329, 2017.
- [160] A. Abaspour, S. H. Sadati, and M. Sadeghi, “Nonlinear optimized adaptive trajectory control of helicopter,” *Control Theory and Technology*, vol. 13, no. 4, pp. 297–310, 2015.
- [161] L. Ljung and T. Söderström, *Theory and practice of recursive identification*, vol. 5. JSTOR, 1983.

- [162] C. Schumacher, P. Khargonekar, and N. McClamroch, “Stability analysis of dynamic inversion controllers using time-scale separation,” in *Guidance, Navigation, and Control Conference and Exhibit*, p. 4322, 1998.
- [163] J.-J. E. Slotine, W. Li, *et al.*, *Applied nonlinear control*, vol. 199. Prentice hall Englewood Cliffs, NJ, 1991.
- [164] M. A. Henson and D. E. Seborg, “Critique of exact linearization strategies for process control,” *Journal of Process Control*, vol. 1, no. 3, pp. 122–139, 1991.
- [165] C.-M. Lin and C.-H. Chen, “Robust fault-tolerant control for a biped robot using a recurrent cerebellar model articulation controller,” *IEEE Transactions on Systems, Man, and Cybernetics, Part B (Cybernetics)*, vol. 37, no. 1, pp. 110–123, 2007.
- [166] Y.-X. Li and G.-H. Yang, “Adaptive fuzzy decentralized control for a class of large-scale nonlinear systems with actuator faults and unknown dead zones,” *IEEE Transactions on Systems, Man, and Cybernetics: Systems*, vol. 47, no. 5, pp. 729–740, 2017.
- [167] A.-R. Merheb, H. Noura, and F. Bateman, “Emergency control of ar drone quadrotor uav suffering a total loss of one rotor,” *IEEE/ASME Transactions on Mechatronics*, 2017.
- [168] Y. Song, Y. Wang, and C. Wen, “Adaptive fault-tolerant pi tracking control with guaranteed transient and steady-state performance,” *IEEE Transactions on Automatic Control*, vol. 62, no. 1, pp. 481–487, 2017.
- [169] M. Van, S. S. Ge, and H. Ren, “Robust fault-tolerant control for a class of second-order nonlinear systems using an adaptive third-order sliding mode control,” *IEEE Transactions on Systems, Man, and Cybernetics: Systems*, vol. 47, no. 2, pp. 221–228, 2017.
- [170] R. Ahmed, M. El Sayed, S. A. Gadsden, J. Tjong, and S. Habibi, “Automotive internal-combustion-engine fault detection and classification using artificial neural network techniques,” *IEEE Transactions on vehicular technology*, vol. 64, no. 1, pp. 21–33, 2015.
- [171] P. Aboutaleb, A. Abbaspour, P. Forouzaneshad, and A. Sargolzaei, “A novel sensor fault detection in an unmanned quadrotor based on adaptive neural observer,” *Journal of intelligent & robotic systems*, vol. 90, no. 3-4, pp. 473–484, 2018.

- [172] L. Wang, Y. He, Z. Zhang, and C. He, “Trajectory tracking of quadrotor aerial robot using improved dynamic inversion method,” *Intelligent Control and Automation*, vol. 4, no. 04, p. 343, 2013.
- [173] G. Campa, Y. Gu, B. Seanor, M. R. Napolitano, L. Pollini, and M. L. Fravolini, “Design and flight-testing of non-linear formation control laws,” *Control Engineering Practice*, vol. 15, no. 9, pp. 1077–1092, 2007.
- [174] J. Roskam and C.-T. E. Lan, *Airplane aerodynamics and performance*. DARcorporation, 1997.
- [175] J. Reiner, G. J. Balas, and W. L. Garrard, “Robust dynamic inversion for control of highly maneuverable aircraft,” *Journal of Guidance, Control, and Dynamics*, vol. 18, no. 1, pp. 18–24, 1995.
- [176] A. Abaspour, M. Sadeghi, and S. H. Sadati, “Using fuzzy logic in dynamic inversion flight controller with considering uncertainties,” in *Fuzzy Systems (IFSC), 2013 13th Iranian Conference on*, pp. 1–6, IEEE, 2013.
- [177] E. J. Smeur, Q. Chu, and G. C. de Croon, “Adaptive incremental nonlinear dynamic inversion for attitude control of micro air vehicles,” *Journal of Guidance, Control, and Dynamics*, vol. 38, no. 12, pp. 450–461, 2015.
- [178] Q. Shen, B. Jiang, P. Shi, and C.-C. Lim, “Novel neural networks-based fault tolerant control scheme with fault alarm,” *IEEE transactions on cybernetics*, vol. 44, no. 11, pp. 2190–2201, 2014.
- [179] S. A. Snell, D. F. Nns, and W. L. Arrard, “Nonlinear inversion flight control for a supermaneuverable aircraft,” *Journal of guidance, control, and dynamics*, vol. 15, no. 4, pp. 976–984, 1992.
- [180] K. W. Iliff and K.-S. C. Wang, “Flight-determined subsonic longitudinal stability and control derivatives of the f-18 high angle of attack research vehicle (harv) with thrust vectoring,” 1997.
- [181] W. K. Na and B. Gou, “Feedback-linearization-based nonlinear control for pem fuel cells,” *IEEE Transactions on Energy Conversion*, vol. 23, no. 1, pp. 179–190, 2008.
- [182] E. T. Hillstrom, M. Canova, Y. Guezennec, and G. Rizzoni, “Modeling the cathode pressure dynamics in the buckeye bullet ii 540 kw hydrogen pem fuel cell system,” *Journal of Power Sources*, vol. 241, pp. 33–45, 2013.

- [183] K. Brik, F. B. Ammar, A. Djerdir, and A. Miraoui, “Causal and fault trees analysis of proton exchange membrane fuel cell degradation,” *Journal of Fuel Cell Science and Technology*, vol. 12, no. 5, p. 051002, 2015.
- [184] Q. Li, W. Chen, Z. Liu, J. Huang, and L. Ma, “Net power control based on linear matrix inequality for proton exchange membrane fuel cell system,” *IEEE Transactions on Energy Conversion*, vol. 29, no. 1, pp. 1–8, 2014.
- [185] G. Park and Z. Gajic, “A simple sliding mode controller of a fifth-order non-linear pem fuel cell model,” *IEEE transactions on energy conversion*, vol. 29, no. 1, pp. 65–71, 2014.
- [186] M. R. Hayati, A. Khayatian, and M. Dehghani, “Simultaneous optimization of net power and enhancement of pem fuel cell lifespan using extremum seeking and sliding mode control techniques,” *IEEE Transactions on Energy Conversion*, vol. 31, no. 2, pp. 688–696, 2016.
- [187] X. Wu and B. Zhou, “Fault tolerance control for proton exchange membrane fuel cell systems,” *Journal of Power Sources*, vol. 324, pp. 804–829, 2016.
- [188] F. D. Bianchi, C. Ocampo-Martinez, C. Kunusch, and R. S. Sánchez-Pena, “Fault-tolerant unfalsified control for pem fuel cell systems,” *IEEE Transactions on Energy Conversion*, vol. 30, no. 1, pp. 307–315, 2015.
- [189] M. Manohar and S. Das, “Current sensor fault-tolerant control for direct torque control of induction motor drive using flux-linkage observer,” *IEEE Transactions on Industrial Informatics*, vol. 13, no. 6, pp. 2824–2833, 2017.
- [190] M. Ghanavati, A. Chakravarthy, and P. Menon, “Pde-based analysis of automotive cyber-attacks on highways,” in *American Control Conference (ACC), 2017*, pp. 1833–1838, IEEE, 2017.
- [191] E. Dijoux, N. Y. Steiner, M. Benne, M.-C. Péra, and B. G. Pérez, “A review of fault tolerant control strategies applied to proton exchange membrane fuel cell systems,” *Journal of Power Sources*, vol. 359, pp. 119–133, 2017.
- [192] C. Lebreton, C. Damour, M. Benne, B. Grondin-Perez, and J.-P. Chabriat, “Passive fault tolerant control of pemfc air feeding system,” *International Journal of Hydrogen Energy*, vol. 41, no. 34, pp. 15615–15621, 2016.

- [193] H.-J. Rong, N. Sundararajan, P. Saratchandran, and G.-B. Huang, “Adaptive fuzzy fault-tolerant controller for aircraft autoland under failures,” *IEEE Transactions on Aerospace and Electronic Systems*, vol. 43, no. 4, 2007.
- [194] M. G. Perhinschi, M. R. Napolitano, G. Campa, B. Seanor, J. Burken, and R. Larson, “Design of safety monitor schemes for a fault tolerant flight control system,” *IEEE Transactions on Aerospace and Electronic Systems*, vol. 42, no. 2, pp. 562–571, 2006.
- [195] X. Wu and D. Gao, “Optimal fault-tolerant control strategy of a solid oxide fuel cell system,” *Journal of Power Sources*, vol. 364, pp. 163–181, 2017.
- [196] X. He, Z. Wang, L. Qin, and D. Zhou, “Active fault-tolerant control for an internet-based networked three-tank system,” *IEEE Transactions on Control Systems Technology*, vol. 24, no. 6, pp. 2150–2157, 2016.
- [197] A. Abbaspour, A. Khalilnejad, and Z. Chen, “Robust adaptive neural network control for pem fuel cell,” *International Journal of Hydrogen Energy*, vol. 41, no. 44, pp. 20385–20395, 2016.
- [198] M. Kamal, D. Yu, and D. Yu, “Fault detection and isolation for pem fuel cell stack with independent rbf model,” *Engineering Applications of Artificial Intelligence*, vol. 28, pp. 52–63, 2014.
- [199] C. Lebreton, M. Benne, C. Damour, N. Yousfi-Steiner, B. Grondin-Perez, D. Hissel, and J.-P. Chabriat, “Fault tolerant control strategy applied to pemfc water management,” *International Journal of Hydrogen Energy*, vol. 40, no. 33, pp. 10636–10646, 2015.
- [200] C. Jeppesen, S. S. Araya, S. L. Sahlin, S. Thomas, S. J. Andreasen, and S. K. Kær, “Fault detection and isolation of high temperature proton exchange membrane fuel cell stack under the influence of degradation,” *Journal of Power Sources*, vol. 359, pp. 37–47, 2017.
- [201] S. Li, H. Cao, and Y. Yang, “Data-driven simultaneous fault diagnosis for solid oxide fuel cell system using multi-label pattern identification,” *Journal of Power Sources*, vol. 378, pp. 646–659, 2018.
- [202] A. Rosich, R. Sarrate, and F. Nejjari, “On-line model-based fault detection and isolation for pem fuel cell stack systems,” *Applied Mathematical Modelling*, vol. 38, no. 11, pp. 2744–2757, 2014.

- [203] S. De Lira, V. Puig, J. Quevedo, and A. Husar, “Lpv observer design for pem fuel cell system: Application to fault detection,” *Journal of Power Sources*, vol. 196, no. 9, pp. 4298–4305, 2011.
- [204] J. Liu, W. Luo, X. Yang, and L. Wu, “Robust model-based fault diagnosis for pem fuel cell air-feed system,” *IEEE Transactions on Industrial Electronics*, vol. 63, no. 5, pp. 3261–3270, 2016.
- [205] M. Davoodi, N. Meskin, and K. Khorasani, “Event-triggered multiobjective control and fault diagnosis: A unified framework,” *IEEE Transactions on Industrial Informatics*, vol. 13, no. 1, pp. 298–311, 2017.
- [206] A. Abbaspour, K. K. Yen, P. Forouzannezhad, and A. Sargolzaei, “Active adaptive fault-tolerant control design for pem fuel cells,” in *2018 IEEE ENERGY CONVERSION CONGRESS & EXPO*, pp. 1–6, IEEE, 2018.
- [207] J. Hamelin, K. Agbossou, A. Laperriere, F. Laurencelle, and T. Bose, “Dynamic behavior of a pem fuel cell stack for stationary applications,” *International Journal of Hydrogen Energy*, vol. 26, no. 6, pp. 625–629, 2001.
- [208] L. Xu, M.-Y. Chow, J. Timmis, and L. S. Taylor, “Power distribution outage cause identification with imbalanced data using artificial immune recognition system (airs) algorithm,” *IEEE Transactions on Power Systems*, vol. 22, no. 1, pp. 198–204, 2007.
- [209] A. Sargolzaei, A. Abbaspour, M. A. Al Faruque, A. S. Eddin, and K. Yen, “Security challenges of networked control systems,” in *Sustainable Interdependent Networks*, pp. 77–95, Springer, 2018.
- [210] J. Hare, X. Shi, S. Gupta, and A. Bazzi, “Fault diagnostics in smart micro-grids: A survey,” *Renewable and Sustainable Energy Reviews*, vol. 60, pp. 1114–1124, 2016.
- [211] C.-K. Zhang, L. Jiang, Q. Wu, Y. He, and M. Wu, “Delay-dependent robust load frequency control for time delay power systems,” *IEEE Transactions on Power Systems*, vol. 28, no. 3, pp. 2192–2201, 2013.
- [212] H. Zhang, W. Meng, J. Qi, X. Wang, and W. X. Zheng, “Distributed load sharing under false data injection attack in inverter-based microgrid,” *IEEE Transactions on Industrial Electronics*, 2018.

- [213] Y. Liu, P. Ning, and M. K. Reiter, “False data injection attacks against state estimation in electric power grids,” *ACM Transactions on Information and System Security (TISSEC)*, vol. 14, no. 1, p. 13, 2011.
- [214] M. Chlela, G. Joos, M. Kassouf, and Y. Brissette, “Real-time testing platform for microgrid controllers against false data injection cybersecurity attacks,” in *Power and Energy Society General Meeting (PESGM), 2016*, pp. 1–5, IEEE, 2016.
- [215] P. Risbud, N. Gatsis, and A. Taha, “Vulnerability analysis of smart grids to gps spoofing,” *IEEE Transactions on Smart Grid*, 2018.
- [216] A. Jafarnia-Jahromi, A. Broumandan, J. Nielsen, and G. Lachapelle, “Gps vulnerability to spoofing threats and a review of antispoofing techniques,” *International Journal of Navigation and Observation*, vol. 2012, 2012.
- [217] K. Emami, T. Fernando, H. H.-C. Iu, B. D. Nener, and K. P. Wong, “Application of unscented transform in frequency control of a complex power system using noisy pmu data,” *IEEE Transactions on Industrial Informatics*, vol. 12, no. 2, pp. 853–863, 2016.
- [218] H. M. Khalid and J. C.-H. Peng, “Immunity toward data-injection attacks using multisensor track fusion-based model prediction,” *IEEE Transactions on Smart Grid*, vol. 8, no. 2, pp. 697–707, 2017.
- [219] Z.-H. Yu and W.-L. Chin, “Blind false data injection attack using pca approximation method in smart grid,” *IEEE Transactions on Smart Grid*, vol. 6, no. 3, pp. 1219–1226, 2015.
- [220] P. Bangalore and L. B. Tjernberg, “An artificial neural network approach for early fault detection of gearbox bearings,” *IEEE Transactions on Smart Grid*, vol. 6, no. 2, pp. 980–987, 2015.
- [221] A. Abdullah, “Ultrafast transmission line fault detection using a dwt based ann,” *IEEE Transactions on Industry Applications*, 2017.
- [222] S. Jana and A. De, “A novel zone division approach for power system fault detection using ann-based pattern recognition technique,” *Canadian Journal of Electrical and Computer Engineering*, vol. 40, no. 4, pp. 275–283, 2017.

- [223] M. Ozay, I. Esnaola, F. T. Y. Vural, S. R. Kulkarni, and H. V. Poor, “Machine learning methods for attack detection in the smart grid,” *IEEE Transactions on Neural Networks and Learning Systems*, vol. 27, no. 8, pp. 1773–1786, 2016.
- [224] J. Yan, H. He, X. Zhong, and Y. Tang, “Q-learning-based vulnerability analysis of smart grid against sequential topology attacks,” *IEEE Transactions on Information Forensics and Security*, vol. 12, no. 1, pp. 200–210, 2017.
- [225] S. A. Foroutan and F. R. Salmasi, “Detection of false data injection attacks against state estimation in smart grids based on a mixture gaussian distribution learning method,” *IET Cyber-Physical Systems: Theory & Applications*, vol. 2, no. 4, pp. 161–171, 2017.
- [226] Y. He, G. J. Mendis, and J. Wei, “Real-time detection of false data injection attacks in smart grid: A deep learning-based intelligent mechanism,” *IEEE Transactions on Smart Grid*, vol. 8, no. 5, pp. 2505–2516, 2017.
- [227] J. Hao, R. J. Piechocki, D. Kaleshi, W. H. Chin, and Z. Fan, “Sparse malicious false data injection attacks and defense mechanisms in smart grids,” *IEEE Transactions on Industrial Informatics*, vol. 11, no. 5, pp. 1–12, 2015.
- [228] N. S. Nise, *CONTROL SYSTEMS ENGINEERING, (With CD)*. John Wiley & Sons, 2007.

## VITA

### ALI REZA ABBASPOUR

March 4, 1988	Born, Mashhad, Iran
2011	B.S., Electrical Engineering-Control Sadjad University of Technology Mashhad, Iran
2013	M.S., Guidance and Control System Malek-Ashtar University of Technology Tehran, Iran
2016	Ph.D. Student Florida International University Miami, Florida

### SELECTED PUBLICATIONS AND PRESENTATIONS

A. Abbaspour, K. Yen, P. Forouzannezhad, A. Sargolzaei. *A Neural Adaptive Approach for Active Fault-tolerant Control Design in UAV*, IEEE Transactions on Systems, Man, and Cybernetics: Systems, 2018.

A. Abbaspour, P. Aboutalebi, K. Yen, A. Sargolzaei. *Neural adaptive observer-based sensor and actuator fault detection in nonlinear systems: Application in UAV*, ISA Transactions, Vol. 67, pp. 317-329, 2017.

A. Abbaspour, A. Khalilnejad, Z. Chen, *Robust adaptive neural network control for PEM fuel cell*, International Journal of Hydrogen Energy, Vol. 41, No. 44, pp.20385-20395, 2016.

A. Abbaspour, K. Yen, S. Noei, A. Sargolzaei. *Detection of Fault Data Injection Attack on UAV Using Adaptive Neural Network*, Procedia Computer Science, Vol. 95, pp: 193-200, 2016.

A. Abbaspour, M. Sanchez, A. Sargolzaei, K. Yen, N. Sornkhampan. *Adaptive Neural Network based Fault Detection Design for Unmanned Quadrotor under Faults and Cyber Attacks*, 25th INTERNATIONAL CONFERENCE ON SYSTEMS ENGINEERING ICSEng , August, 2017.

A. Abbaspour, A. Sargolzaei, K. Yen , *Detection of False Data Injection Attack on Load Frequency Control in Distributed Power Systems* , 49th North American

Power Symposium, Sep. 2017.

A. Abbaspour, A. Sargolzaei, K. Yen *A Neural Network based Resilient Control Design For Distributed Power Systems under Faults and Attacks* , IEEE International Conference on Environment and Electrical Engineering and 2018 IEEE Industrial and Commercial Power Systems Europe (EEEIC / I&CPS Europe), June 2018.

A. Abbaspour, K. Yen, P. Frouzannezhad, A. Sargolzaei, Active Adaptive Fault-Tolerant Control Design for PEM Fuel Cells, IEEE Energy Conversion Congress and Exposition, Portland, OR , September, 2018.

A. Abbaspour, A. Sargolzaei, K. Yen, *A Neural Network-based Cyber-Attack Resilient Design for Load Frequency Control System*, IEEE Transaction on Industrial Electronics, (Under Review).

A. Abbaspour, K. Yen, A. Sargolzaei *Active Nonlinear Fault-Tolerant Control Design for PEM Fuel Cells*, IEEE Transaction on Industry Application, (Under Review).

A. Sargolzaei , A. Abbaspour, M.A. Al Faruque, A. Salah Eddin, K. Yen *Security Challenges of Networked Control Systems Sustainable Interdependent Networks from Theory to Application*, Springer International Publishing, 2018.

P. Aboutalebi, A. Abbaspour, P. Forouzannezhad, A.Sargolzaei *A Novel Sensor Fault Detection in an Unmanned Quadrotor Based on Adaptive Neural Observer*, Journal of Intelligent & Robotic Systems,90(3-4):473-84, 2018.

A Khalilnejad, A Sundararajan, A Abbaspour, A Sarwat, *Optimal Operation of Combined Photovoltaic Electrolyzer Systems*, Journal of Energies 9 (5), 332, 2016.

Khalilnejad, A., A. Abbaspour, and A. I. Sarwat. *Multi-level optimization approach for directly coupled photovoltaic-electrolyser system.*” International Journal of Hydrogen Energy, Vol.41, No. 28, pp. 11884-11894 (2016).

S. Noei , A. Sargolzaei, A. Abbaspour, K. Yen. *A Decision Support System for Improving Resiliency of Cooperative Adaptive Cruise Control Systems*, Procedia Computer Science, Vol.95, pp.489-496, 2016.

A. Sargolzaei, K. Yen, M. Abdelghani, A. Abbaspour, S. Sargolzaei *Generalized Attack Model for Networked Control Systems, Evaluation of Control Method*, Intelligent Control and Automation, Vol. 8, No. 3, 2017.